Patterns in stream biofilm communities and organic matter processing in an agricultural stream network: A multi-scale assessment of the influence of groundwater

by

Lauren Katherine Banks

A thesis

presented to the University of Waterloo

in fulfillment of the

thesis requirement for the degree of

Doctor of Philosophy

in

Biology (Water)

Waterloo, Ontario, Canada, 2024

© Lauren Katherine Banks 2024

Examining Committee Membership

The following served on the Examining Committee for this thesis. The decision of the Examining Committee is by majority vote.

Supervisor	Dr. Adam G. Yates *Associate Professor* *Department of Biology*
External Examiner	Dr. John D. Wehr *Professor* *Fordham University*
Internal Member	Dr. Rebecca C. Rooney *Associate Professor* *Department of Biology*
Member	Dr. Clare E. Robinson *Professor* *Western University* *Adjunct, Department of Biology, University of Waterloo*
Internal-external Member	Dr. Simon C. Courtenay *Professor* *School of Environment, Resources and Sustainability* *Faculty of Environment*

Author's Declaration

This thesis consists of material all of which I authored or co-authored: see Statement of Contributions included in the thesis. This is a true copy of the thesis, including any required final revisions, as accepted by my examiners.

I understand that my thesis may be made electronically available to the public.

Statement of Contributions

I am the sole author of Chapters 1 and 5, which are not intended for publication. The three data chapters (Chapters 2 – 4) will be, or have been, published as stand-alone manuscripts.

The work in Chapter 2 is published in Aquatic Ecology[1] co-authored with Dr. I. Lavoie, Dr. M. Boreux, S.L. Kroeze, N. Gotkowski, Dr. C.E. Robinson, Dr. J.W. Roy, and Dr. A.G. Yates. I co-designed the study, conducted the field work and laboratory work, completed the data analysis, and wrote the resulting manuscript and Dr. A.G. Yates co-designed the study, assisted with field work, contributed to data analysis, and authoring the manuscript. Dr. C.E. Robinson and Dr. J.W. Roy co-designed the study and edited/reviewed the manuscript. Technical support and editing/reviewing of the manuscript was provided by Dr. M. Boreux, S.L. Kroeze, N. Gotkowski. The work presented in Chapter 3 is published in Hydrobiologia[2] with Dr. I. Lavoie, Dr. C.E. Robinson, Dr. J.W. Roy, and Dr. A.G. Yates as co-authors. I co-designed the study, conducted the fieldwork and laboratory work, completed the data analysis, and wrote the resulting manuscript and Dr. A.G. Yates co-designed the study, contributed to, and authoring the manuscript. Dr. C.E. Robinson, Dr. J.W. Roy, co-designed the study and

[1] Banks, L.K., Lavoie, I., Boreux, M.P., Kroeze, S.L., Gotkowski, N., Robinson, C.E., Roy, J.W., and Yates, A.G. 2023. Intra-annual patterns in biofilm communities and cellulose decomposition in a headwater stream network with spatially variable groundwater inputs. Aquatic Ecology. https://doi.org/ 10.1007/s10452-023-10038-6. Springer – as it appears on our copyright page.

[2] Banks, L.K., Lavoie, I., Robinson, C.E., Roy, J.W., and Yates, A.G. 2023. Effects of groundwater inputs on algal assemblages and cellulose decomposition differ based on habitat type in an agricultural stream. *Hydrobiologia*. https://doi.org/10.1007/s10750-023-05251-1. Springer – as it appears on our copyright page.

edited/reviewed the manuscript. Dr. I. Lavoie provided technical support and edited/reviewed the manuscript.

Chapter 4 was co-authored by myself, Dr. I. Lavoie, Dr. C.E. Robinson, Dr. J.W. Roy, and Dr. A.G. Yates. In this chapter, I co-designed the study, conducted the field work and laboratory work, completed the data analysis, and wrote the resulting manuscript. Dr. A.G. Yates co-designed the study, contributed to data analysis, and co-authored the manuscript. Dr. C.E. Robinson, Dr. J.W. Roy, co-designed the study and edited/reviewed the manuscript. Dr. I. Lavoie provided technical support and edited/reviewed the manuscript. As each data chapter is meant to stand alone as a research paper, I have maintained the use of "we" throughout the data chapters to recognize the contributions of others to these projects.

Abstract

Benthic stream biofilm communities support stream ecosystem structure and function by mediating nutrient and carbon cycling. Understanding how environmental factors shape biofilm communities in stream ecosystems is therefore essential. Biofilm communities have been shown to be strongly influenced by nutrient availability and temperature, factors that can be modified by groundwater input at multiple spatial scales. However, in enriched streams, groundwater input as a driver of heterogeneity in surface water environmental conditions has not been well-explored among stream reaches (kilometer scale), habitat types (meter scale), and patches (centimeter scale), nor has the seasonal consistency of these relationships been studied. To investigate the association of groundwater input to biofilm communities, I conducted three interconnected field studies in Kintore Creek, a nutrient-rich agricultural stream network in Ontario, Canada. First, I assessed if variability in groundwater input altered patterns of biofilm communities and cellulose decomposition among reaches over four temperate seasons (Chapter 2). Next, I compared habitats (i.e., riffles and runs) in reaches with high, moderate, and low groundwater inputs to determine if habitat type modified the effects of groundwater input on stream biofilm communities and cellulose decomposition by varying environmental conditions (Chapter 3). Lastly, I assessed the response of stream biofilm communities and cellulose decomposition to a gradient of groundwater upwelling at the patch scale and tested whether small scale variations in environmental conditions are associated with biofilm communities and cellulose decomposition (Chapter 4). The results of Chapter 2 showed no within season association of groundwater input to biofilm communities, with

seasonality driving heterogeneity in biofilm communities. Findings in Chapter 3 demonstrated that habitat type modified effects of groundwater input on biofilm communities. Groundwater influence was expressed by greater primary production and decomposition in runs in reaches with groundwater input compared to runs in the reach with no groundwater input. At the patch scale (Chapter 4), groundwater upwelling did not appear to generate substantial variation in surface water conditions, and variability stream velocity was the primary driver of heterogeneity in stream biofilm communities. The findings of this this thesis are in contrast to past work that found effects of groundwater on stream biofilm communities in nutrient-poor streams. These results may be due to cumulative effects of groundwater input throughout the stream network, thereby limiting the ability to detect environmental drivers of groundwater influence at small spatial (i.e., habitat, patch) scales. Therefore, additional studies comparing catchments with differing levels of groundwater are needed to fully understand the influence of groundwater on stream biofilm communities in differing landscape contexts. A major challenge across spatial scales was the ability to represent the impact of groundwater inputs through environmental measures and biofilm communities, suggesting further investigations at the stream water – biofilm interface is required to disentangle the environmental drivers associated to heterogeneity in biofilm communities. The results of this thesis suggest that the influence of groundwater input on stream biofilm communities and processes depends on the context of stream ecosystem, therefore understanding effects of groundwater input requires future research across a diverse range of stream ecosystems.

Keywords: Streams, Biofilm, Diatoms, Chlorophyll-*a*, Biomass, Cellulose Decomposition, Groundwater, Spatial Scale, Ecological heterogeneity

Acknowledgments

To my supervisor, Dr. Adam Yates, thank you for taking me on as a PhD student and providing invaluable guidance, expertise, editing, and continued support as I have navigated the highs and lows of this degree. Your mentorship has helped me develop into the scientist I am today. Thank you to my examining committee members, Dr. Rebecca Rooney, Dr. Simon Courtenay, and Dr. John Wehr, who have generously provided their time to improve this work through their review and feedback.

I would like to acknowledge the contributions of my collaborators to this work. Thank you to Dr. Isabelle Lavoie for your support and expertise on diatom taxonomy, I have fallen in love with diatoms too! Laura Malbezin, thank you for your technical assistance. To the RESTORE lab at Western University, particularly Dr. Clare Robinson and the groundwater team: Dr. Max Boreux, Kyle Robinson, Shuyang Wang, and Meghan Vissers, thank you for funding, technical assistance, and data exchange. Thanks to Dr. Jim Roy of Environment and Climate Change Canada for your technical expertise and advice on all things groundwater. Our stream ecology – environmental engineering collaboration made this research possible.

I would like to thank Erika Hill for her support during the initial stages of this work and fieldwork throughout this project. Your problem solving, electric screwdriver skills, and dedication to successful research were crucial to the completion of my lab and fieldwork goals.

I would also like to extend my appreciation to the landowners in Kintore, ON for their support and permission to access streams to conduct my research.

Thank you to the Canadian taxpayer for making graduate research scholarships possible. I have been generously supported by OGS and NSERC throughout this degree. Research in Canada would not be possible without funding for graduate students.

To members of StrEAMS lab, past and present, thank you for being there through this rollercoaster of a journey. To Shayla Kroeze, Nicole Gotkowski, Megan Sauro, Amy White, Cora Bilhorn, and Matthew Volk – thank you all for the hard work and fun days in the field.

To my adopted academic community in the Faculty of Environment – Natasha Serrao, Isabel Jorgensen, Maria Battaglia, Rodrigo Curty Pereira, Nathanael Bergbusch, and Lauren Smith – thank you for making UWaterloo a truly memorable experience filled with laughs, personal and academic growth, and real talk.

To my long distance lifetime bestie, Hayley Thomas, I quite literally wouldn't be here without you. You always believe in me and push me to show up as my best self. I'm so glad we are doing life together.

Lastly, I could not have completed this journey without the unwavering support of my parents, Hazen and Lynne, who have always supported my absurd adventures and allowed me the freedom to follow my dreams.

Table of Contents

List of Figures

List of Tables

List of Abbreviations

%	Percent
^{222}Rn	Radon-222
AFDM	Ash-Free Dry Mass
AIC_c	Akaike Information Criterion corrected for small sample sizes
AEM	Asymmetric Eigenvector Mapping
Avg.Dis	Average Dissimilarity
C	Carbon
Chl-*a*	Chlorophyll-*a*
C:N	Carbon to Nitrogen
C:P	Carbon to Phosphorus
CSA	Cotton-Strip Assay
DI	Deionized
DOC	Dissolved Organic Carbon
°C	Degrees Celsius
FLA	Flow Injection Analysis automated ion analyzer
GLM	Generalized Linear Model
GNSS	Global Navigation Satellite System
HG	High Groundwater Reach
LDL	Lower Detection Limit
LG	Low Groundwater Reach
LMEM	Linear mixed effects models
MG	Moderate Groundwater Reach

N	Nitrogen
NH_4^+	Ammonium
nMDS	Non-Metric Multidimensional Scaling
NO_3^--N	Nitrate as N
P	Phosphorus
PAR	Photosynthetically Active Radiation
PERMANOVA	Permutational Analysis of Variance
PLS	Partial Least Squares
PCA	Principal Components Analysis
SRP	Soluble Reactive Phosphorus
TN	Total Nitrogen
TP	Total Phosphorus

1 General Introduction

1.1 Overview

Stream ecosystems are hierarchically structured, where successively smaller sub-systems such as stream segment, reach, habitat, and patch exist within a stream system (Frissell et al., 1986). The interconnectedness of sub-systems among spatial scales within a stream ecosystem are controlled by spatially nested environmental drivers, where each lower level is constrained by environmental conditions at higher levels (Frissell et al., 1986; Thorp et al., 2008). The spatial template generated by the inherently nested spatial scales in streams controls patterns in biological response (Palmer & Poff, 1997; Poff, 1997; Thorp et al., 2006).

In streams, benthic stream biofilms, hereafter biofilms, are a crucial part of stream ecosystems. Biofilm communities are composed of autotrophic and heterotrophic microorganisms that include algae, bacteria, and fungi, that have a key role in biogeochemical processing of organic and inorganic materials that influence nutrient cycling and carbon cycling in streams (Borchardt, 1996; Battin et al., 2003a; Besemer, 2015). Biofilm communities can be used as a valuable tool to assess stream ecosystems because their diverse community composition and high sensitivity to changes in environmental conditions positions these communities at the interface of biological response and the environment (Lowe & Pan, 1996; Lavoie et al., 2004).

Biofilm communities can be influenced by environmental factors in stream surface water including nutrients, water temperature, and water chemistry, across multiple spatially nested scales (Stevenson, 1997; Royer & Minshall, 2003; Graça et al., 2015). Groundwater

inputs into stream surface water can also alter surface water nutrient availability, water temperature, and water chemistry (Boulton & Hancock, 2006; Boano et al., 2014). However, groundwater inputs have also been shown to be spatially heterogeneous, creating patchiness in groundwater – surface water exchange across spatial scales in a stream network (Dent et al., 2001; Conant et al., 2019).

Groundwater generated variability in surface water conditions has been shown to generate heterogeneity in biological response at multiple spatial scales within a stream network (Brunke & Gonser, 1997; Wyatt et al., 2008; Tang et al., 2019; Burrows et al., 2020). In past studies, assessments of the association of groundwater inputs to heterogeneity in biofilm communities are typically performed in low-nutrient (i.e., < 5 μg P L^{-1} SRP, < 0.5 mg N L^{-1} NO_3^- - N), alluvial rivers at a single spatial or temporal scale (but see Tang et al., 2019). Thus, how groundwater inputs influence biofilm communities in more nutrient-rich surface waters among nested spatial scales and over multiple temperate seasons is largely unknown. Thus, the research presented in this thesis seeks to use the spatially nested hierarchical structure of streams as a template to assess the role of groundwater input in generating heterogeneity in stream biofilm communities (i.e., biomass and diatom composition) and organic matter processing (i.e., cellulose decomposition).

1.1.1 Stream biofilm communities

Biofilms are ubiquitous in freshwater ecosystems, where they can develop on nearly any interfacial environment, ranging from Antarctic ice sheets to alpine streams, and can establish communities on both organic and inorganic substrates, contributing to biodiversity

and ecosystem processes (Costerton et al., 1995; Stoodley et al., 2002; Dang & Lovell, 2015). Stream benthic biofilm communities are composed of highly diverse microbial communities of bacteria, archaea, algae, fungi, protozoa, and viruses that colonize streambed substrates (Besemer 2015). The autotrophic component of the biofilm includes algae (e.g., diatoms, green algae, and red algae) and cyanobacteria, whereas the heterotrophic component, consists of primarily bacteria and fungi (Battin et al., 2016). Benthic biofilms are a major component of stream ecosystem function, where biofilms process organic and inorganic materials through direct assimilation or transformation (Sabater et al. 2016).

The autotrophic component of stream biofilms generally consists of diatoms, green algae, and cyanobacteria, hereafter collectively referred to as benthic autotrophs. In streams, benthic autotroph assemblages assimilate and transform bioavailable forms of nutrients (i.e., soluble reactive phosphorus (SRP), nitrate (NO_3^-), and ammonium (NH_4^+)) into benthic autotroph biomass (Biggs, 1996). Nutrients stored in benthic autotroph biomass can also be transported downstream during sloughing of biofilm communities (Minshall et al., 2017). Benthic autotrophic mediated nutrient cycles including assimilation, storage, and transportation can lead to short transport distances and rapid cycling of nutrients in the stream, influencing the quantity of dissolved materials and extent of downstream eutrophication potential. The rate of assimilation and subsequent growth of benthic autotroph communities directly impacts production of basal resources in the stream food web (Allan & Castillo, 2007a). Benthic autotrophs can be a high-quality food source for freshwater consumers, primarily stream invertebrates, due to lower C:N and C:P ratios in autotrophic tissue compared

to terrestrial matter (Frost & Elser, 2002; Guo et al., 2016). The extent that benthic autotroph assemblages can perform biogeochemical processes, which are integral to stream ecosystem function, is determined by variability in habitat quality that arise due to heterogeneity in environmental conditions across multiple spatial and temporal scales that controls assemblage biomass and community composition (Stevenson, 1997; Soininen, 2007).

The heterotrophic component of stream biofilms is largely composed of bacteria and fungi, which have a key role in the breakdown and mineralization of organic material (Cummins, 1974; Petersen & Cummins, 1974). The major processes for breakdown of organic material through the detrital pathway undergo a well-defined sequence beginning with initial leaching of soluble compounds (Webster & Benfield, 1986). Detritus is then assimilated and mineralized through colonization and processing by heterotrophic microbes, specifically bacteria and fungi, who condition detritus (i.e., make it more palatable) for subsequent consumption by invertebrate consumers (Suberkropp, 1992; Suberkropp & Weyers, 1996; Allan & Castillo, 2007d). Physical fragmentation within the detrital pool is linked to abrasion and shear stress by streamflow, which also leads to downstream transport of detritus (Gessner et al., 1999). The processing of organic material through the detrital pathway creates an important link in carbon cycling, nutrient mineralization, and energy transfer in stream ecosystems (Enríquez et al., 1993). Identifying environmental factors that generate heterogeneity in patterns of organic matter processing across multiple spatial and temporal has been of keen interest due to the important role heterotrophic microbes have in supporting

stream ecosystem processes (e.g., Royer & Minshall, 2003; Rinehart et al., 2015; Follstad Shah et al., 2017; Costello et al., 2022).

1.1.2 Review of methods for sampling stream biofilm communities

Streambed substrate consistently has been shown to be a key driver biofilm community characteristics (e.g., Battin et al., 2001; Cardinale et al., 2002; Hanrahan et al., 2018; Wijewardene et al., 2021). Among and within reaches in a stream network, substrate size can vary widely (e.g., cobbles, gravel, sand, silt), posing a challenge for direct comparisons of biofilm communities (Burkholder, 1996). Thus, methods that employ a standardized approach are required to compare biofilm communities across spatial and temporal scales. Various standardized approaches to capture the autotrophic and heterotrophic components of biofilm communities in streams have been developed.

Biofilm biomass can be sampled directly from natural substrata in the stream, or from a standardized substrate that has been incubated in the stream (*sensu* Steinman et al., 2007). Biofilm biomass accrual follows a well-defined accrual curve, where colonization and exponential growth results in peak biomass at approximately 28 days, depending on season (Biggs, 1996; Royer & Minshall, 2003). This is a disadvantage of biomass sampling from natural substrata, as peak biomass cannot be identified for each sampling period. Further, there may not be consistent size substrata (e.g., cobble) among or within reaches in a stream network. Scraping a known area from an artificial substrate that has been deployed for a known amount of time allows for direct comparisons of biomass accrual.

Assessing biomass accrual also allows for insights into both the autotrophic and heterotrophic component of the biofilm. Pigments in algae, such as chlorophyll-*a*, have been widely applied to estimate algal biomass and require relatively straightforward lab equipment and protocols (*sensu* Steinman et al., 2007). Pigment analyses of chlorophyll-*a* allows for a distinction of algal biomass from other biofilm biomass, however, the amount of chlorophyll-*a* in a cell depends on autotroph community composition and environmental factors (*sensu* Steinman et al., 2007). Further, biofilm biomass can be estimated by measuring ash-free dry mass using well-described methods and commonly available lab equipment, although this method does not distinguish autotrophic and heterotrophic biomass, nor does it identify whether biomass is alive or senescent (*sensu* Steinman et al., 2007). By simultaneously measuring autotrophic and biofilm biomass from a standardized substrate, associations with environmental conditions can be readily assessed.

Changes in benthic autotroph assemblages have been consistently linked to spatio-temporal heterogeneity in environmental conditions (e.g., Stevenson, 1997; Biggs et al., 1998; Stevenson & Pan, 2010; Passy & Larson, 2011; Lange et al., 2016). Benthic autotroph assemblages broadly consist of three dominant groups: green algae, cyanobacteria, and diatoms (DeNicola, 1996). Though each green algae, cyanobacteria, and diatoms respond to changes in the environment, diatoms have been shown to be a more robust indicator of changes in environmental conditions (e.g., Pan et al., 1996; Winter & Duthie, 2000; Lavoie et al., 2004; Stevenson & Pan, 2010; Carayon et al., 2019). Diatom assemblages can provide insight into environmental conditions because diatom assemblages are taxonomically rich, including

hundreds of taxa in temperate streams, are sensitive to changes in environmental conditions, and have a well-established autecology (Van Dam et al., 1994; Lavoie et al., 2006). Diatom communities can be readily sampled in streams by scraping a known area of a natural or artificial substrate, and number of samples required can be easily altered to match the spatial scale of the research question (Biggs, 1996; Lavoie et al., 2005). Diatom taxa can been identified and enumerated using microscopy or molecular methods (Bailet et al., 2019; Rimet et al., 2019). Protocols for analysis of diatom communities after identification are robust, such as inclusion and exclusion criteria for rare taxa (Cao et al., 2001; Lavoie et al., 2009; Lavoie & Campeau, 2016). Though in its infancy, there is potential to apply machine learning to existing valve view diatom images to assist with more rapid taxonomic identification (Pu et al., 2023). A key limitation of using compiled diatom images is that identification of diatoms in girdle view is not yet possible. Identification of individual diatoms using microscopy can be challenging primarily due to analyst skill level, time required, availability of microscope equipment, and ongoing updates and changes to diatom taxonomy. However, with the required taxonomic expertise and equipment availability, identification of diatom taxa is a useful bioindicator to assess associations between diatom community composition and environmental conditions (Passy, 2001; Soininen, 2007; Lavoie et al., 2014).

1.1.3 Review of sampling organic matter processing

Biofilm biomass accrual provides a metric for comparison of the quantity of biofilm community at a given sampling location, biomass accrual does not account for the function of processing of organic material biofilms perform in streams. Because of the importance of a

function-based metric of organic matter processing, various techniques to assess organic matter processing have been developed.

The litter-bag assay was developed as a method to assess organic matter processing in stream ecosystems (Gessner & Chauvet, 2002). The litter-bag assay involves placing a known mass of plant litter in a mesh bag, deploying in a stream, collecting, and re-weighing plant litter to measure mass loss during deployment. The difference in mass loss provides a decomposition rate, as amount of organic matter lost during breakdown over a known incubation period (Boulton & Boon, 1991). A benefit of this method is that allochthonous litter can be used to assess realized decomposition processes, providing further insight into nutrient cycling in streams (Robbins et al., 2023). However, a major disadvantage of the litter-bag assay is the lack of consistency such as across mesh sizes, litter taxa, litter quality, and amount of plant litter used, which limits comparability among studies (*sensu* Tiegs et al., 2013). The lack of standardization with the litter-bag assay led to the development of the cotton-strip assay, which measures decomposition rate as a loss of tensile strength rather than mass loss (Boulton & Boon, 1991; Boulton & Quinn, 2000). The cotton-strip assay provides a standardized and ecologically relevant material, as cotton is 95 % cellulose as plant litter is primarily cellulose (Egglishaw, 1972). The cotton-strip assay has shown sensitivity to differences in environmental conditions at multiple spatial scales (e.g., Clapcott & Barmuta, 2010; Webb et al., 2019). Additionally, cotton-strips tend to decompose more rapidly than plant litter, requiring shorter incubation time (Tiegs et al., 2007). A disadvantage of the cotton-strip assay is that the assay provides a relative measure of decomposition among locations, but does not necessarily reflect the actual rate of C processing in the stream (Tiegs et al., 2007, 2013).

However, overall, the cotton-strip assay does provide a standardized indicator of measuring organic matter processing.

1.2 Review of environmental drivers of biofilm communities

1.2.1 Nutrient availability & Water chemistry

Nutrient availability, as phosphorus (P; dissolved inorganic P) and nitrogen (N; nitrate and ammonia), in surface water can limit stream biofilm accrual (Suberkropp & Chauvet, 1995; Borchardt, 1996; Gulis & Suberkropp, 2003). Surface water nutrient availability has also been shown to be influenced by groundwater inputs (Brunke & Gonser, 1997; Boulton et al., 1998). Generally, autotrophic biomass accrual has a positive association with nutrient availability in the water column (Biggs, 2000; Dodds & Welch, 2000). Heterotrophic microbial activity depends on both water column nutrient availability and litter quality (Royer & Minshall, 2001; Ferreira et al., 2015). Because of the varying nutrient requirements for different taxa in the biofilm, autotrophs and heterotrophs typically have different nutrient limitation thresholds (Tank & Dodds, 2003). In southern Ontario streams, nutrient threshold for ensuring protection from eutrophication effects in agricultural streams has been estimated as 0.026 mg P L^{-1} for total P, and 1.06 mg N L^{-1} for total N for benthic algae (Chambers et al., 2012). Estimates for surface water SRP and NO_3^- - N thresholds for heterotrophic microbial activity have been estimates as 0.018 – 0.053 mg P L^{-1} for SRP and 0.16 – 3.03 mg N L^{-1} for NO_3^- - N (Rosemond et al. 2002; Ferreira et al. 2006; Gulis et al. 2006).

Nutrient availability is not the only resource that can influence stream biofilm communities. Indeed, in temperate streams, nutrient availability only explained 10 – 40 % of

the variation in benthic algal biomass (Dodds et al., 2002). Further, in agricultural streams, where nutrients tend not to be limiting, and biofilm communities may be limited by other habitat factors (e.g., light availability, stream velocity) (Munn et al., 2010). Therefore, nutrient availability must be considered in the context of other habitat factors (e.g., water chemistry, water temperature, stream velocity, and/or light availability).

Water chemistry can also have a modifying role on biofilm communities. Past work that the role of pH in influencing microbial activity where ranges in pH were greater than 2.0, though common aquatic hyphomycetes (fungi) can tolerate a wide range of pH (Suberkropp, 1992; Griffith & Perry, 1994; Webb et al., 2019). In streams, greater pH tends to be correlated to increased conductivity, which may be associated with erosion and runoff adding major ions and nutrients into the surface water, particularly in agricultural streams (Biggs, 1990; Pan et al., 1996; Leland & Porter, 2000). Dissolved oxygen concentration can also influence biofilm community function. Oxygen can also limit microbial respiration and photosynthesis due to changes in diel demand for oxygen, and may be reduced where there increased loading of organic material into a stream (Allan & Castillo, 2007b). Groundwater inputs can also alter water chemistry in the surface waters, for example, groundwater inputs tend to be less oxygen rich than surface waters (Valett et al., 1997; Malard & Hervant, 1999).

1.2.2 Temperature

Surface water temperature can influence biofilm growth rates, thereby altering productivity and biomass accrual. Groundwater inputs can also influence surface water temperatures, where a temperature differential between groundwater and surface waters exist

(Kaandorp et al., 2019; Tang et al., 2019) Generally, warmer water temperatures increase microbial metabolic activity, however, taxa in the biofilm have varying preferred temperature ranges (Brown et al., 2004; Battin et al., 2016; Delgado et al., 2017). For the autotrophic component of the biofilm, the major groups of autotrophs tend to have differing temperature ranges of maximum growth rates and contribution to community composition, where diatoms (Bacillariophyceae) typically range between 5 °C and 20 °C, green algae (Chlorophyta) between 15 °C and 30 °C, and cyanobacteria (Cyanobacteria) are typically above 30 °C (DeNicola, 1996). The differences in temperature tolerance of these groups have implications for expected autotrophic biomass and community composition among temperate seasons. Seasonal shifts in benthic autotroph assemblage composition have observed in temperate streams, where in cooler seasons diatom tend to dominate autotroph assemblages, and in warmer seasons autotroph community composition shifts tends to include a more diverse range of autotrophic taxa (Flinders et al., 2019; Snell et al., 2019; Tang et al., 2019). Surface water temperature acts as a key regulator for autotrophic community composition and metabolic activity, even while other resources (e.g., light, nutrients) are readily available, thereby constraining autotrophic assemblages in the biofilm (Mulholland et al., 1985; Allan & Castillo, 2007c).

Surface water temperature has also been shown to be a primary environmental driver of organic matter processing, where warmer temperatures are associated with faster rates of organic matter processing (Ferreira & Chauvet, 2011; Fernandes et al., 2012; Costello et al., 2022). In streams, aquatic hyphomycetes may constitute nearly 90 % of heterotrophic biofilm

biomass, representing the majority of heterotrophic activity in the biofilm (Aumen et al., 1983; Findlay & Arsuffi, 1989; Tank & Winterbourn, 1995). Like autotrophs, heterotrophic aquatic hyphomycetes (fungi) have optimal temperatures for growth rates at temperatures of 15 – 25 °C, and have been shown to exhibit seasonal shifts on taxa composition in temperate streams (Suberkropp, 1984; Sridhar & Bärlocher, 1993). Heterotrophic bacteria show a similar optimal temperatures to aquatic hyphomycetes, with peak respiration rates estimated to be between 15 and 25 °C, and highly diverse bacterial communities have been associated with water temperatures of 16 – 19 °C, (Cherry & Guthrie, 1973; Sand-Jensen et al., 2007). Warmer surface water temperatures generally increase the metabolic activity of heterotrophic microbes, and past work has demonstrated that higher nutrient availability in the surface water can interact synergistically with temperature to increase rates of organic matter processing (Gulis & Suberkropp, 2003; Ferreira & Chauvet, 2011; Geraldes et al., 2012). Variation in surface water temperature due to seasonality in temperate streams can also affect decomposition rates. Under cooler (e.g., winter) conditions, decomposition rates can vary widely within small thermal range (Griffiths & Tiegs, 2016). Past findings suggest that faster rates of organic matter processing are likely to occur where surface water is warmer (i.e., 15 – 25 °C) and surplus nutrients are available (Woodward et al., 2012; Tiegs et al., 2019).

1.2.3 Stream velocity

Stream velocity can effect ecological response in stream ecosystems by influencing access to resources (e.g., nutrients) and habitat quality (e.g., sheer stress) (Poff et al., 1997; Stevenson, 1997; Royer & Minshall, 2003). Indeed, stream velocity has been associated with

variation in algal biomass, algal assemblage composition, and organic matter processing (Horner et al., 1990; Biggs & Gerbeaux, 1993; Biggs & Hickey, 1994; Biggs et al., 1998; Tiegs et al., 2009; Webb et al., 2019). Within the biofilm, benthic algae have been shown to be affected by trade-offs in resource subsidy – shear stress responses to increasing stream velocity. For example, slower stream velocity (< 0.2 m/s) limits mass transfer (i.e., nutrient diffusion) whereas faster stream velocity (> 0.4 m/s) can result in sloughing of algal biomass, and where biomass typically peaks at ~ 0.2 m/s (Biggs et al., 1998). Stream velocity also has a key role in determining which taxa dominate algal assemblages. Generally, green algae establish in slower velocities than diatoms (Biggs & Hickey, 1994; Biggs & Thomsen, 1995). Further, within the diatom assemblage, taxa vary in their preferences for stream velocity, where low profile and motile taxa tend to be observed in faster velocities and high profile taxa are more common in slower velocities (Van Dam et al., 1994; Passy, 2007).

Faster stream velocity has consistently been shown to enhance rates of organic matter breakdown, attributed to greater physical abrasion (Tiegs et al., 2009; Clapcott & Barmuta, 2010; Webb et al., 2019). Physical abrasion allows for greater fragmentation of organic matter, which can be transported in areas of faster velocity (i.e., riffles), but organic matter may be depositional in areas of slow velocity (i.e., runs and pools), thereby influencing carbon cycling throughout the stream continuum (Vannote et al., 1980; Clapcott & Barmuta, 2010; Nogaro et al., 2010).

1.2.4 Light

Light availability, through shading by tree canopy cover or attenuation by turbid surface waters, can influence biofilm communities. Canopy cover can obstruct over 95 % of photosynthetically active radiation, limiting photosynthesis of autotrophic communities (PAR) (Hill, 1996). Similarly, suspended sediments in surface waters can further attenuate PAR before reaching biofilm communities (Dodds & Welch, 2000). Benthic autotroph community composition and biomass accrual can be affected by light availability because of the response of different taxa to irradiance (Hill, 1996). Typically, green algae require higher light intensities than diatoms or cyanobacteria (Hill, 1996). Taxa traits may also contribute to shifts in community composition in response to light availability. Low profile taxa, attached to the substrate, may decrease in abundance in response to shading, whereas high profile and motile taxa may increase in abundance due to better access to light (Passy, 2007). Further, access to light may vary among seasons, where there is greater light availability during spring (prior to leaf out) and autumn (post leaf fall) than summer. Light availability may also be a limiting resource for biofilm accrual due to interaction with other environmental factors.

Light availability can interact with other environmental factors, such as nutrient availability, to limit biofilm accumulation. For example, Munn et al., (1989) found that a stream network in Illinois, USA with agricultural riparian cover (i.e., grasses and shrubs) in the headwaters and more forest riparian vegetation in the downstream, with a concomitant gradient of turbidity from upstream to downstream, likely reduced light penetration into the stream, despite experimental surface water nutrient enrichment (0.33 – 0.85 mg P L^{-1} for SRP and 1.8 – 2.1 mg N L^{-1} for NO_3^- - N). Similarly, a 2-year nutrient enrichment (~0.88 mg P L^{-1}

for SRP and ~1.9 mg N L^{-1} for NO_3^- - N) study in a forested stream in Georgia, USA, resulted in little change in benthic algal biomass or biofilm biomass, or any change in the dominant taxa in the algal assemblage (Greenwood & Rosemond, 2005). However, nutrient enrichment of a moderately shaded, forested Mediterranean stream resulted in higher chlorophyll-*a* concentration and algal density, but there was not a corresponding shift in community composition (Sabater et al., 2005). Light may also have a role in the priming effect for heterotrophic microbial decomposers, where greater light availability may stimulate algal productivity and exudates, allowing for more rapid decomposition of more recalcitrant organic matter (Danger et al., 2013; Howard-Parker et al., 2020) Thus, light availability may have an important limiting role on stream biofilm biomass and community composition.

1.2.5 Influence of groundwater input

Contributions to stream flow can originate from various sources such as precipitation, surface water runoff, and groundwater input (Hynes, 1983). Stream ecosystems often receive a substantial proportion of their streamflow from groundwater input, particularly during periods of baseflow in the winter and summer months in temperate regions (Boulton & Hancock, 2006; Bertrand et al., 2012). Groundwater flow paths are often spatially and temporally heterogeneous due to variability subsurface hydrogeological structures and climate at large scales (e.g., stream segments, catchments), as well as small scale (e.g., reach, habitat, patch) differences in hydraulic gradients between groundwater and surface waters (Boano et al., 2014; Conant et al., 2019). Groundwater – surface water exchange in a stream system is defined by areas of groundwater upwelling, or input, where groundwater enters the surface

water and, conversely, areas of downwelling where surface water enters the groundwater (Winter et al., 1998; Boulton & Hancock, 2006). Large scale determinants of groundwater – surface water exchange include topography, geology, and climate (Sophocleous, 2002; Boulton & Hancock, 2006; Boano et al., 2014; Conant et al., 2019). Topography controls the depth and structure of the water table, and the geology drives spatial arrangement of the soil and bedrock determines where groundwater – surface water exchange occurs (Winter et al., 1998). Climate, including seasonality in temperate regions, influences frequency and intensity of precipitation events, as well as annual patterns in baseflow dominated streamflow (Sophocleous, 2002). Groundwater inputs are the predominant contributor to stream flow during summer and winter baseflow periods in temperate climates (Bertrand et al., 2012). Temperate seasons can also generate temperature variation in thermal regimes of groundwater – surface water exchange, where groundwater inputs are cooler than surface waters summer, and warmer than surface water in winter (Kaandorp et al., 2019).

Large scale drivers constrain local factors such as streambed topography and sediment grain size which lead to shallow groundwater flow paths that differ at multiple spatial scales, leading to variable groundwater influence within a stream network (Dent et al., 2001; Malard et al., 2002; Cardenas et al., 2004; Korbel & Hose, 2015). Streambed topography generates differences in patchiness in groundwater inputs due to hydraulic head where areas of faster stream velocity generate surface water downwelling and areas of slower stream velocity where groundwater can enter the surface water (Harvey & Bencala, 1993; Brunke & Gonser, 1997). Differences in sediment grain size creates heterogeneity in streambed permeability where more

coarse sediment usually results in greater exchange, whereas finer sediment reduces exchange (Renard & Allard, 2013).

Shallow groundwater flow paths can result in an interface of groundwater – surface water exchange known as the hyporheic zone, a subsurface layer of streambed sediment where groundwater – surface water can exchange at small scales (i.e., meter, centimeter) within a reach (Boulton et al., 1998; Dent et al., 2001). The hyporheic zone has a steep physiochemical gradient, with complex patterns of aerobic and anaerobic conditions that interaction with geochemically and microbially-rich streambed sediments, as well as stream biofilms, increasing opportunities for higher rates of biogeochemical activity and transformation of organic carbon and nutrients (Anderson-Glenna et al., 2008; Krause et al., 2011; Harvey & Gooseff, 2015). Further, in areas where groundwater is upwelling, there is generally a more moderated thermal regime compared to areas of no groundwater influence (Brunke & Gonser, 1997; Valett et al., 1997; Baxter & Hauer, 2000; Kaandorp et al., 2019). The dynamic interactions of hydrological and biogeochemical processes where groundwater – surface water exchange creates heterogeneous environmental conditions that can affect stream biofilm communities (Valett et al., 1994; Jones et al., 1995; Wyatt et al., 2008; Mejia et al., 2016; Tang et al., 2019; Burrows et al., 2020).

Patchiness in groundwater inputs have been associated with heterogeneity in stream biofilm communities and organic matter processing because of the role of groundwater input in influencing surface water nutrient availability, water temperature, and water chemistry (Brunke & Gonser, 1997; Boulton & Hancock, 2006; Boano et al., 2014). Groundwater inputs

have been associated with patches of greater primary productivity within reaches, largely attributed to nutrient subsidies from groundwater (Wyatt et al., 2008; Roy et al., 2011; Mejia et al., 2016; Burrows et al., 2020). Groundwater inputs also can generate more stable temperature conditions that can promote algal growth during cooler and warmer seasons, and reduce annual variability in benthic algal biomass over a hydrologic year (Sear et al., 1999; Mejia et al., 2016; Kaandorp et al., 2019; Tang et al., 2019). Stream velocity has also been shown to influence the effect of groundwater input within a reach, where autotrophic growth is stimulated by groundwater resource subsidies (e.g., nutrients and chemical constituents) in areas of slower velocity, but not in areas of faster velocity (Burrows et al., 2020). In addition, groundwater inputs have also been shown to alter diatom assemblage composition (Stevenson et al., 2009; Roy et al., 2011).

Organic matter processing has also been shown to be influenced by groundwater inputs. Faster rates of organic matter processing have been associated with groundwater input, likely due to additional nutrients from groundwater (Griffiths & Tiegs, 2016). In reaches with groundwater, groundwater input provide microbial communities additional resources from groundwater, thereby increase organic matter processing (Tiegs et al., 2009; Webb et al., 2019). However, the cooling effect of groundwater inputs on surface water during warmer seasons has been found to slow organic matter processing (Webb et al., 2019; Poisson & Yates, 2022). Further, low levels of dissolved oxygen in areas of groundwater input may also hinder organic matter processing (Cornut et al., 2010). In the streambed sediment subsurface, cooler groundwater input with lower levels of dissolved oxygen have been associated with lower

heterotrophic activity, resulting in slower rates of organic matter processing (Strommer & Smock, 1989; Malard & Hervant, 1999; Crenshaw et al., 2002; Cornut et al., 2010). Given that groundwater input can alter key environmental drivers, such as nutrient availability and temperature, understanding the extent that groundwater input can modify heterogeneity of stream biofilm communities and organic matter processing is crucial to our understanding of stream ecosystems (Boulton & Hancock, 2006; Conant et al., 2019).

1.2.5.1 Review of methods to measure groundwater input

Methods to measure groundwater can often be intrusive and destructive, involving extraction of streambed sediments and/or drilling into streambed sediments and installing equipment directly into the streambed for the duration of a study (Kalbus et al., 2006). The scale of measurement of groundwater inputs can influence estimates of groundwater in a stream. For example, differences between point measurements in a reach compared with tracer techniques stream network scale. Therefore, understanding groundwater input in stream network may be best represented by employing several techniques across multiple spatial scales (Kalbus et al., 2006).

At kilometer scales, non-destructive methods to investigate groundwater inputs include incremental streamflow, hydrograph separation, and environmental tracers. Measurements of incremental streamflow are optimal when there are low flow conditions and require gauging of both stream velocity and tracer dilution throughout each reach. These measurements are cumbersome and may be inaccurate during periods of high flow (e.g., spring). If detailed hydrographic information is limited, then another method should be employed (Kalbus et al.,

2006). Environmental tracers are used to identify any change in surface water properties that can be attributed to groundwater inputs and can be naturally occurring in streams. The use of ions as tracers (e.g., conductivity) may not accurately represent groundwater inputs, as biogeochemical reactions may alter concentrations of ions in the surface water, and the presence of ions may not be related to concentrations in groundwater (Cook et al., 2003).

Where groundwater contributes to surface water, concentrations of radon-222 (^{222}Rn) can be two or three orders of magnitude greater in the groundwater compared to surface waters (Atkinson et al., 2015). Further, because ^{222}Rn has a short half-life (3.82 days) and readily degasses into the atmosphere, there is a rapid decline in downstream concentrations of ^{222}Rn. Thus high ^{222}Rn concentrations are only found in surface waters where there is groundwater input at, or immediately upstream of, the sampling location (Cook et al., 2003). Additionally, ^{222}Rn is relatively easy to sample and non-intrusive, requiring only a grab sample. Further, a mass balance approach can be taken at each reach that integrates upstream and downstream ^{222}Rn concentration, stream discharge, stream velocity, and reach width, allowing for estimates of groundwater discharge in a reach (Atkinson et al., 2015). At the among reach scale, ^{222}Rn provides insight into groundwater inputs throughout the reach, while allowing for comparison among reaches over multiple seasons because of the consistent sampling and measuring methods. However, ^{222}Rn as a proxy for groundwater is limited to detecting patterns in groundwater at large spatial scales (i.e., among reaches) (Cook et al., 2003).

With consideration of the potential patch dynamics of within reach scale hyporheic exchange and the requirement for minimally disturbing the streambed, temperature as a tracer

can be employed as a method to quantify groundwater – surface water exchange. Heat, as streambed and surface water temperatures, is assumed to be empirically associated with quantitative measures of groundwater flux (Conant 2004). Heat is a useful tracer in this context, as groundwater temperatures are generally more stable throughout a year, whereas surface water temperatures tend to vary throughout a day and over temperate seasons (Kalbus et al., 2006). However, an important assumption is that differences in temperature between the streambed and surface water are not attributable to solar warming due to time required to measure streambed and surface water temperature (Kalbus et al., 2006). In warmer seasons, groundwater is typically cooler than surface water, therefore where groundwater is present in the shallow streamed, it is expected that there will be greater difference between surface and subsurface temperatures (Kalbus et al., 2006). Although point measurements of surface and subsurface temperatures are measured, discrete surface and subsurface temperature points can be measured across transects and interpolated to create spatial maps of subsurface temperature and surface water – subsurface temperature gradient within a reach (Fleckenstein et al., 2010; Boano et al., 2014; Rau et al., 2014). Within a reach, groundwater inputs can be patchy at a small (centimeter) scale, therefore spatial mapping of subsurface temperature and stream water – subsurface temperature gradient can be used as a proxy to create a template of small-scale groundwater – surface water exchange throughout a reach (Conant 2004). The template can be used as a proxy to identify locations of groundwater input, surface water downwelling, or no exchange within a reach (Robinson et al., 2022). This is a particularly useful method as temperature can be measured rapidly and non-intrusively, measurements do not impact streamflow, and can provide insight into small-scale (i.e., < 1 meter) spatial patterns in

groundwater flux within habitats and patches in a reach (Rau et al., 2014, Conant 2004). However, physical factors in the stream must also be taken into consideration. Streambed topography associated with sequences of slow stream velocity (i.e., runs) and fast stream velocity (i.e., riffles) has also been shown to modify patterns of groundwater input within a reach, therefore stream velocity may modify groundwater influence (Harvey & Bencala, 1993; Krause et al., 2011).

At the within reach scale, findings of spatial temperature mapping can also be supported by direct point measurements of groundwater – surface water exchange, such as hydraulic head, using pipes installed in the streambed. Where groundwater is upwelling, the hydraulic head of groundwater is greater than that of the stream, conversely, where surface water is downwelling, the hydraulic head of stream is greater than that of groundwater (Winter et al., 1988). Additionally, this method also allows for direct measurements of groundwater nutrients and chemistry (Conant et al., 2019). The challenge of measuring hydraulic head is that these point measurements potentially only integrate a small (sub-meter) area of groundwater – surface water exchange (Kalbus et al., 2006). This method is intrusive, as pipes need to be installed directly into the streambed, which may affect streamflow and alter environmental conditions biota experience. Further, streambed sediment type may determine placement of wells, as dense clay or cobbles inhibit pipe installation (Cey et al., 1998). Therefore, direct point measurements of groundwater – surface water exchange may be used to support findings from other methods but may not be feasible to employ throughout all biological sampling locations reach.

1.3 Research objectives

The goal of my thesis was to understand how heterogeneity in stream biofilm communities (i.e., biomass and diatom assemblage composition) and organic matter breakdown (i.e., cellulose decomposition) are associated with patterns of groundwater input at multiple spatial and temporal scales. To achieve this goal, I conducted three interrelated studies at different spatial scales, one of which was also completed over four temperate seasons. Each study was performed in the baseflow-driven, headwater stream system (i.e., Kintore Creek) in an agricultural landscape in Ontario, Canada. For my second chapter, I conducted a field study to assess if there is an association between heterogeneity in stream biofilm communities and cellulose decomposition to groundwater input among reaches the headwater stream network. Additionally, I evaluated whether spatial patterns in the association of stream biofilm communities and cellulose decomposition to groundwater input varied among four temperate seasons. In my third chapter, I compared stream biofilm communities and cellulose decomposition between habitat types (i.e., riffle and run) in reaches with high, moderate, and low groundwater to determine if effects of groundwater input vary with habitat type. I also assessed the association between heterogeneity in biofilm communities and cellulose decomposition and environmental variables that can be modified by groundwater input. Chapter 4 examined the response of stream biofilm communities and cellulose decomposition to a gradient of groundwater upwelling at the patch scale within a reach. Collectively, the three chapters represent a hierarchical, multi-scale assessment of the influence of groundwater input on biofilm communities and cellulose decomposition. My last chapter summarizes and

integrates my findings from the three data chapters, while also providing suggestions for future research.

2 Intra-annual patterns in biofilm communities and cellulose decomposition in a headwater stream network with spatially variable groundwater inputs

2.1 Introduction

Stream biofilms are an important component of stream communities that contribute to ecosystem structure and function by performing biogeochemical processing of organic and inorganic materials (Battin et al. 2003; Marmonier et al. 2012; Sabater et al. 2016). Stream biofilms consist of both primary producers and heterotrophic microbes including algae, bacteria, fungi, and micro-meiofauna (Besemer 2015). Algae are the dominant primary producers in biofilms, providing basal resources to higher trophic levels, and influence nutrient cycling through nutrient uptake from surface water and subsequently transforming, and/or remineralizing nutrients (Minshall 1978; Vannote et al. 1980; Mulholland 1996). Likewise, heterotrophic microbes contribute to carbon cycling in streams by processing organic matter and can be an important food source for organisms at higher trophic levels (Royer and Minshall 2003; Graça et al. 2015).

The critical roles that biofilms play in streams has led to significant efforts to determine the environmental controls of the structure (e.g., biomass and community composition) and function (e.g., organic matter processing) of biofilms (Stevenson 1997; Biggs et al. 1998; Tiegs et al. 2019). Previous studies have established that spatial patterns in stream biofilm communities and organic matter processing are influenced by a number of local habitat factors including nutrient availability (Stevenson 1997; Ferreira et al. 2015) and water temperature (Morin et al. 1999; Ferreira and Chauvet 2011; Martínez et al. 2014). These factors can also vary according to season (Francoeur et al. 1999; Griffiths and Tiegs 2016). However, many

key environmental controls, including temperature and nutrient availability, can be influenced by the amount of groundwater inputs to streams (Boulton and Hancock 2006; Conant et al. 2019). It is therefore important to establish the extent to which variability in groundwater inputs may alter spatial and temporal heterogeneity of stream biofilm communities and organic matter processing.

Groundwater inputs to streams are often spatially variable due to the complexity of subsurface hydrogeological units and associated groundwater flow paths (Conant et al. 2019). Variability in groundwater inputs can increase environmental spatial heterogeneity in streams, influencing autotrophic and heterotrophic components of stream biofilms through addition of nutrients and moderated temperature regimes (Brunke and Gonser 1997; Boulton and Hancock 2006). Indeed, past studies have shown spatial heterogeneity of biofilms in streams to be strongly linked to variability in groundwater inputs (Baxter and Hauer 2000; Wyatt et al. 2008; Mejia et al. 2016; Burrows et al. 2020). For example, variability in groundwater inputs along a stream can create heterogeneity in surface water temperature at multiple spatial scales (e.g., within and between stream reaches) when and where a temperature differential between discharging groundwater and the receiving stream exists (Malard et al. 2002). Moderating thermal effects of groundwater inputs have been shown to increase algal biomass at the patch scale (Pepin and Hauer 2002; Mejia et al. 2016) and linked to slower cellulose decomposition in warmer seasons (Griffiths and Tiegs 2016; Poisson and Yates 2022). Moreover, inputs of nutrient-rich groundwater have been shown to stimulate primary production (Wyatt et al. 2008; Roy et al. 2011; Mejia et al. 2016) as well as accelerate organic matter processing due to

stimulation of microbial activity (Gulis and Suberkropp 2003; Ferreira and Chauvet 2011). However, past studies of stream biofilms have been largely limited to a single season in low-nutrient (i.e., < 5 μg P L^{-1} SRP, < 0.5 mg N L^{-1} NO_3^- - N) alluvial rivers, leaving more nutrient-rich surface waters that experience multiple temperate seasons understudied (but see Tang et al. 2019).

Groundwater inputs to a stream can potentially modify effects of seasonality on biofilms by moderating variation in surface water temperature because groundwater is typically more thermally stable throughout a year. Indeed, stream reaches with high groundwater inputs generally have cooler surface water temperatures in summer and warmer surface water temperatures in winter (Kaandorp et al. 2018, 2019). Such groundwater mediated thermal regimes have been shown to increase primary production during cooler and warmer seasons (Wyatt et al. 2008; Mejia et al. 2016). Indeed, Tang et al., (2019) observed that groundwater inputs reduced variation in benthic algal biomass over an annual cycle because of moderated thermal regimes. This pattern was in contrast to reaches without groundwater, where effects of seasonality on benthic algal biomass were more apparent (Tang et al. 2019). Moderated surface water temperature attributed to groundwater inputs have also been linked to slower decomposition rates during warmer seasons and increased decomposition rates in cooler seasons (Griffiths and Tiegs 2016; Webb et al. 2019). Variation in stream water nutrients over an annual cycle also likely had a role in driving differences in cellulose decomposition in a stream in Walker Branch, Tennessee, USA (Griffiths and Tiegs 2016). Moreover, the impact of groundwater inputs may vary with season, as groundwater can be a

more important source of stream flow during baseflow periods, typically in summer and winter in temperate climates (Bertrand et al. 2012). Yet, although groundwater inputs have been shown to affect stream ecological condition, few studies have examined the effect of groundwater inputs on biofilms in all seasons of a hydrologic year (but see Griffiths and Tiegs 2016; Tang et al. 2019).

Our study assessed how variability in the magnitude of groundwater input may influence spatial and temporal patterns of biofilm communities and cellulose decomposition among reaches of a nutrient-rich headwater stream network in an agricultural area of southern Ontario, Canada. Specifically, we predicted that: (i) seasonal patterns of stream biofilm communities (e.g., chl-*a* accumulation, biofilm growth rate, diatom assemblage composition) and cellulose decomposition would be associated with the magnitude of groundwater inputs at the reach scale, and (ii) differences in the magnitude of groundwater inputs between stream reaches (i.e., spatial heterogeneity) would be associated with spatial patterns in stream biofilm communities and cellulose decomposition.

2.2 Methods

2.2.1 Study area and site selection

Our study was conducted in the two headwater branches of Kintore Creek (43 º08’20” N, 81º01’48” W) in southern Ontario, Canada (Fig. 1). Kintore Creek watershed experiences a temperate climate with four distinct seasons (autumn, winter, spring, summer), with mean annual low and high air temperatures of - 6.0 °C (minimum) and 20.2 °C (maximum), respectively, and an average annual precipitation of 1069.5 mm (Environment and Climate

Change Canada 2010). Land use in Kintore Creek watershed is predominantly agriculture (80 %), with forest (12 %) and residential (4 %) uses constituting smaller fractions (Agricutlure and Agri-Food Canada 2020). Agriculture in the catchment is dominated by row crops of soybean and corn, and subsurface tile drainage is present in many agricultural fields. Within the catchment, surficial geology has variable permeability over the landscape due to glacial deposits of sand-silt tills. High permeability zones are generally on the uppermost parts of the catchments, and throughout the western part of the catchment where sediments are predominantly sand. The stream channels are predominantly silt with some organics, sand, and gravel and vary in permeability (Ontario Geological Survey 2010). Direct groundwater discharges are the main source of flow during baseflow conditions in the headwaters of Kintore Creek as there are no reservoirs or other major wetlands contributing water to the stream. The exception is when the groundwater level is high and groundwater via agricultural tile drains also contributes water to the stream during baseflow conditions.

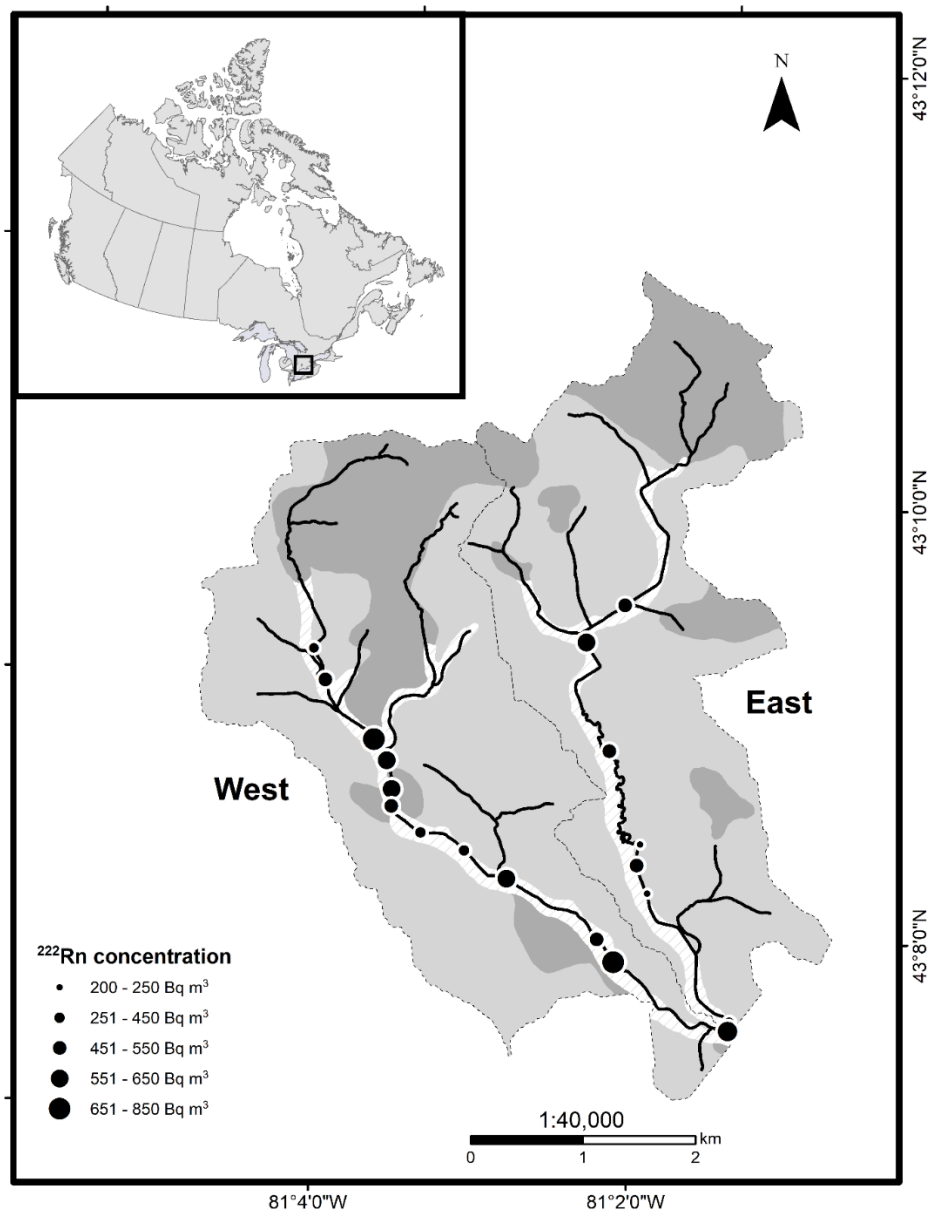

Figure 2.1 Location of headwater catchments (grey dashed lines) of Kintore Creek (solid black lines), located in Southern Ontario, Canada (inset) and 19 study reaches (filled circles) with varying groundwater inputs as indicated by median concentrations of radon-222 (^{222}Rn, Bq m^{-3}). Sub-watersheds exhibit varying permeability of surface sediments (high permeability: dark grey; low-medium permeability: light grey; variable permeability: grey hatched lines.

(Permeability: Ontario Geological Survey 2010; Catchment boundaries/stream network: Forsyth et al. 2016)

Nineteen stream reaches that exhibited a range of groundwater inputs were included in our study. The magnitude of groundwater inputs were estimated based on proportional radon-222 (^{222}Rn, Bq m^{-3}) concentration. ^{222}Rn is produced from the radioactive decay of radium and is commonly used as a tracer for evaluating groundwater inputs to surface waters as it: i) is often naturally present in groundwater at considerably higher concentrations than in the receiving surface waters, ii) is chemically inert, and iii) typically dissipates from surface waters quickly because it is a gas and given its short half-life of 3.82 days (Cook 2013). The distribution of selected reaches extended from near the top of the network to the confluence of the two branches (Fig. 2.1; Appendix A1.). Within each selected reach, sampling locations were established in riffle habitats. Selected reaches exhibited comparable amounts of canopy cover (average = 85 %, range = 21 %) determined during leaf-out seasons using a densiometer (Forestry Suppliers, 2008), thereby controlling for the effect of light availability on algal growth.

2.2.2 Sample Collection & Processing

2.2.2.1 Environmental Characterization

The magnitude of groundwater inputs along the stream network was estimated from stream ^{222}Rn (Bq m^{-3}) was surveyed in autumn of 2018, as well as winter, spring, and summer of 2019. For each survey, ^{222}Rn was measured at 45 sites across the headwaters of Kintore Creek with an average stream distance of 200 m between survey points (study reaches shown

in Supplemental Table 1). Stream water samples were collected in 4 L amber glass bottles and were analyzed for ^{222}Rn within 4 hours using RAD7 electronic radon detectors with the big bottle accessory (Durridge, USA).

Surface water conditions in each of the 19 sampling reaches were characterized by measuring water temperature and water chemistry. Stream water temperature was measured in each reach using temperature loggers (HOBO Pendant, Onset, USA) at 10-minute intervals for the duration of each deployment period. Temperature loggers were fastened to rebar near the streambed. Stream water temperature measurements were used to calculate the mean daily temperature range (°C) and mean daily temperature (°C). Mean daily temperature range was calculated by determining daily maximum and minimum temperatures for each deployment day with the daily ranges then averaged over the incubation period. Mean daily temperature was calculated as the sum of the daily mean temperatures over the deployment period, and was corrected for deployment length by dividing the sum by the number of deployment days of each incubation period (*sensu* Benfield et al. 2017).

Grab water samples were taken at 60 % depth in a well-mixed area of each reach during the four sampling periods for analysis of Dissolved Organic Carbon (DOC), and the dominant bioavailable forms of nitrogen and phosphorus (i.e., nitrate - nitrogen [NO_3^--N]) and Soluble Reactive Phosphorous [SRP], respectively). Nitrate samples were filtered using a 0.45-µm cellulose acetate filter and frozen until analyzed. SRP samples were filtered using the 0.45-µm cellulose acetate filter, kept in the fridge, and analyzed within 24 hrs of filtering. NO_3^--N was analyzed using liquid chromatography (HPLC) (Thermo Scientific Dionex Aquion Ion

Chromatography System with Dionex AS-DV autosampler) and SRP was analyzed on Flow Injection Analysis automated ion analyzer (FIA) (Lachat QuikChem, QC8500 FIA Automated Ion Analyzer) (AWWA 2004) using external standards to calibrate standard curves. The lower detection limits were 0.25 mg L^{-1} for NO_3^- - N and 1 μg L^{-1} for SRP. DOC was analyzed using a Shimadzu TOC-5000A Total Organic Carbon Analyzer using USEPA Organic Carbon, Total (Combustion or Oxidation) Method (US EPA 1974). Additionally, pH and specific conductivity (μS cm^{-1}) were measured in a well-mixed, flowing section of each reach during each sampling period using a handheld YSI probe (YSI, Professional Plus).

2.2.2.2 Biofilms

Biofilms were sampled using standardized artificial substrates (unglazed ceramic tiles; 21.24 cm^2 each) to provide a consistent surface for stream biofilm accumulation (*sensu* Steinman et al. 2007). Three tiles were placed in a tile holder and attached to a brick anchor using cable binders. Tile holders and brick anchors were secured by burying the brick in the streambed and leaving approximately 2 cm above the streambed.

Tile holders were placed in riffle habitats and deployed at the same location in each of the four seasons. Incubation length was adjusted for each season to ensure peak biomass and was 25 or 28 days in autumn (September – October), 33 or 34 days in winter (January – February), 33 or 34 days in spring (May – June), and 26 or 27 days in summer (August). In each season, one of the three tiles was sampled for each of diatom taxonomy, chlorophyll-*a* [chl-*a*], and ash-free dry mass [AFDM]). The entire tile area was scraped using a toothbrush and well-rinsed with deionized water between samples. Diatom taxonomy samples were

preserved with Lugol's iodine (~1 % v/v) and biomass (chl-*a* and AFDM) samples were stored frozen until analysis.

Diatom frustules were first cleaned of organic matter to ensure visible frustules by digesting samples in 5 mL of 100 % (v/v) nitric acid for 15 h. Then, 1 mL of hydrogen peroxide 30 % (v/v) was added and tubes were immersed in a water bath at 60 °C for 1 h. Samples were then centrifuged at 5500 rpm for 10 minutes. Following centrifugation, the acid supernatant was disposed of, and the pellet was retained. Deionized water was then added to rinse the pellet. This process was repeated until supernatant reached a pH above 6. Taxonomy samples were mounted on microscope slides with Naphrax® (refractive index: 1.74; Brunel microscopes Ltd., Wiltshire, UK). Diatom assemblages were enumerated using a Zeiss Axio Imager 2 light microscope equipped with Differential Interference Contrast optical components and a digital camera. A minimum of 400 diatom valves per sample were enumerated at 1000x magnification. Diatoms were identified to species level where possible following Lavoie et al., (2008b) and Bey & Béranger (2014).

Chl-*a* samples were thawed and filtered onto Whatman GF/C filters and placed in 50 mL centrifuge tubes with 10 mL of 90 % ethanol. Next, hot ethanol non-acidification extraction was performed by partially submerging centrifuge tubes in an 80 °C hot water bath for 7 min. Chl-*a* concentration was determined using a Turner Designs Trilogy Fluorometer (Model: 7200e000). The extracted liquid was diluted if maximum detection limits (> 75 µg/mL) were surpassed.

AFDM samples were thawed and filtered through pre-ashed Whatman GF/C filters for determination of organic mass. Filtered samples were then dried at 105 °C for a minimum of 12 h and weighed. Next, samples were ashed in a muffle furnace at 550 °C for 1 h and weighed to determine mass loss on ignition. Samples were then re-wetted, due to high levels of silt/clay, and dried at 105 °C for a minimum of 12 h and weighed to correct for water loss by clay and other minerals.

2.2.2.3 Cellulose Decomposition

Cellulose decomposition was measured using the cotton-strip assay, with preparation, deployment, and retrieval following Tiegs et al. (2013). Fredrix-brand unprimed 12-oz. heavyweight cotton fabric, Style #548 (Fredrix, Lawrenceville, GA, USA) was used to construct 2.5 cm x 8 cm strips, with 3 mm of frayed 'fuzz' along the lengths of the strip. Five cotton strips were then randomly assigned to each sampling reach and deployed in the riffle habitat. Strips were attached to a 1.5 m chain using cable binders. The chain was anchored to the bed using rebar. Incubation times varied among seasons due to changes in expected time to reach approximately 50 % tensile loss. Incubation was 18 days in autumn (September – October), 33 or 34 days for winter (January – February), 15 days in spring (May – June), and15 days in summer (August).

On retrieval, strips were submerged in a tray with 70 % ethanol for 7 minutes to sterilize the strip, stopping microbial activity. After sterilization, strips were carefully brushed to remove excess debris and sediment, then laid flat and covered with aluminum foil. Strips were

placed on ice in a cooler until returning to the lab. In the lab, strips were dried at 40 °C for 24 h, and subsequently analyzed for tensile strength.

Tensile strength of the strips, defined as force required to break the strip, was measured using a tensiometer and motorized test stand (Force Gauge, Model M3-100). Following Tiegs et al. (2013), equal lengths of each end were placed in the tensiometer grips (Mark-10 brand, Model #MG100) and were then pulled at a constant rate of 2 cm/min until the strip ripped, indicating peak tension. To determine the overall percent loss of tensile strength, the measured tensile strength of test strips was compared to mean tensile strength of reference strips. Fifty reference strips underwent saturation in distilled water, cleaning in 70 % ethanol for 7 minutes, and were dried at 40 °C for 24 h, and their tensile strength was measured. The tensile strength was measured for each sample strip, and percent (%) tensile loss per day was calculated using Eq.1 (*sensu* Tiegs et al. 2013).

$$\%\ \text{tensile loss per day} = \frac{\left(\frac{\text{Tensile Strength}^{REF} - \text{Tensile Strength}^{SAMP}}{\text{Tensile Strength}^{REF}}\right) \text{x } 100}{\text{Incubation time}}$$

(Eq. 1)

Prior to analyses, % tensile loss per day of the five cotton strips in each reach were averaged to establish a representative % tensile loss rate for each reach.

2.2.3 Data Analysis

In R (version 4.0.3), we employed Pearson product-moment correlations using *cor.test* (stats package, R Core Team, 2020) to determine if there were associations between ^{222}Rn concentration, our proxy for groundwater input, and environmental variables (SRP, NO_3^- - N,

DOC, specific conductivity, pH, mean daily temperature range, and mean daily temperature) in each season ($\alpha = 0.05$). Environmental variables that failed the Shapiro-Wilk test of normality using *shaprio.test* (stats package, R Core Team, 2020) were log-transformed prior to the correlation analysis.

Partial least squares (PLS) regression was used to evaluate the association of temperature and water chemistry variables with spatio-temporal patterns of biofilm biomass (chl-*a* accumulation and biofilm growth rate) and cellulose decomposition (% tensile loss per day). We performed a PLS for all seasons to determine effects of seasonality. We also completed a PLS on each individual season to identify with-season associations of environmental predictors to biological response. PLS regression is a multivariate analysis used to identify associations between predictor (environment) and response (ecological) variables (Wold et al. 2001; Carrascal et al. 2009). PLS regression is particularly useful when predictors are highly correlated, and there are many predictors relative to observations (Carrascal et al. 2009). Environmental predictor variables (X: SRP, NO_3^- - N, DOC, specific conductivity, pH, ^{222}Rn, mean daily temperature range, and mean daily temperature) are used to create a set of components (PLS loadings) that explain the most variance in biofilm biomass and cellulose decomposition (Y), based on simultaneous decomposition of X and Y matrices (Eriksson et al. 2013). All environmental predictor variables were min-max normalized prior to analysis. Model performance was assessed using the cross-validated goodness of prediction (Q^2), where goodness of prediction ($Q^2 > 0.097$) is the difference between predicted and observed values. Goodness of prediction was estimated using a tenfold cross-validation method with 999

iterations. The sum of explanatory capacity (R^2Y) for each component represents the total explanatory capacity of the PLS model. Components that explained 10 % or more of the variation of response (Y) variables were retained. The influence of each predictor (X) variable was evaluated using variable importance projection (VIP) scores. Predictors with a VIP greater than one were identified as important for explaining response (Y) variables. For important predictor variables, the direction of the association to and response variables was evaluated by assessing the loadings on the biplot. PLS analyses were completed in R (version 4.0.3) using *plsreg2* (plsdepot package, Sanchez 2016).

Spatial and temporal patterns in diatom assemblage composition were assessed by performing Non-Metric Multidimensional Scaling (nMDS). An nMDS was performed using diatom assemblages from all seasons to assess whether seasons had different assemblage composition. If seasonal diatom assemblage composition differed, then an nMDS was performed on diatom assemblages for each individual season. The nMDS was performed on Hellinger transformed relative abundances using Bray-Curtis distance. Only taxa with a relative abundance of ≥ 2 % in at least one sample in a given season were included (Legendre and Gallagher 2001). nMDS ordination was completed using two dimensions with a maximum of 1000 iterations or until two convergent solutions were found. Analyses were completed using *metaMDS* function (vegan package, Oksanen et al., 2020) in R (version 4.0.3).

A one factor permutational analysis of variance (PERMANOVA) was performed to compare variation in diatom assemblages in response to the fixed factor of season (levels: autumn, winter, spring, summer). If seasonal diatom assemblages were determined to be

significantly different ($p \leq 0.05$), then we evaluated the taxa that most contributed to dissimilarity among seasons using similarity percentages (SIMPER) analysis on Hellinger transformed relative abundance. SIMPER calculated the contribution (percentage) of dissimilarity between two groups that each taxa contributes (Clarke 1993). Taxa contributing greater than 5 % of the average dissimilarity between seasons were retained in results. We also assessed cumulative change in assemblage by assessing average dissimilarity of non-adjacent seasons. Analyses were completed with PRIMER software package (version 7.0 with PERMANOVA+, Primer-E Ltd., Plymouth, UK; Clarke & Gorley, 2015).

A BIOENV (matching of biotic and environmental patterns; Clarke and Warwick 1994) was used to assess potential within season associations between diatom assemblages and measured environmental variables (SRP, NO_3^--N, DOC, specific conductivity, pH, ^{222}Rn, mean daily temperature range, and mean daily temperature). BIOENV calculates the extent of the association between two similarity matrices (biotic and environment) based on Spearman rank correlation, where pairs of samples that have a similar environment would produce a similar diatom assemblage (Clarke and Warwick 1994). For each season, the biotic matrices were created using Hellinger transformed relative abundance was used to calculate Bray-Curtis distance between samples. Environmental variables were min-max normalized, then Euclidean distance was used to generate environmental similarity matrices. Analyses were completed with *bioenv* function and significance was tested using *mantel* function with 999 permutations using environmental distances extracted from *bioenv* results (vegan package, Oksanen et al. 2020).

2.3 Results

2.3.1 Chl-*a* accumulation, biofilm growth rate, and cellulose decomposition

Seasonal and spatial variation was observed among measures of chl-*a* accumulation, biofilm growth rate, and cellulose decomposition (Fig. 2.2). Chl-*a* accumulation was greatest in summer followed by spring and autumn, and slowest in winter (Fig. 2.2a). In contrast to chl-*a* accumulation, biofilm growth rate was greatest in autumn, then summer and spring, and remained slowest in winter (Fig. 2.2b). Cellulose decomposition (% tensile loss day^{-1}) was slowest in winter, faster in summer and autumn, and fastest in spring (Fig. 2.2c).

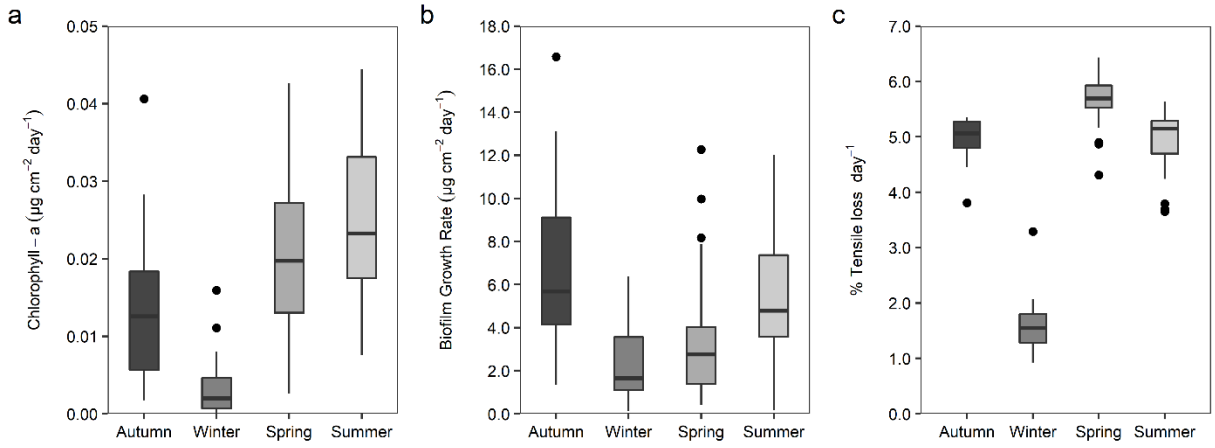

Figure 2.2. Boxplots of (a) chl-*a* accumulation (µg cm^{-2} day^{-1}), (b) biofilm growth rate (µg cm^{-2} day^{-1}), and (c) cellulose decomposition (% tensile loss day^{-1}) for 19 sampled reaches in Kintore Creek in autumn, winter, spring and summer seasons. Boxplots show the median (dark bar), interquartile range (box), upper and lower quartiles (vertical lines), and outliers (black circles)

2.3.2 Groundwater related environmental parameters

Seasonal and spatial differences in ^{222}Rn, mean daily temperature range (°C), and mean daily temperature were observed in the Kintore Creek headwaters (Fig. 3). Among study

reaches, ^{222}Rn concentrations were generally greater in areas where the surrounding surficial sediment permeability was higher (Fig. 2.1). Stream ^{222}Rn concentrations among study reaches varied among seasons and was generally highest in the winter followed by spring, and lowest in autumn and summer (Fig. 2.3a).

Mean daily temperature (°C) was highest in summer, then autumn and spring, and lowest in winter (Fig. 2.3b). Mean daily temperature (°C) and ^{222}Rn were negatively correlated (r = -0.73, $p < 0.001$) in spring, but were not associated ($p > 0.05$) for all other seasons (Supplementary Fig. 1). Mean daily temperature range (°C) was generally largest in the spring and summer and smallest in autumn and winter (Fig. 2.3c). Mean daily temperature range and ^{222}Rn were positively correlated in spring (r = 0.54, $p = 0.016$), but were not significant ($p > 0.05$) for all other seasons (Appendix A2.).

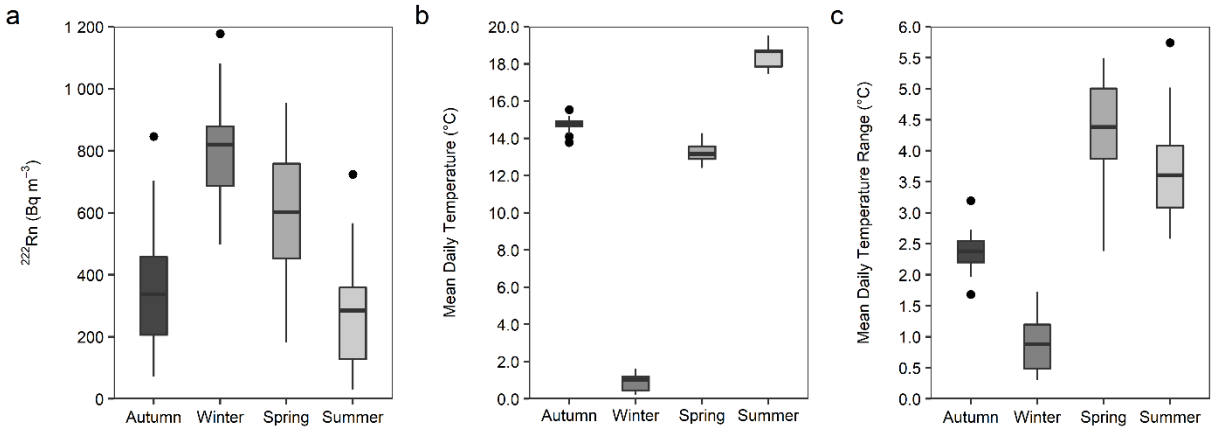

Figure 2.3 Boxplots of (a) ^{222}Rn (Bq m^{-3}), (b) mean daily temperature (°C), and (c) mean daily temperature range (°C) for 19 sampled reaches in Kintore Creek in autumn, winter, spring and summer seasons. Boxplots show the median (dark bar), interquartile range, upper and lower quartiles (vertical lines), and outliers (black circles)

Measures of stream water chemistry showed variability among seasons (Fig. 2.4). SRP (mg P L^{-1}) concentration was highest in autumn followed by summer then winter, and lowest in spring (Fig. 2.4a). SRP and ^{222}Rn were negatively associated in summer (r = -0.54, p = 0.02), but were not associated (p > 0.05) in any other season (Appendix A2.). NO_3^- - N concentrations were lowest in autumn, and characterized by high variability in summer, winter, and spring, though spring tended to have the highest NO_3^- - N (Fig. 2.4b). NO_3^- - N and ^{222}Rn were negatively associated in autumn (r = -0.51, p = 0.026) and positively associated in summer (r = 0.53, p = 0.020), but were not associated (p > 0.05) in winter or spring (Appendix A2.). DOC was highest in spring, with autumn, winter, and summer showing similar ranges in DOC (Fig. 2.4c). Correlations of DOC and ^{222}Rn were not significant (p > 0.05) for any season. Specific conductivity (µS cm^{-1}) was lowest in spring and summer, and highest in autumn and winter (Fig. 2.4d). Correlations between specific conductivity and ^{222}Rn were not significant (p > 0.05) for any season. pH was generally highest in spring followed by summer and autumn, and lowest in winter (Fig. 2.4e). pH and ^{222}Rn were negatively correlated summer (r = -0.46, p = 0.048), but were not correlated (p > 0.05) for any other season (Appendix A2.).

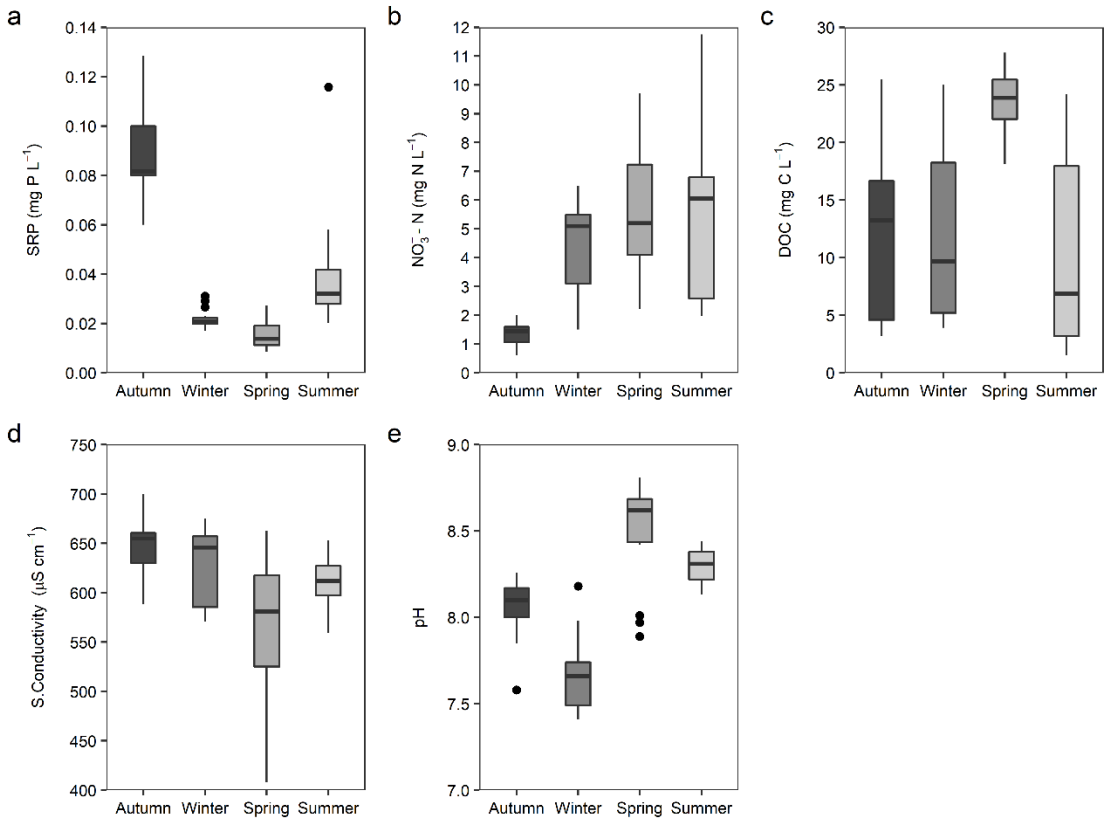

Figure 2.4 Boxplots of water quality parameters (a) SRP (mg P L^{-1}), (b) NO_3^- - N (mg N L^{-1}), (c) DOC (mg C L^{-1}), (d) specific conductivity (µS cm^{-1}), and (e) pH for 19 sampled reaches in Kintore Creek in autumn, winter, spring and summer seasons. Boxplots show the median (dark bar), interquartile range, upper and lower quartiles (vertical lines), and outliers (black circles)

2.3.3 Environmental drivers of stream biofilm biomass & cellulose decomposition

PLS regression of chl-*a*, AFDM, and % tensile loss for all seasons produced an interpretable model ($Q^2 = 0.58$, $R^2X = 0.58$, $R^2Y = 0.39$), comprised of two components that explained 58% of variance in environmental variables and 39% of the variance in biological variables (Fig. 2.5). The first component organized sites based on seasonal variation in ^{222}Rn, mean daily temperature and mean daily temperature range. ^{222}Rn was negatively associated

with chl-*a* accumulation, biofilm growth rate, and % tensile loss (VIP >1.0). Mean daily temperature and mean daily temperature range and pH were positively associated with chl-*a* accumulation, biofilm growth rate, and % tensile loss (VIP >1.0). pH was also positively associated with variance in the biological variables (VIP >1.0). Winter samples were clustered apart from all other seasons, and samples in autumn, spring, and summer showed a high degree of overlap.

On the second component, variance in the biological variables was also influenced by mean daily temperature, mean daily temperature range, pH, as well as SRP (VIP > 1.0). Sites on the second component were organized by SRP concentration, with autumn generally having the highest SRP, and spring and summer showing similar SRP concentrations based on the clustering of sites. Mean daily temperature was positively associated with chl-*a* accumulation, biofilm growth rate, and % tensile loss. Conversely, mean daily temperature range and pH were negatively associated with chl-*a* accumulation, biofilm growth rate, and % tensile loss.

Based on the observed differentiation of biological variables by seasonal variation in temperature, separate PLS regressions were run on samples from each of the four seasons. However, environmental variables had no association with biological variables for any of the four individual seasons ($Q^2 < 0.097$).

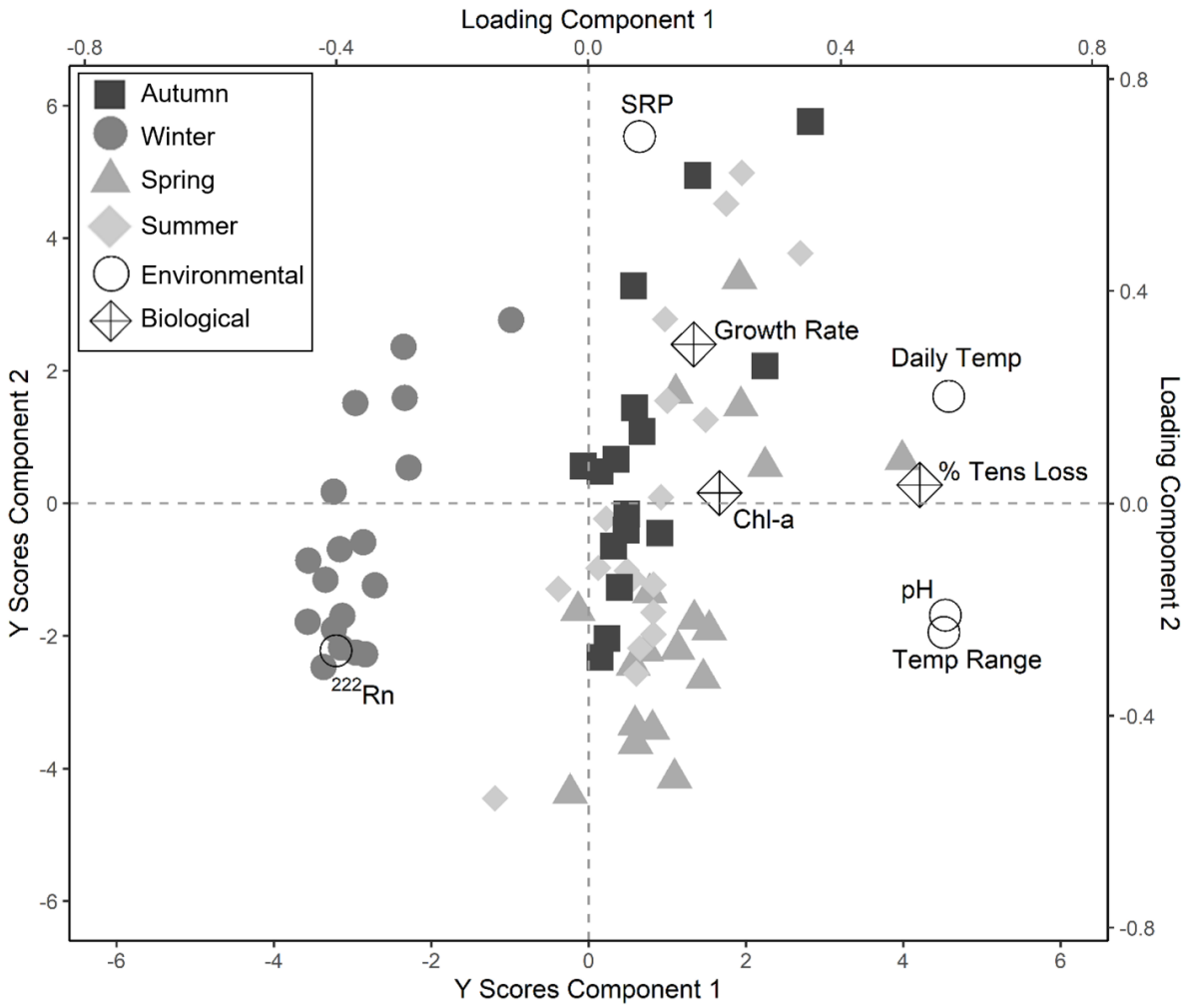

Figure 2.5 Scores and loadings biplot for PLS regression of chl-*a* accumulation (Chl-a), biofilm growth rate (Growth Rate), and % tensile loss (% Tens Loss) (hollow diamond plus) associated with environmental descriptor variables (hollow circles). Site scores shown on primary axes and loadings on secondary axes. Descriptor locations show association between predictor environmental variables and the biological response variables by their proximity to the origin

2.3.4 Diatom assemblage patterns and drivers

Ninety-nine diatom taxa (most of them identified to the species level) were enumerated in the network across all sites and all seasons. Taxa richness varied among seasons, with the total taxonomic richness in autumn at 76 taxa compared to 75 taxa in winter, 56 taxa in spring, and 37 taxa in summer.

Diatom species contributing 5 % or more to total relative abundance of all sites within any season were *Achnanthidium eutrophilum* (Lange-Bertalot) (ADEU), *Amphora pediculus* (Kützing) (APED), *Cocconeis placentula* (Ehrenberg sensu Hofmann) (CPLA), *Eunotia* spp. (EUNO), *Navicula lanceolata* (C. Agardh) (NLAN), *Planothidium frequentissimum* (Lange-Bertalot) (PLFR), and *Tabellaria flocculosa* (Roth) (TFLO) (Fig. 2.6). In autumn 4 taxa contributed to nearly 80 % of total relative abundance. These were *A. pediculus* (30 %), *C. placentula* (23 %) *A. eutrophilum* (14 %) and *P. frequentissimum* (12 %). In contrast, taxa contributing nearly half of the total relative abundance in winter were *N. lanceolata* (33 %), *A. eutrophilum* (23 %), *T. flocculosa* (7 %) and *Eunotia* spp. (6 %). In spring, *A. eutrophilum* contributed nearly half (40 %) of the total relative abundance and four other taxa cumulatively contributed 39 % (*C. placentula* (14 %), *A. pediculus* (10 %), *P. frequentissimum* (10 %), and *C. pediculus* (5 %)). Summer had similar species composition to spring but differed in the relative abundance of taxa. *C. placentula* was the most abundant taxa (53 %), with 3 taxa cumulatively contributing an additional 35 % to total relative abundance (*A. pediculus* (19 %), *P. frequentissimum* (10 %), and *A. eutrophilum* (6 %)).

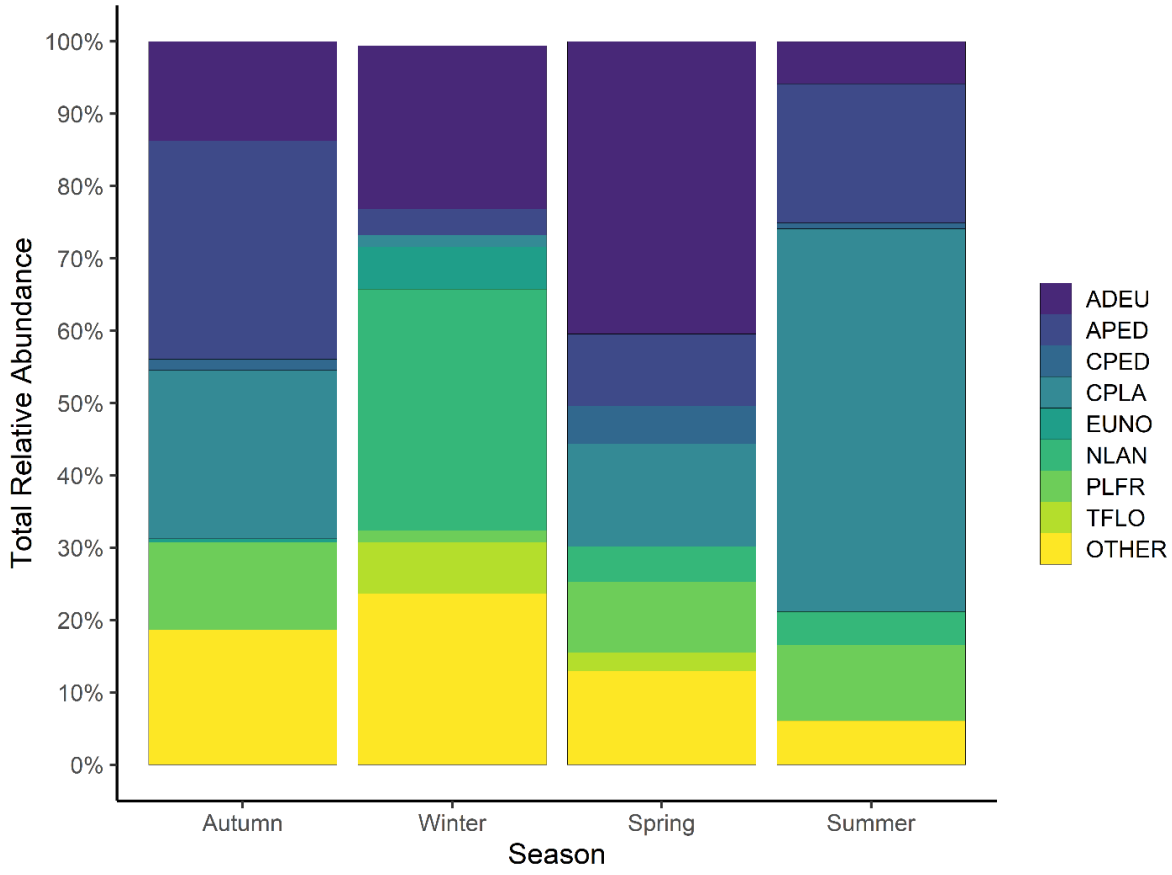

Figure 2.6 Relative abundance of diatom taxa contributing > 5% to total abundance from any season. Key taxa are: *Achnanthidium eutrophilum* (Lange-Bertalot) (ADEU), *Amphora pediculus* (Kützing) (APED), *Cocconeis pediculus* (Ehrenberg) (CPED), *Cocconeis placentula* (Ehrenberg sensu Hofmann) (CPLA), *Eunotia* spp. (EUNO), *Navicula lanceolata* (C. Agardh) (NLAN), *Planothidium frequentissimum* (Lange-Bertalot) (PLFR), *Tabellaria flocculosa* (Roth) (TFLO), and all other taxa (OTHER)

Ordination of the diatom assemblages indicated that winter assemblages were strongly dissimilar from all other seasons, with assemblages being more similar in spring, summer, and autumn (Fig. 2.7.). Five taxa, *A. eutrophilum*, *A. pediculus*, *C. placentula*, *N. lanceolata*, and *P. frequentissimum* were shown to be disproportionately influencing dissimilarity among

seasons based on SIMPER analyses. Average dissimilarity (Avg.Dis) between autumn and winter was 74.2 %, with five taxa contributing one-third of average dissimilarity, *A. eutrophilum* (Avg.Dis = 7.2 %), *A. pediculus* (Avg.Dis = 8.6 %), *C. placentula* (Avg.Dis = 8.2 %), *N. lanceolata* (Avg.Dis = 10.7 %), and *P. frequentissimum* (Avg.Dis = 5.0 %). A third of total average dissimilarity (67.5 %) between winter and spring was attributed to four taxa, *A. eutrophilum* (Avg.Dis = 8.7 %), *C. placentula* (Avg.Dis = 5.7 %), *N. lanceolata* (Avg.Dis = 11.0 %), and *P. frequentissimum* (Avg.Dis = 5.1 %). Spring showed an average dissimilarity of 61.0 % with summer with approximately a third of overall average dissimilarity contributed by *A. eutrophilum* (Avg.Dis = 16.8 %) and *C. placentula* (Avg.Dis = 16.3 %) and another one-fifth of total average dissimilarity was attributed to three taxa, *A. pediculus* (Avg.Dis = 8.4 %), *N. lanceolata* (Avg.Dis = 5.9 %), and *P. frequentissimum* (Avg.Dis = 7.9 %).

Assessment of non-adjacent seasons revealed that autumn had an average dissimilarity of 57.9% with spring with four taxa contributing one-thirds of overall average dissimilarity, *A. eutrophilum* (Avg.Dis = 12.5 %), *A. pediculus* (Avg.Dis = 10.2 %), *C. placentula* (Avg.Dis = 8.9 %), and *P. frequentissimum* (Avg.Dis = 5.8 %). Autumn showed an average dissimilarity of 56.3 % with summer of which five taxa, *A. eutrophilum* (Avg.Dis = 8.7 %), *A. pediculus* (Avg.Dis = 11.2 %), *C. placentula* (Avg.Dis = 12.4 %), *N. lanceolata* (Avg.Dis = 5.9 %), and *P. frequentissimum* (Avg.Dis = 8.4 %), accounted for nearly half of the overall average dissimilarity. Average dissimilarity was greatest between winter and summer (75 %), with approximately 40 % of overall average dissimilarity attributed to four taxa: *A. eutrophilum*

(Avg.Dis = 8.7 %), *A. pediculus* (Avg.Dis = 6.5 %), *C. placentula* (Avg.Dis = 15.0 %), and *N. lanceolata* (Avg.Dis = 10.0 %).

A one-factor PERMANOVA showed that diatom assemblages were significantly different among seasons (pseudo-$F_{(371)}$ =13.19, p = 0.001). A post-hoc pairwise comparison revealed that assemblages in all adjacent and non-adjacent seasonal pairings were significantly different (p = 0.001). Due to seasonal differences among diatom assemblages, further analyses of diatom assemblages were conducted within each season.

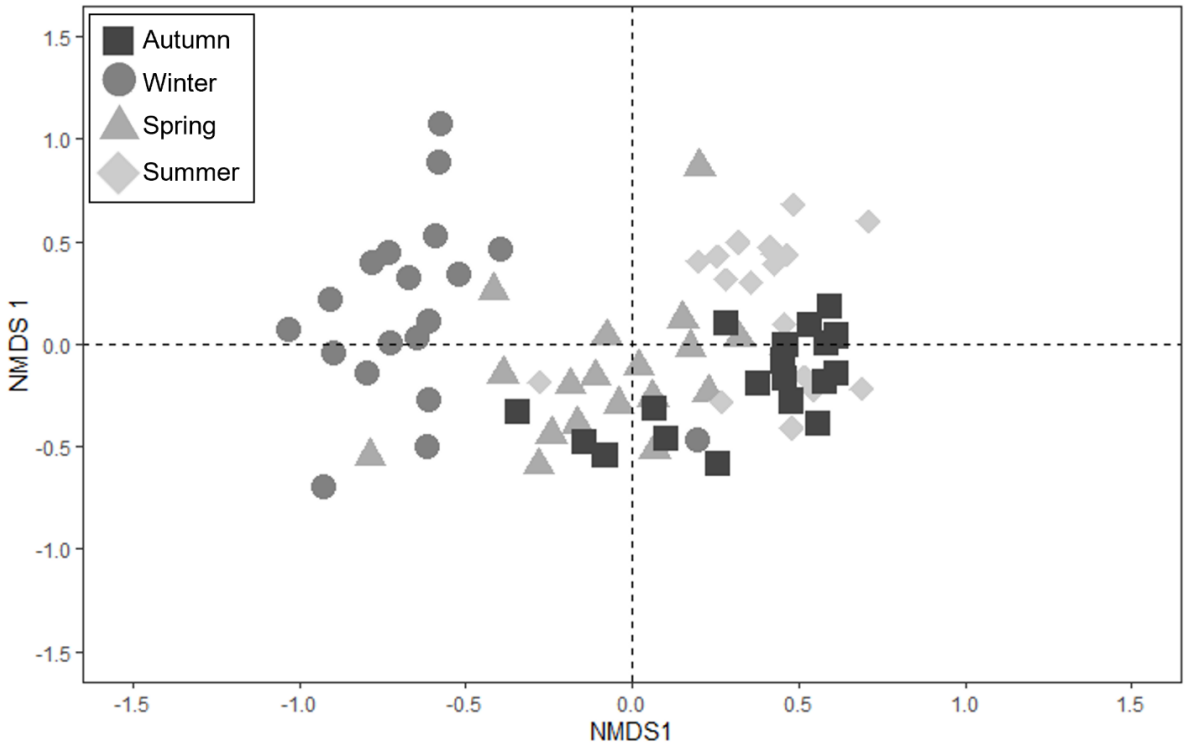

Figure 2.7 nMDS using Bray-Curtis dissimilarity index displaying separation of diatom assemblage relative abundance at 19 reaches of Kintore Creek based on season (stress = 0.19)

In autumn, diatom assemblages tended to cluster together regardless of ^{222}Rn concentration (Fig. 2.8a). SIMPER analyses showed over half of the average dissimilarity

(53.5 %) among autumn assemblage were contributed by three taxa, *A. pediculus* (Avg.Dis = 21.5 %), *C. placentula* (Avg.Dis = 22.8 %), and *P. frequentissimum* (Avg.Dis = 13.6 %). BIOENV analysis revealed that increasing NO_3^--N, pH, ^{222}Rn, and mean daily temperature range were associated (r = 0.40, p = 0.002) with dissimilarities among autumn assemblages.

In contrast to autumn, diatom assemblages in winter were largely scattered in both axes with no pattern among levels of ^{222}Rn (Fig. 2.8b). One-third of total average dissimilarity (42.1 %) observed among winter assemblages was driven by two taxa, *A. eutrophilum* (Avg.Dis = 16.8 %) and *N. lanceolata* (Avg.Dis = 21.3 %). Greater dissimilarity of winter assemblages was associated with increasing NO_3^- - N (r = 0.44, p = 0.001).

Spring showed stronger clustering of diatom assemblages than winter, though there were no trends associated with ^{222}Rn concentration (Fig. 2.7c). Four taxa contributed three-quarters of the average dissimilarity (50.0 %) in spring. With *A. eutrophilum* (Avg.Dis = 35.2 %) contributing at least 3-times as much to dissimilarity as *A. pediculus* (Avg.Dis = 12.5 %), *C. placentula* (Avg.Dis = 11.0 %) or *P. frequentissimum* (Avg.Dis = 12.9 %). BIOENV analysis showed that increasing NO_3^- - N, specific conductivity, and mean daily temperature range were associated with greater dissimilarity in autumn diatom assemblages (r = 0.25, p = 0.044).

For summer diatom assemblages, two-thirds of sites were clustered together, whereas the other third was clustered together, though this clustering was not associated with ^{222}Rn concentration (Fig. 2.7d). Nearly half of average dissimilarity (54.2 %) was attributed to *C. placentula* (Avg.Dis = 43.1 %), with an additional 20 % of dissimilarity contributed by *A.*

pediculus. However, this dissimilarity was not associated with any of the measured environmental variables ($p > 0.05$).

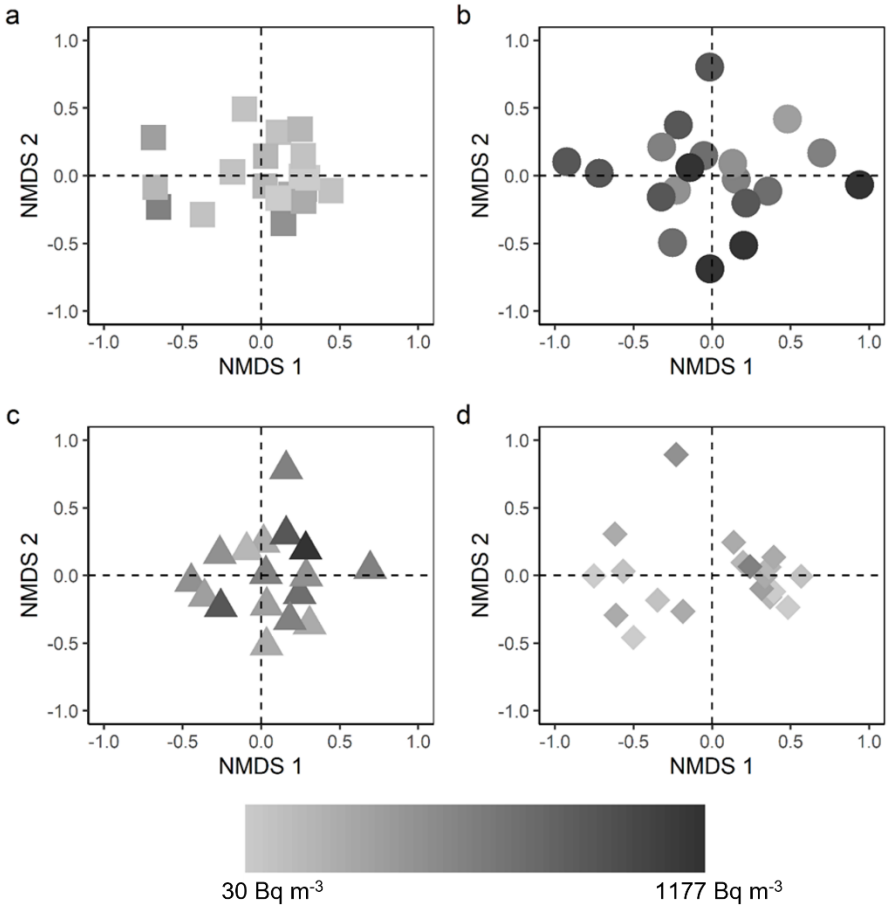

Figure 2.8 nMDS using Bray-Curtis dissimilarity index displaying separation of diatom assemblage relative abundance at 19 reaches of Kintore Creek in each season (a) autumn (stress = 0.16), (b) winter (stress = 0.14), (c) spring (stress = 0.13), and (d) summer (stress = 0.094) relative to lowest to highest ^{222}Rn concentration

2.4 Discussion

2.4.1 Groundwater influence on stream biofilms

Our study found no evidence of associations between spatio-temporal variation in groundwater inputs and stream biofilm communities, nor between groundwater inputs and cellulose decomposition in the assessed headwater stream network. The findings of our study are in contrast to several past studies that have shown that groundwater contributes to ecological heterogeneity in streams through moderated water temperature (Tang et al. 2019), maintenance of stream flow (Sear et al. 1999), as well as delivery of nutrients and other chemical constituents to surface waters (Valett et al. 1994; Wyatt et al. 2008; Mejia et al. 2016). However, unlike past studies we did not observe consistent or strong associations between our indicator of groundwater input, ^{222}Rn, and spatio-temporal variation in key environmental drivers such as stream water nutrients (nitrogen [N], phosphorus [P]), water chemistry, and temperature. Thus, we hypothesize that groundwater inputs were not associated with spatial heterogeneity in stream biofilms because variation in groundwater inputs was insufficient to generate substantive variability in the key environmental conditions among the sampled reaches.

The relative importance of groundwater inputs in modifying nutrient concentrations in the stream reaches and thereby inducing spatial heterogeneity in stream biofilms in the agricultural headwaters of Kintore Creek may have been limited by consistently high surface water nutrient availability throughout the network. Indeed, with the exception of SRP in spring, median concentrations of SRP and nitrate were up to 3-times greater and between 5- and 20-

times greater, respectively, than nutrient saturation thresholds previously identified for benthic algal growth in southern Ontario streams (i.e., 0.026 mg P L^{-1} for total P, and 1.06 mg N L^{-1} for total N, Chambers et al. 2012). Similarly, surface water SRP and NO_3^- - N concentrations exceeded estimated thresholds for heterotrophic microbial activity in all seasons as previous work have estimated thresholds (0.018 – 0.053 mg P L^{-1} for SRP and 0.16 – 3.03 mg N L^{-1} for NO_3^- - N; Rosemond et al. 2002; Ferreira et al. 2006; Gulis et al. 2006) for surface water nutrient limitation of heterotrophic microbial activity in freshwater ecosystems. Consequently, any additional nutrients added to the stream via groundwater inputs likely had limited effects on biofilm activity and accumulation. Alternatively, some reaches may have received different amounts of groundwater input among seasons. Indeed, varying groundwater input may explain why correlations of NO_3^- - N and ^{222}Rn were in opposing directions for summer (positive) and autumn (negative). Preliminary analysis of shallow groundwater in the streambed along Kintore Creek does indicate variability in nutrient groundwater concentrations between reaches (C.E. Robinson, unpublished data). Additional work is thus needed to determine if groundwater inputs are sufficient to generate localized differences in biofilms given the enriched surface water nutrient concentrations.

We found no measurable within season effects of temperature on among site variation in biofilm metrics. Across all reaches and seasons, temperature measures exhibited a limited thermal gradient (less than 2 °C) and were not associated with spatial variation in groundwater inputs (i.e., stream ^{222}Rn concentrations). Some past studies have suggested that a warming of at least 3 °C is required to consistently increase chl-*a* in warmer seasons (Godwin and Carrick

2008; Ylla et al. 2014; Delgado et al. 2017). Likewise, previous work at global and reach scales suggest that significant differences in organic matter breakdown are generally observed where surface water temperatures differ from 4 – 5 °C (Griffiths and Tiegs 2016; Follstad Shah et al. 2017; Tiegs et al. 2019). Based on these limits, it is likely that groundwater mediated differences in surface water temperature among sites in our study stream were too small to elicit spatial heterogeneity in biofilms.

Our observations of limited temperature variation are in contrast with past studies that have assessed the impacts of variable groundwater inputs among reaches (e.g., Griffiths and Tiegs 2016; Tang et al. 2019). For example, Tang et al., (2019) found that groundwater input in a reach moderated thermal regimes and was associated with greater benthic algal biomass, whereas in reaches without groundwater, effects of seasonality were more evident. Likewise, Griffiths and Tiegs (2016) found smaller diel temperature ranges at upstream reaches that were strongly groundwater gaining. However, the moderated temperature effect dissipated at downstream reaches where larger diel temperature ranges were associated with slower tensile loss (Griffiths and Tiegs 2016). Our results thus suggest that prevailing surface water conditions more strongly influenced stream water temperature in the headwater network of Kintore Creek than did groundwater inputs limiting effects groundwater induced environmental heterogeneity at the reach scale.

Our findings indicate that the amount of groundwater input occurring along a stream reach may have less effect on benthic algal growth or organic matter breakdown in nutrient-rich, agricultural stream networks than in previously assessed oligotrophic streams (e.g., Pepin

& Hauer, 2002; Wyatt et al., 2008). The limited variability of measured environmental conditions we observed among reaches within a season may have been due to thermal or chemical effects of groundwater input being dissipated by cumulative upstream contributions of surface waters. Indeed, in nutrient-poor streams, the influence of spatially variable groundwater inputs on environmental conditions within the stream, has typically been detected at a smaller scales (e.g., patch) and extrapolated to the reach (e.g. Wyatt et al., 2008; Mejia et al., 2016). However, our study aimed to assess how groundwater inputs influenced ecological variation among reaches within a stream network, and it appears that at this scale, dilution of patch scale thermal effects and high surface water nutrient availability may overwhelm any biologically meaningful differences. Therefore, the role of groundwater influence as a contributor to environmental heterogeneity may be best identified where environmental conditions are measured at a more localized patch scale.

Although we observed limited evidence that groundwater was affecting ecological conditions in the headwater network of Kintore Creek it does not appear that it was because of limited groundwater inputs to the stream. Indeed, the range of ^{222}Rn concentrations we measured in the Kintore Creek network (30 – 1177 Bq m^{-3}) exceeds that of past studies that have equated observed radon values with significant inputs of groundwater using isotopes and mass balance models. For example, Martinez et al. (2015), equated a ^{222}Rn range of 200 – 715 Bq m^{-3} with a groundwater contribution of 20 – 70 % to stream flow in headwater streams. Similarly, Unland et al. (2013) observed ^{222}Rn concentrations varying from 52 to 604 Bq m^{-3} for a river where groundwater was estimated to contribute up to 21% of river discharge under

baseflow conditions. Moreover, Burrows et al. (2020) found that chl-*a* concentrations were associated with variations in ^{222}Rn concentrations similar to what we observed across the Kintore Creek headwater network. However, care needs to be taken in inferring the magnitude of groundwater discharge to the stream based on the stream ^{222}Rn concentrations alone because; 1) ^{222}Rn concentrations in groundwater vary with mineralogy near the stream, and; 2) ^{222}Rn losses from the stream via gas evasion and decay relative to transport down the stream vary with stream properties (e.g., stream gradient, width, depth). ^{222}Rn evasion to the atmosphere and its decay relative to its transport will also vary with stream properties (e.g., stream gradient). Indeed, studies conducted in groundwater receiving streams have reported a wide range of ^{222}Rn values (e.g., 70 to 150 Bq m^{-3} in Gleeson & Richter 2018, and up to 7800 Bq m^{-3} in Lefebvre et al. 2015). Overall, the measured ^{222}Rn concentrations indicate that Kintore Creek had significant variation in groundwater inputs throughout its headwater network.

2.4.2 Seasonality

^{222}Rn concentrations were found to vary seasonally with higher concentrations observed in winter and spring compared to summer and autumn. Seasonal ^{222}Rn have also been observed in other temperate environment streams (e.g., Mullinger et al. 2007) and have been attributed to changes in the height of the local water table. A higher groundwater table facilitating tile drainage flow and higher groundwater discharge to the stream may explain the larger winter and spring ^{222}Rn concentrations in Kintore Creek because although sampling was conducted under baseflow conditions in all seasons, stream flows were higher in spring and

winter. Indeed, the higher measured ^{222}Rn concentrations during winter and spring likely resulted from the activation of these additional subsurface flow paths combined with the faster transport of ^{222}Rn down the stream (higher flows) compared to the rates of ^{222}Rn decay and gas evasion.

However, the strong seasonal differences we observed in Kintore Creek biofilm communities did not appear to be the result of changes in groundwater inputs but rather network-wide control of stream temperature by seasonally associated variations in air temperature. Indeed, the particularly large seasonal shift observed in biofilm biomass between winter and the warmer seasons appeared to be due to cold winter surface water temperatures that likely limited microbial activity. Our findings are concordant with past assessments of biofilm communities that indicated reduced primary production and microbial activity in winter (Francoeur et al. 1999; Brown et al. 2004). Moreover, seasonality also appears to have been the primary determinant of chl-*a* accumulation in Kintore Creek during warmer seasons as we found that greater chl-*a* was associated with increasing surface water temperatures in warmer seasons, with peak chl-*a* occurring in summer. Seasonal shifts in autotrophic taxonomic composition may have contributed to greater amount of chl-*a* accumulation during warmer seasons in Kintore Creek as the algal component of the biofilm has been shown to transition from diatom dominated assemblages in cooler seasons to more chl-*a* rich cyanobacteria and green algae dominated assemblages in warmer seasons (Biggs 1996; Piggott et al. 2015).

Our assessment of diatom assemblages across four temperate seasons in an agricultural stream network showed that composition varied among the seasons due to changes in relative abundance of a small number of dominant taxa. The seasonal shifts in dominant taxa appeared to reflect the suitability of autecological attributes for seasonal environmental conditions. Our finding that seasonal shifts in diatom composition was limited to a small number of dominant taxa is consistent with other multi-season assessments of diatom assemblages (Tang et al. 2016; Flinders et al. 2019; Snell et al. 2019). For example, winter diatom assemblages were dominated by *N. lanceolata*, a high profile and motile taxon known to be common in temperate winter assemblages due to its wide-ranging thermal tolerance and ability to move through the biofilm matrix (Passy 2007; Hofmann et al. 2011; Shore et al. 2017; Snell et al. 2019). Moreover, the high profile character of *N. lanceolata* may reflect resource (e.g light and/or nutrients) scarcity or decreased grazing pressure (Passy 2007; Stenger-Kovács et al. 2013; Lange et al. 2016) often associated with winter conditions. In contrast, *A. eutrophilum*, a pioneer species that is typically the first to colonize substrates (Ponader and Potapova 2007) and can maintain its position due to resistance to dynamic flow because of its low profile attachment (Rimet and Bouchez 2012; Ockenden et al. 2016), was dominant in spring, likely reflecting dynamic stream flow conditions typical in spring in temperate environments. In summer and autumn, *C. placentula* and *A. pediculus* were co-dominant. Both taxa are epiphytic, with *C. placentula* generally preferring warmer surface waters (Jahn et al. 2009), and *A. pediculus* typically observed in high surface water nutrient conditions (Rimet and Bouchez 2012). The co-dominance of *C. placentula* and *A. pediculus* suggests that the simultaneous seasonal increase in surface water temperature and likely increase of filamentous

green algae in the biofilm matrix allowed for the proliferation of *C. placentula* and *A. pediculus* in summer and autumn.

We found faster cellulose decomposition in warmer seasons compared to winter. Reduced breakdown in association with colder temperatures is consistent with past studies (e.g. Swan and Palmer 2004; Ferreira and Canhoto 2013; Griffiths and Tiegs 2016). Indeed, our findings are comparable to those of Poisson and Yates (2022) who found that cellulose breakdown was 0.57 to 1.15 % per day when winter stream temperatures were consistently below 5 °C. However, unlike past studies, we observed that spring had the fastest cellulose decomposition. Indeed, because summer had the greatest surface water temperatures, summer would be expected to have the fastest breakdown rates due to enhanced microbial activity (Chauvet and Suberkropp 1998; Griffiths and Tiegs 2016). A possible explanation for increased breakdown in spring is that our spring sampling occurred prior to leaf-out. As such, greater light availablity may have accelerated decomposition through increased algal priming of the cotton strips (Howard-Parker et al. 2020). Additionally, the increased stream flows observed in spring may have led to greater physical abrasion, further increasing cellulose breakdown. Overall, our findings provide additional evidence of the role of seasonality in driving temporal differences in cellulose breakdown in nutrient-rich, agricultral streams in temperature ecosystems.

2.5 Conclusions

Our assessment of spatio-temporal heterogeneity in stream biofilms in an agricultural, headwater stream network with varying groundwater inputs showed that seasonal variation

was the overriding environmental control shaping biofilm communities and cellulose decomposition. Indeed, our findings provide evidence of seasonal shifts in streams in temperate ecosystems. These seasonal shifts in ecological response emphasize the importance of including multi-season sampling in ecological monitoring frameworks to foster a stronger understanding of ecological function across discrete and recurring seasonal conditions. Yet, despite apparent variation in groundwater inputs among reaches within a season, our findings do not support our hypothesis of correspondence between reach scale heterogeneity in ecological condition and groundwater inputs. We postulate that variations in groundwater influence among reaches may have been masked by cumulative upstream effects of groundwater and surface water mixing in Kintore Creek headwaters. Consequently, groundwater influence on biofilm communities and cellulose decomposition may be expressed in a more local fashion than can be detected by reach scale measurements.

2.6 References

Agriculture and Agri-Food Canada (2020) AAFC annual crop inventory 2019. https://open.canada.ca/data/en/dataset/d90a56e8-de27-4354-b8ee-33e08546b4fc. Accessed 13 Feb 2021

American Water Works Association, AWWA (2004) Flow injection analysis for orthophosphate. Standard methods for the examination of water and wastewater, 22nd edn. American Public Health Association, American Water Works Association, Water Environment Federation, 4500-P-G

Battin TJ, Kaplan LA, Newbold JD, et al (2003) Effects of current velocity on the nascent architecture of stream microbial biofilms. Appl Environ Microbiol 69:5443–5452. https://doi.org/10.1128/AEM.69.9.5443

Baxter C V., Hauer FR (2000) Geomorphology, hyporheic exchange, and selection of spawning habitat by bull trout (*Salvelinus confluentus*). Can J Fish Aquat Sci 57:1470–1481. https://doi.org/10.1139/f00-056

Benfield EF, Fritz KM, Tiegs SD (2017) Leaf-litter breakdown. In: Lamberti GA, Hauer FR (eds) Methods in Stream Ecology, Volume 2: Ecosystem Function, 3rd edn. Elsevier, Academic Press, pp 71–82

Bertrand G, Goldscheider N, Gobat JM, Hunkeler D (2012) Review: From multi-scale conceptualization to a classification system for inland groundwater-dependent ecosystems. Hydrogeol J 20:5–25. https://doi.org/10.1007/s10040-011-0791-5

Besemer K (2015) Biodiversity, community structure and function of biofilms in stream ecosystems. Res Microbiol 166:774–781. https://doi.org/10.1016/j.resmic.2015.05.006

Bey M, Béranger L (2014) Atlas des diatomées. In: Cent. Res. Public Gabriel Lippman. http://www.auvergne-rhone-alpes.developpement-durable.gouv.fr/atlas-des-diatomees-a3480.html. Accessed 8 Jan 2019

Biggs BJF (1996) Patterns in benthic algae of streams. In: Stevenson RJ, Bothwell ML, Lowe RL (eds) Algal ecology: freshwater benthic ecosystems, 2nd edn. Academic Press, San Diego, CA, USA, pp 31–56

Biggs BJF, Goring DG, Nikora VI (1998) Subsidy and stress responses of stream periphyton to gradients in water velocity as a function of community growth form. J Phycol 34:598–607. https://doi.org/10.1046/j.1529-8817.1998.340598.x

Boulton AJ, Hancock PJ (2006) Rivers as groundwater-dependent ecosystems: A review of degrees of dependency, riverine processes and management implications. Aust J Bot 54:133–144. https://doi.org/10.1071/BT05074

Brown JH, Gillooly JF, Allen AP, et al (2004) Toward a metabolic theory of ecology. Ecology 85:1771–1789. https://doi.org/10.1890/03-9000

Brunke M, Gonser T (1997) The ecological significance of exchange processes between rivers and groundwater. Freshw Biol 37:1–33. https://doi.org/10.1046/j.1365-2427.1997.00143.x

Burrows RM, Beesley L, Douglas MM, et al (2020) Water velocity and groundwater upwelling influence benthic algal biomass in a sandy tropical river: implications for water-resource development. Hydrobiologia 847:1207–1219. https://doi.org/10.1007/s10750-020-04176-3

Carrascal LM, Galván I, Gordo O (2009) Partial least squares regression as an alternative to current regression methods used in ecology. Oikos 118:681–690. https://doi.org/10.1111/j.1600-0706.2008.16881.x

Chambers PA, McGoldrick DJ, Brua RB, et al (2012) Development of environmental thresholds for nitrogen and phosphorus in streams. J Environ Qual 41:7–20. https://doi.org/10.2134/jeq2010.0273

Chauvet E, Suberkropp K (1998) Temperature and sporulation of aquatic hyphomycetes. Appl Environ Microbiol 64:1522–1525. https://doi.org/10.1128/aem.64.4.1522-1525.1998

Clarke KR (1993) Non-parametric multivariate analyses of changes in community structure. Aust J Ecol 18:117–143. https://doi.org/10.1111/j.1442-9993.1993.tb00438.x

Clarke KR, Gorley RN (2015) Primer v7: User manual/tutorial. Primer-E 93

Clarke KR, Warwick RM (1994) Similarity-based testing for community pattern: the two-way layout with no replication. Mar Biol 118:167–176. https://doi.org/10.1007/BF00699231

Conant B, Robinson CE, Hinton MJ, Russell HAJ (2019) A framework for conceptualizing groundwater-surface water interactions and identifying potential impacts on water quality, water quantity, and ecosystems. J Hydrol 574:609–627. https://doi.org/10.1016/j.jhydrol.2019.04.050

Cook PG (2013) Estimating groundwater discharge to rivers from river chemistry surveys. Hydrol Process 27:3694–3707. https://doi.org/10.1002/hyp.9493

Delgado C, Almeida SFP, Elias CL, et al (2017) Response of biofilm growth to experimental warming in a temperate stream. Ecohydrology 10:1–9. https://doi.org/10.1002/eco.1868

Environment and Climate Change Canada (2010) Canadian Climate Normals. http://climate.weather.gc.ca/climate_normals/index_e.html#1981. Accessed 1 Nov 2021

Eriksson L, Bryne T, Johansson E, et al (2013) Multi-and megavariate data analysis: part I: basic principles and applications., 3rd edn. Umetrics AB, Umeå

Ferreira V, Canhoto C (2013) Effect of experimental and seasonal warming on litter decomposition in a temperate stream. Aquat Sci 76:155–163. https://doi.org/10.1007/s00027-013-0322-7

Ferreira V, Castagneyrol B, Koricheva J, et al (2015) A meta-analysis of the effects of nutrient enrichment on litter decomposition in streams. Biol Rev 90:669–688. https://doi.org/10.1111/brv.12125

Ferreira V, Chauvet E (2011) Synergistic effects of water temperature and dissolved nutrients on litter decomposition and associated fungi. Glob Chang Biol 17:551–564. https://doi.org/10.1111/j.1365-2486.2010.02185.x

Ferreira V, Gulis V, Graça MAS (2006) Whole-stream nitrate addition affects litter decomposition and associated fungi but not invertebrates. Oecologia 149:718–729. https://doi.org/10.1007/s00442-006-0478-0

Flinders CA, Ragsdale RL, Ikoma J, et al (2019) Spatial and temporal patterns of diatom assemblages, and their drivers, in four US streams: Evidence from a long-term dataset. Hydrobiologia 846:159–179. https://doi.org/10.1007/s10750-019-04061-8

Follstad Shah JJ, Kominoski JS, Ardón M, et al (2017) Global synthesis of the temperature sensitivity of leaf litter breakdown in streams and rivers. Glob Chang Biol 23:3064–3075. https://doi.org/10.1111/gcb.13609

Forsyth DK, Riseng CM, Wehrly KE, et al (2016) The Great Lakes hydrography dataset: Consistent, binational watersheds for the Laurentian Great Lakes basin. J Am Water Resour Assoc 52:1068–1088. https://doi.org/10.1111/1752-1688.12435

Francoeur SN, Biggs BJE, Smith RA, Lowe R (1999) Nutrient limitation of algal biomass accrual in streams: seasonal patterns and a comparison of methods. J North Am Benthol Soc 18:242–260. https://doi.org/10.2307/1468463

Gleeson T, Richter B (2018) How much groundwater can we pump and protect environmental flows through time? Presumptive standards for conjunctive management of aquifers and rivers. River Res Appl 34:83–92. https://doi.org/10.1002/rra.3185

Godwin CM, Carrick HJ (2008) Spatio-temporal variation of periphyton biomass and accumulation in a temperate spring-fed stream. Aquat Ecol 42:583–595. https://doi.org/10.1007/s10452-007-9133-z

Graça MAS, Ferreira V, Canhoto C, et al (2015) A conceptual model of litter breakdown in low order streams. Int Rev Hydrobiol 100:1–12. https://doi.org/10.1002/iroh.201401757

Griffiths NA, Tiegs SD (2016) Organic-matter decomposition along a temperature gradient in a forested headwater stream. Freshw Sci 35:518–533. https://doi.org/10.1086/685657

Gulis V, Ferreira V, Graça MAS (2006) Stimulation of leaf litter decomposition and associated fungi and invertebrates by moderate eutrophication: Implications for stream assessment. Freshw Biol 51:1655–1669. https://doi.org/10.1111/j.1365-2427.2006.01615.x

Gulis V, Suberkropp K (2003) Leaf litter decomposition and microbial activity in nutrient-enriched and unaltered reaches of a headwater stream. Freshw Biol 48:123–134. https://doi.org/10.1046/j.1365-2427.2003.00985.x

Guo F, Kainz MJ, Sheldon F, Bunn SE (2016) The importance of high-quality algal food sources in stream food webs - current status and future perspectives. Freshw Biol 61:815–831. https://doi.org/10.1111/fwb.12755

Hofmann G, Werum M, Lange-Bertalot H (2011) Diatomeen im Süßwasser-Benthos von Mitteleuropa: Bestimmungsflora Kieselalgen für die ökologische Praxis: über 700 der häufigsten Arten und ihre Ökologie. A.R.G. Gantner Verlag Kommanditgesellschaft, Rugell.

Howard-Parker B, White B, Halvorson HM, Evans-White MA (2020) Light and dissolved nutrients mediate recalcitrant organic matter decomposition via microbial priming in experimental streams. Freshw Biol 65:1189–1199. https://doi.org/10.1111/fwb.13503

Jahn R, Kusber W, Romero OE (2009) Cocconeis pediculus Ehrenberg and C. placentula Ehrenberg var. placentula (Bacillariophyta): Typification and taxonomy. Fottea 9:275–288. https://doi.org/10.5507/fot.2009.027

Kaandorp VP, Doornenbal PJ, Kooi H, et al (2019) Temperature buffering by groundwater in ecologically valuable lowland streams under current and future climate conditions. J Hydrol X 3:1–16. https://doi.org/10.1016/j.hydroa.2019.100031

Kaandorp VP, Molina-Navarro E, Andersen HE, et al (2018) A conceptual model for the analysis of multi-stressors in linked groundwater–surface water systems. Sci Total Environ 627:880–895. https://doi.org/10.1016/j.scitotenv.2018.01.259

Lange K, Townsend CR, Matthaei CD (2016) A trait-based framework for stream algal communities. Ecol Evol 6:23–36. https://doi.org/10.1002/ece3.1822

Lavoie I, Hamilton P, Campeau S, et al (2008) Guide d'identification des diatomées des rivières de l'Est du Canada. Presses de L'Université du Québec, Québec

Lefebvre K, Barbecot F, Larocque M, Gillon M (2015) Combining isotopic tracers (222Rn and δ13C) for improved modelling of groundwater discharge to small rivers. Hydrol Process 29:2814–2822. https://doi.org/10.1002/hyp.10405

Legendre P, Gallagher ED (2001) Ecologically meaningful transformations for ordination of species data. Oecologia 129:271–280. https://doi.org/10.1007/s004420100716

Malard F, Tockner K, Dole-Olivier MJ, Ward J V. (2002) A landscape perspective of surface-subsurface hydrological exchanges in river corridors. Freshw Biol 47:621–640. https://doi.org/10.1046/j.1365-2427.2002.00906.x

Marmonier P, Archambaud G, Belaidi N, et al (2012) The role of organisms in hyporheic processes: Gaps in current knowledge, needs for future research and applications. Ann Limnol 48:253–266. https://doi.org/10.1051/limn/2012009

Martínez A, Larrañaga A, Pérez J, et al (2014) Temperature affects leaf litter decomposition in low-order forest streams: field and microcosm approaches. Microbiol Ecol 87:257–267. https://doi.org/10.1111/1574-6941.12221

Martinez JL, Raiber M, Cox ME (2015) Assessment of groundwater-surface water interaction using long-term hydrochemical data and isotope hydrology: Headwaters of the Condamine River, Southeast Queensland, Australia. Sci Total Environ 536:499–516. https://doi.org/10.1016/j.scitotenv.2015.07.031

Mejia FH, Baxter C V., Berntsen EK, Fremier AK (2016) Linking groundwater – surface water exchange to food production and salmonid growth. Can J Fish Aquat Sci 73:1650–1660. https://doi.org/10.1139/cjfas-2015-0535

Minshall GW (1978) Autotrophy in stream ecosystems. Bioscience 28:767–771. https://doi.org/10.2307/1307250

Morin A, Lamoureux W, Busnarda J (1999) Empirical models predicting primary productivity from chlorophyll a and water temperature for stream periphyton and lake and ocean phytoplankton. J North Am Benthol Soc 18:299–307. https://doi.org/10.2307/1468446

Mulholland PJ (1996) Role in nutrient cycling in streams. In: Stevenson RJ, Bothwell M, Lowe R (eds) Algal ecology: freshwater benthic ecosystems, 2nd edn. Academic Press, San Diego, CA, USA, pp 609–639

Mullinger NJ, Binley AM, Pates JM, Crook NP (2007) Radon in Chalk streams: Spatial and temporal variation of groundwater sources in the Pang and Lambourn catchments, UK. J Hydrol 339:172–182. https://doi.org/10.1016/j.jhydrol.2007.03.010

Ockenden MC, Deasy CE, Benskin CMWH, et al (2016) Changing climate and nutrient transfers: evidence from high temporal resolution concentration-flow dynamics in headwater catchments. Sci Total Environ 548–549:325–339. https://doi.org/10.1016/j.scitotenv.2015.12.086

Oksanen J, Blanchet FG, Friendly M, et al (2020) vegan: community ecology package

Ontario Geological Survey (2010) Surficial geology of southern Ontario; Ontario Geological Survey, Miscellaneous Release Data 128 - Revised

Passy SI (2007) Diatom ecological guilds display distinct and predictable behavior along nutrient and disturbance gradients in running waters. Aquat Bot 86:171–178. https://doi.org/10.1016/j.aquabot.2006.09.018

Pepin DM, Hauer FR (2002) Benthic responses to groundwater-surface water exchange in 2 alluvial rivers in northwestern Montana. J North Am Benthol Soc 21:370–383. https://doi.org/10.2307/1468476

Piggott JJ, Salis RK, Lear G, et al (2015) Climate warming and agricultural stressors interact to determine stream periphyton community composition. Glob Chang Biol 21:206–222. https://doi.org/10.1111/gcb.12661

Poisson R, Yates AG (2022) Impaired cellulose decomposition in a headwater stream receiving subsurface agricultural drainage. Ecol Process 11:1–17. https://doi.org/10.1186/s13717-022-00406-9

Ponader KC, Potapova MG (2007) Diatoms from the genus *Achnanthidium* in flowing waters of the Appalachian Mountains (North America): Ecology, distribution and taxonomic notes. Limologica 37:227–241. https://doi.org/10.1016/j.limno.2007.01.004

R Core Team (2020) R: A language and environment for statistical computing.

Rimet F, Bouchez A (2012) Life-forms, cell-sizes and ecological guilds of diatoms in European rivers. Knowl Manag Aquat Ecosyst 406:1–12. https://doi.org/10.1051/kmae/2012018

Rosemond AD, Pringle CM, Ramírez A, et al (2002) Landscape variation in phosphorus concentration and effects on detritus-based tropical streams. Limnol Oceanogr 47:278–289. https://doi.org/10.4319/lo.2002.47.1.0278

Roy JW, Zaitlin B, Hayashi M, Watson SB (2011) Influence of groundwater spring discharge on small-scale spatial variation of an alpine stream ecosystem. 670:661–670. https://doi.org/10.1002/eco

Royer T V, Minshall GW (2003) Controls on leaf processing in streams from spatial-scaling and hierarchical perspectives. J North Am Benthol Soc 22:352–358. https://doi.org/https://doi.org/10.2307/1468266

Sabater S, Timoner X, Borrego C, Acuña V (2016) Stream biofilm responses to flow intermittency: From cells to ecosystems. Front Environ Sci 4:1–10. https://doi.org/10.3389/fenvs.2016.00014

Sanchez G (2016) plsdepot: partial least squares data analysis methods.

Sear DA, Armitage PD, Dawson FH (1999) Groundwater dominated rivers. Hydrol Process 13:255–276. https://doi.org/10.1002/(SICI)1099-1085(19990228)13:3<255::AID-HYP737>3.0.CO;2-Y

Shore M, Murphy S, Mellander PE, et al (2017) Influence of stormflow and baseflow phosphorus pressures on stream ecology in agricultural catchments. Sci Total Environ 590–591:469–483. https://doi.org/10.1016/j.scitotenv.2017.02.100

Snell MA, Barker PA, Surridge BWJ, et al (2019) Strong and recurring seasonality revealed within stream diatom assemblages. Sci Rep 9:1–7. https://doi.org/10.1038/s41598-018-37831-w

Steinman AD, Lamberti GA, Leavitt PR (2007) Biomass and pigments of benthic algae. In: Hauer FR, Lamberti G (eds) Methods in Stream Ecology, 2nd edn. Academic Press, San Diego, CA, USA, pp 357–379

Stenger-Kovács C, Lengyel E, Crossetti LO, et al (2013) Diatom ecological guilds as indicators of temporally changing stressors and disturbances in the small Torna-stream, Hungary. Ecol Indic 24:138–147. https://doi.org/10.1016/j.ecolind.2012.06.003

Stevenson RJ (1997) Scale-dependent determinants and consequences of benthic algal heterogeneity. J North Am Benthol Soc 16:248–262. https://doi.org/10.2307/1468255

Swan CM, Palmer MA (2004) Leaf diversity alters litter breakdown in a Piedmont stream. J North Am Benthol Soc 23:15–28. https://doi.org/10.1899/0887-3593(2004)023<0015:LDALBI>2.0.CO;2

Tang T, Guo S, Tan L, et al (2019) Temporal effects of groundwater on physical and biotic components of a karst stream. Water 11:1–17. https://doi.org/10.3390/w11061299

Tang T, Jia X, Jiang W (2016) Multi-scale temporal dynamics of epilithic algal assemblages: evidence from a Chinese subtropical mountain river network. Hydrobiologia 770:289–299. https://doi.org/10.1007/s10750-015-2603-8

Tiegs SD, Clapcott JE, Griffiths NA, Boulton AJ (2013) A standardized cotton-strip assay for measuring organic-matter decomposition in streams. Ecol Indic 32:131–139. https://doi.org/10.1016/j.ecolind.2013.03.013

Tiegs SD, Costello D, Isken M, et al (2019) Global patterns and drivers of ecosystem functioning in rivers and riparian zones. Sci Adv 5:1–8. https://doi.org/10.1126/sciadv.aav0486

Unland NP, Cartwright I, Andersen MS, et al (2013) Investigating the spatio-temporal variability in groundwater and surface water interactions: A multi-technique approach. Hydrol Earth Syst Sci 17:3437–3453. https://doi.org/10.5194/hess-17-3437-2013

US EPA (1974) EPA Method 415.1: Total organic carbon (combustion or oxidation).

Valett HM, Fisher SG, Grimm NB, Camill P (1994) Vertical hydrologic exchange and ecological stability of a desert stream ecosystem. Ecology 75:548–560. https://doi.org/10.2307/1939557

Vannote RL, Minshall GW, Cummins KWC, et al (1980) River continuum concept. Can J Fish Aquat Sci 37:130–137. https://doi.org/10.1139/f80-017

Webb JR, Pearce NJT, Painter KJ, Yates AG (2019) Hierarchical variation in cellulose decomposition in least-disturbed reference streams: a multi-season study using the cotton strip assay. Landsc Ecol 34:2353–2369. https://doi.org/10.1007/s10980-019-00893-w

Wold S, Sjöström M, Eriksson L (2001) PLS-regression: A basic tool of chemometrics. Chemom Intell Lab Syst 58:109–130. https://doi.org/10.1016/S0169-7439(01)00155-1

Wyatt KH, Hauer FR, Pessoney GF (2008) Benthic algal response to hyporheic-surface water exchange in an alluvial river. Hydrobiologia 607:151–161. https://doi.org/10.1007/s10750-008-9385-1

Ylla I, Canhoto C, Romaní AM (2014) Effects of warming on stream biofilm organic matter use capabilities. Microb Ecol 68:132–145. https://doi.org/10.1007/s00248-014-0406-5

3 Effects of groundwater inputs on algal assemblages and cellulose decomposition differ based on habitat type in an agricultural stream

3.1 Introduction

Stream biofilms are an essential component of stream ecosystem structure and function because of their role in biogeochemical processing of organic and inorganic materials (Borchardt, 1996; Battin et al., 2003; Besemer, 2015). Stream biofilms are composed of autotrophic and heterotrophic microorganisms that include algae, bacteria, and fungi (Besemer, 2015). The algal component of biofilms influences nutrient cycling in streams through uptake and subsequent transformation and/or remineralization of nutrients, and generates primary production that is a source of basal resources for higher trophic levels (Minshall, 1978; Borchardt, 1996; Mulholland, 1996). Likewise, heterotrophic microorganisms in the biofilm contribute to carbon cycling in streams through conversion of organic material into smaller particles, as well as mineralization and assimilation into microbial biomass (Cummins, 1974; Petersen & Cummins, 1974). Due to the critical functions biofilms perform in streams, considerable effort has been made to identify environmental factors that influence biofilm communities (e.g., biomass and diatom assemblage composition) and organic matter breakdown (e.g., cellulose decomposition) (Biggs, 1995; Biggs et al., 1998; Lavoie et al., 2014; Battin et al., 2016; Tiegs et al., 2019).

Environmental factors that have been found to be important determinants of stream biofilm communities and organic matter breakdown include light, nutrients, water temperature, water chemistry, and stream velocity (Stevenson, 1997; Royer & Minshall, 2003; Graça et al., 2015). Further, these environmental factors act on biofilm communities and organic matter breakdown at different spatial scales. For example, previous work has shown that surface water nutrients, water temperature, and water chemistry can vary at the reach scale (Biggs, 1995; Stevenson, 1997; Martínez et al., 2014; Graça et al., 2015). Stream velocity is a key environmental factor that varies at the habitat scale (Biggs et al., 1998, 2005; Passy, 2007; Webb et al., 2019). Surface water nutrient availability, water temperature, and water chemistry can also be influenced by groundwater inputs at reach and habitat scales (Boulton & Hancock,

2006; Boano et al., 2014). However, the extent that habitat type may modify the effect of groundwater inputs and subsequently alter patterns in stream biofilm communities and organic matter breakdown has not been well-studied.

In streams, groundwater inputs are often spatially heterogeneous due to varying hydraulic gradients between groundwater and surface waters, as well as subsurface hydrogeological structures that result in variable groundwater flow paths (Conant et al., 2019). Within reaches, groundwater flow paths can be modified by hydrogeomorphic features including sequences of faster stream velocity (i.e., riffle habitats) to slower stream velocity (i.e., run habitats), with changing stream velocities and streambed topography resulting in patchiness in groundwater inputs due to differences in hydraulic head (Harvey & Bencala, 1993; Brunke & Gonser, 1997). Additionally, heterogeneity in streambed permeability can affect the connectivity patterns in groundwater – surface water exchange. For example, coarse sediment typically allows for greater exchange, whereas finer sediment inhibits exchange (Renard & Allard, 2013). Groundwater inputs can modify a stream's environmental conditions when the surface water and groundwater have different physical and chemical characteristics. For example, depending on season, upwelling groundwater can have lower (summer) or higher (winter) water temperature than surface waters (Krause et al., 2011). Alternatively, groundwater can be more reducing compared to surface waters leading to redox gradients near the groundwater – surface water interface that can affect the release and retention of nutrients (Lewandowski et al., 2019; Vissers et al., 2023).

Changes in environmental conditions due to spatially heterogeneous groundwater inputs have been linked to patterns in stream biofilm communities and cellulose decomposition. At the reach and habitat scales, input of groundwater has been associated with elevated primary production (Coleman & Dahm, 1990; Roy et al., 2011; Mejia et al., 2016; Burrows et al., 2020). Further, past work has suggested that groundwater inputs can stimulate cellulose decomposition by providing nutrient subsidies (Griffiths & Tiegs, 2016), but may also reduce cellulose decomposition through stream cooling (Webb et al., 2019, Poisson & Yates, 2022). Additionally, lower dissolved oxygen in groundwater inputs may also lead to slower decomposition rates (Cornut et al., 2010). However, there has been limited work

explicitly assessing how the impact of groundwater inputs on stream environmental conditions, biota, and processes may differ among habitats (but see Burrows et al., 2020).

Within a reach, habitat type can generate environmental heterogeneity that could modify the impact of groundwater inputs and associated patterns in stream biofilm communities and cellulose decomposition (Webb et al., 2019; Burrows et al., 2020). Habitat type is often defined by relative stream velocity, where fast moving water is associated with riffles and slower moving water is associated with runs and/or pools (Jowett, 1993). Differences in stream velocity have been shown to alter biofilm communities and organic matter processing. For example, faster stream velocity produces increased shear stress, which is an important driver in determining which taxa establish in algal assemblages (Biggs & Hickey, 1994; Biggs et al., 1998). Rates of organic matter processing are also enhanced by faster stream velocity due to greater physical abrasion (Clapcott & Barmuta, 2010). Further, physical differences between habitat types have been associated with spatial heterogeneity in groundwater input. In riffles, a sudden steepening of the slope of the streambed results in faster stream velocities, but can also create a pressure differential at the streambed surface along the riffle driving surface water to downwell at the start of riffles and upwell at the end of the riffle (i.e., a hyporheic flow path) (Harvey & Bencala, 1993). This hyporheic flow across the riffle can result in groundwater inputs being restricted to the end of the riffle or beginning of the adjacent run, and to the edges of the stream. In contrast, for a run, the streambed topography and slope are more muted, resulting in lower stream velocities and limited pressure differentials, and thus limited hyporheic flow to restrict groundwater inputs (Dent et al., 2001).

Our study compared stream biofilm communities and cellulose decomposition in riffle and run habitats in reaches with high, moderate, and low groundwater inputs and determined if impacts of groundwater input were habitat dependent. We also assessed if environmental variables modified by groundwater inputs were associated with habitat scale patterns in biofilm communities and cellulose decomposition. We hypothesized that differences in groundwater inputs and subsequent changes in environmental conditions would result in heterogeneity in biofilm biomass and composition and cellulose breakdown among reaches with varying groundwater inputs. Our results provide insight into the role of groundwater inputs as a driver

of biofilm communities and cellulose decomposition, and how habitat type may constrain the impacts of groundwater inputs.

3.2 Methods

3.2.1 Study area and site selection

Our study used a hierarchical design to assess the role of groundwater in generating environmental variation at reach and habitat scales, and if that variation is a driver of ecological heterogeneity in stream biofilm communities (biomass and diatom assemblage) and cellulose decomposition. This study was conducted in three headwater reaches in Kintore Creek, southern Ontario, Canada (Fig. 3.1a, b). Kintore Creek experiences a temperate climate, with mean annual low and high air temperatures of - 6.0 °C and 20.2 °C, respectively, and average annual precipitation of 1069.5 mm (Environment and Climate Change Canada, 2010). Land use in the Kintore Creek catchment is predominantly agricultural (80 %), with forest (12 %) and residential (4 %) uses comprising smaller portions (Agricutlure and Agri-Food Canada, 2020). Crop cover in the catchment consists of soybean, corn, and alfalfa, and many fields are tile drained. Surficial geology in the catchment varies in permeability in association with glacial deposits of tills (low permeability) to sands and gravels (high permeability) (Ontario Geological Survey, 2010).

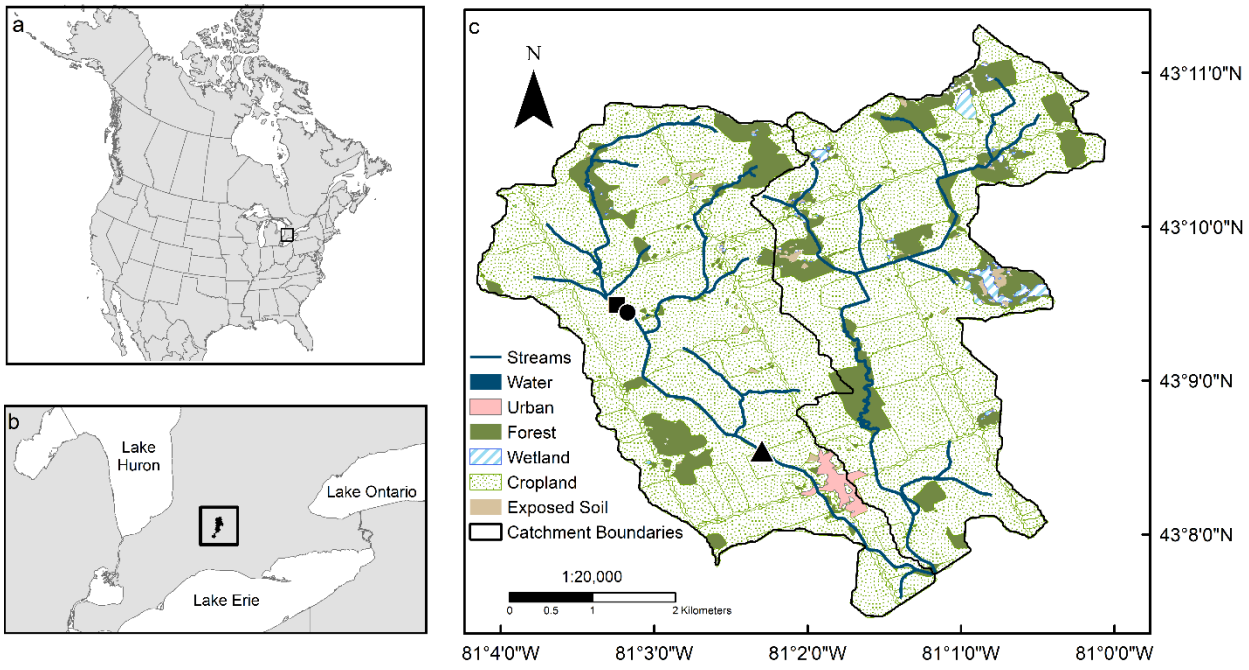

Figure 3.1 Locations of study area in North America (a) and the Kintore creek catchment in southern Ontario (b). Placement of high (HG; filled triangle), moderate (MG; filled square), and low (LG; filled circle) groundwater reaches in western headwater branch of the agriculturally dominated Kintore Creek catchment are indicated in panel c. (Catchment boundaries/stream network in Forsyth et al., 2016; Land use/cover in Agricutlure and Agri-Food Canada, 2020)

Reaches assessed in this study were selected based on differences in groundwater input identified using radon-222 (^{222}Rn, Bq m^{-3}). ^{222}Rn is widely used as a tracer for identifying groundwater inputs as ^{222}Rn concentrations are typically orders of magnitude higher in groundwaters compared to receiving surface waters, where it undergoes gas evasion and decay (Cook, 2013). A single surface water sample was collected above and below each reach using 4 L amber glass bottles and analyzed for ^{222}Rn less than 4 hours after collection using RAD7 electronic radon detectors with the big bottle accessory (Durridge, USA).

A steady state ^{222}Rn mass balance model was then used to estimate net groundwater discharge across each stream reach based on the in-stream ^{222}Rn concentrations (Table 3.1). The model is based on Atkinson et al. (2015) and considers ^{222}Rn inputs to the stream from

groundwater and ^{222}Rn losses due to gas evasion (Appendix B1., B2.). The mass balance model results were used to identify three reaches with varying groundwater inputs: 1) high groundwater reach (hereafter HG); 2) moderate groundwater reach (hereafter MG), and; 3) low groundwater reach (hereafter LG) (Fig. 3.1c). HG is approximately 45 m in length, whereas MG and LG were about 50 m in length. LG is approximately 20 m downstream from MG.

Stream water chemistry and nutrient conditions were measured in each reach. Soluble reactive phosphorus (SRP) and nitrate - nitrogen (NO_3^--N) were measured at three locations in each reach (top, middle, end) three times (beginning, middle, end) during the experiment. SRP was analyzed using a Flow Injection Analysis automated ion analyzer (FIA) (Lachat QuikChem, QC8500 FIA Automated Ion Analyzer, LDL 1 μg L^{-1}). NO_3^--N was analyzed using liquid chromatography (HPLC) (Thermo Scientific Dionex Aquion Ion Chromatography System with Dionex AS-DV autosampler, LDL 0.25 mg L^{-1}). pH and specific conductivity were measured at 5 locations in each habitat mid-way through the experiment using a handheld YSI probe (YSI, Professional Plus). Aside from differences in the groundwater inputs, the three selected reaches showed little variability among most environmental conditions with the exception of channel substrate. HG substrate was generally gravel and sand, substrate in MG was primarily cobble and gravel, whereas at LG the streambed was primarily finer sediment (clay and fine sand). All reaches had open canopies, with surface water nutrients, pH, and specific conductivities (μS cm^{-1}) comparable among the reaches during the deployment period (Table 3.1).

Table 3.1 ^{222}Rn and mean ± standard deviation of stream water chemistry and nutrient conditions in study reaches during deployment. ^{222}Rn Above and ^{222}Rn Below indicate ^{222}Rn concentration above the reach and below the reach, respectively. Groundwater discharge is for entire reach and was calculated using the ^{222}Rn mass balance model.

Environmental Parameter	HG	MG	LG
Radon			
^{222}Rn Above (Bq m^{-3})	1183	295	679

^{222}Rn Below (Bq m^{-3})	1121	679	782
Groundwater discharge (m^3 d^{-1} m^{-1})	7.1	2.7	1.0
Water Chemistry			
SRP (µg P L^{-1})	25.5 ± 3.0	37.6 ± 3.5	38.4 ± 4.7
NO_3-N (mg N L^{-1})	4.9 ± 0.6	3.4 ± 1.0	3.3 ± 1.2
pH	8.07 ± 0.01	8.02 ± 0.01	8.02 ± 0.01
Sp. conductivity (µS cm^{-1})	644 ± 1.6	644.1 ± 0.9	642.5 ± 0.5

3.2.2 Sample Collection and Processing

This study was conducted from July 3rd to August 6th, 2019. Within each reach, sampling locations were established in two riffles and two runs. Riffles and runs were distinguished based on differences in stream velocity (m/s) and depth (cm). Within each habitat unit, five locations in the middle of the channel along the length of the habitat unit were selected for assessment of algal biofilms and cellulose decomposition.

3.2.2.1 Biofilms

To provide a consistent surface for stream biofilm accumulation, we sampled biofilms using standardized artificial substrates (unglazed ceramic tiles; 21.24 cm^2 each, *sensu* Steinman et al., 2007). Three tiles were inserted into a tile holder, then the tile holder was affixed to a brick anchor using cable binders. To secure the tile holder and its brick anchor, the brick was buried in the streambed while ensuring the tile holder 'lip' was placed approximately 2 cm above the streambed. Tile holders were placed at each of the five positions within each habitat unit and were incubated for 26 or 27 days. For each position, two tiles were sampled for biomass (one tile each for chlorophyll-*a* [chl-*a*] and ash-free dry mass [AFDM]) by scraping all biofilm material from entire tile surface using a toothbrush. Because diatoms have shown strong responses to changes in water quality (e.g., nutrients, pH, salinity) (Lavoie et al., 2014), we sampled the third tile for diatom assemblages. Samples for diatom analysis were preserved

with Lugol's iodine (~1% v/v), and biomass samples were placed on ice and stored frozen until chl-*a* and AFDM analyses.

Diatom samples were prepared for enumeration by acid digestion in 5 mL of 100% (v/v) nitric acid for 15 h to remove organic matter, ensuring visible diatom frustules. To complete digestion, 1 mL of hydrogen peroxide 30 % (v/v) was added to each sample, then tubes were immersed in a hot water bath at 60 °C for 1 h. Once cooled to room temperature, samples were centrifuged for 10 minutes at 5500 rpm and the acid supernatant was discarded and pellets retained. Deionized water was added to rinse pellets and this step was repeated until the supernatant was above a pH of 6. Naphrax® (refractive index: 1.74; Brunel microscopes Ltd., Wiltshire, UK) was used to mount diatom frustules on microscope slides. Lastly, diatom assemblages were enumerated at a 1000x magnification using an Olympus BX51 Upright Compound Microscope equipped with differential interference contrast optical components. A minimum of 400 diatom valves per sample were enumerated and identified to species level, where possible, following Lavoie et al. (2008) and Bey & Ector (2013).

Frozen chl-*a* samples were thawed and then filtered onto Whatman GF/C filters. Filters were submerged in 10 mL of 90% ethanol in 50 mL centrifuge tubes. A hot ethanol, non-acidification extraction was done by inserting centrifuge tubes into an 80 °C hot water bath for 7 min. The chl-*a* concentration for each sample was determined using a Turner Designs Trilogy Fluorometer (Model: 7200e000). If maximum detection limits (> 75 µg/mL) were exceeded, then extracted liquid was diluted. We calculated chl-*a* accumulation by dividing chl-*a* concentration by number of days incubated in the stream to standardize samples.

Frozen AFDM samples were thawed prior to analysis. Upon analysis, samples were filtered through pre-ashed Whatman GF/C filters and dried at 105 °C for at least 12 h. For determination of organic mass, the filtered and dried samples were then weighed. Samples were then ashed in a muffle furnace at 550 °C for 1 h. After cooling to room temperature, ashed filters were weighed to determine mass loss on ignition. Because of high levels of silt/clay in the samples, samples were then re-wetted and dried for a minimum of 12 h at 105 °C. The samples were then weighed to correct for water loss due to the presence of clay and other

minerals. To standardize samples, we calculated biofilm growth rate by dividing AFDM by number of days incubated in the stream.

3.2.2.2 Cellulose Decomposition

We used the cotton-strip assay (CSA; Tiegs et al., 2013) to measure cellulose decomposition. Cotton strip preparation, deployment, and retrieval followed Tiegs et al. (2013). Cotton strips were made using Fredrix-brand unprimed 12-oz. heavyweight cotton fabric, Style #548 (Fredrix, Lawrenceville, GA, USA) by producing 2.5 cm x 8 cm strips, with 3 mm of frayed 'fuzz' on the length of the fabric strip.

Ten cotton strips were randomly assigned to each position. Five cotton strips were attached to the tile holder using cable binders, so they laid flat on the surface of the streambed. The remaining five strips were buried at 10 cm depth in the streambed sediment. Both surface and subsurface cotton strips were incubated for 14 days.

Immediately after retrieval, strips were immersed in a tray containing 70 % ethanol for 7 minutes to sterilize the strip, halting microbial activity. Once sterilized, strips were carefully brushed to remove excess debris and sediment. Sterilized and cleaned strips were laid flat and fully covered in folded aluminum foil, then placed on ice in a cooler until we returned to the lab. Strips were then dried at 40 °C for 24 h in the lab, which was then followed by evaluation of tensile strength.

Tensile strength, defined here as the force required to break the strip, was measured for each strip using a tensiometer and motorized test stand (Force Gauge, Model M3-100). Using methods outlined by Tiegs et al. (2013), equal lengths of the strip were positioned in the tensiometer grips (Mark-10 brand, Model #MG100). Next, strips were pulled at a constant rate of 2 cm/min until peak tension, identified as when the strip ripped, was reached. To determine percent loss of tensile strength, mean tensile strength of reference strips were compared to measured tensile strength of incubated strips. To ensure comparability between reference and stream incubated sample strips, reference strips were deployed in a mock field experiment. In the lab, reference strips were saturated in distilled water, then immersed in 70 % ethanol for 7 minutes and gently brushed. Reference strips were dried at 40 °C for 24 h, and the tensile

strength of the reference strip was measured. Tensile strength was measured for each sample strip, which was then used to calculate percent tensile loss per day using Eq.2 (*sensu* Tiegs et al., 2013).

$$\% \text{ tensile loss per day } = \frac{\left(\frac{\text{Tensile Strength}^{REF} - \text{Tensile Strength}^{SAMP}}{\text{Tensile Strength}^{REF}}\right) \text{ x } 100}{\text{Incubation time}}$$

(Eq. 2)

3.2.2.3 Environmental characterization

Surface water temperature and stream velocity were measured in each habitat unit. Near-streambed water temperature was measured at 10-minute intervals using temperature loggers (HOBO Pendant, Onset, USA) that were anchored at the streambed surface in the center of each habitat unit for the duration of the deployment period. However, the loss of the temperature logger in one riffle in HG resulted in the loss of temperature data for that habitat unit. Mean daily temperature range (°C) and mean daily temperature (°C) were calculated from near-streambed water temperature measurements during the deployment period. Mean daily temperature range was calculated by computing daily maximum and minimum temperatures for each deployment day, then these values were averaged over the incubation period. Mean daily temperature was calculated as the sum of the daily mean temperature divided by days in the deployment period (*sensu* Benfield et al., 2017). At each tile holder, stream velocity (m/s) (Hach FH950 Portable Velocity Meter, Hach Ultra Analytics) was measured at the streambed.

Subsurface streambed temperature mapping was conducted on July 5th, 2019 in HG and on July 16th, 2019 in MG and LG. Streambed subsurface temperature can be used as a proxy for groundwater flux with temperature differences between subsurface streambed temperature and stream surface water temperature able to identify areas of groundwater input (Kalbus et al., 2006). Typically, larger temperature gradients (i.e., near-streambed surface water temperature – subsurface streambed temperature) indicates greater groundwater input. For the streambed temperature mapping, streambed temperature readings were taken at 0.3 m intervals across the stream width, with measurement transects every 1 m along the reach. Subsurface

streambed temperature was measured at 10 cm depth below the streambed using a high-accuracy thermometer (Hanna HI98509 Checktemp® 1 Digital Thermometer). For each transect, near-streambed surface water temperature was measured once in the centre of the stream.

3.2.3 Data Analysis

We used generalized linear models (GLMs) to detect effects of groundwater input and habitat on biofilm biomass (i.e., chl-*a* accumulation and biofilm growth rate). We also applied GLMs to assess four diatom assemblage metrics: taxa richness, proportion of the three most abundant taxa (% dominant), taxa evenness, and density of diatoms. Density of diatoms was estimated by correcting the diatom counts in accordance with the proportion of the sample processed to reach 400 valves. The processed sample proportion was measured by the volume of sample used to produce the slides and the number of fields of view necessary to reach the target count of 400 valves.

For all models, fixed effects were groundwater input (three levels: HG, MG, and LG) and habitat (two levels: riffle and run) and their interaction (groundwater input x habitat). Separate GLMs were used to test for differences ($\alpha = 0.10$) in biomass and diatom assemblage metrics. Tukey's post-hoc tests were performed on significant GLM analyses to identify pairwise differences between factor levels. We used $\alpha = 0.10$ for our GLMs to offset risk of Type I and Type II errors due to the combined effects of small sample size ($n = 10$ per habitat type) and inherent variation of biofilm biomass and diatom assemblage metrics in streams. Analyses were completed in R (version 4.0.5) using the *stats* package (R Core Team, 2020) and taxa evenness was calculated using the *vegan* package (Oksanen et al., 2020).

Linear mixed effects models (LMEMs) were used for analyses of streambed and subsurface % tensile loss per day due to the nested structure of our data. For LMEMs, strip position nested within habitat and reach was set as a random effect. Fixed effects were the same as for the GLMs used to analyze the biofilm metrics. Significant LMEM analyses were then further investigated using GLMs to identify patterns in groundwater input, habitat, and their interaction. LMEMs were computed in R (version 4.0.5) with *lme4* and *lmerTest* packages

(Bates et al., 2015; Kuznetsova et al., 2017), using Satterhwaite's method to estimate degrees of freedom and p-value for fixed effects. GLMs were processed in R (version 4.0.5) using the *stats* package (R Core Team, 2020).

Spatial patterns in diatom assemblage composition among groundwater input and habitat units was assessed using non-metric multidimensional scaling (nMDS) on relative abundance data. Relative abundance data included taxa that accounted for at least 2 % relative abundance in at least one sample in any reach, and was subsequently Hellinger transformed (Legendre & Gallagher, 2001). A two-dimensional nMDS was performed using Bray-Curtis distance with a maximum of 1000 iterations or until two convergent solutions were found. Analyses were completed with PRIMER software package (version 7.0 with PERMANOVA+, Primer-E Ltd., Plymouth, UK; Clarke & Gorley, 2015).

A two factor permutational analysis of variance (PERMANOVA) was performed to compare variation in diatom assemblage composition in response to the fixed factors of groundwater input (HG, MG, and LG) and habitat unit (run, riffle). If diatom assemblage composition in reach or habitat or their interaction were identified as significantly different ($\alpha = 0.10$), we then used similarity percentages (SIMPER) routine to identify taxa which contributed most to dissimilarity among reaches and habitats. Analyses were conducted with PRIMER software package (version 7.0 with PERMANOVA+, Primer-E Ltd., Plymouth, UK; Clarke & Gorley, 2015).

To evaluate the association of environmental conditions (i.e., mean daily temperature range [°C], mean daily temperature [°C], tile depth [cm], and stream velocity [m/s]) with spatial patterns in biofilm biomass (chl-*a* accumulation and biofilm growth rate) and cellulose decomposition we used partial least squares (PLS) regression. Separate PLS analyses were conducted for biofilm biomass and % tensile loss per day on the streambed surface. PLS regression can be used to identify associations between predictor (environment) and response (ecological) variables, and is a useful tool when predictors are highly correlated, and there are many predictors relative to observations (Wold et al., 2001; Carrascal et al., 2009). For both % tensile loss per day on the streambed surface and biofilm biomass environmental predictor

variables (X: mean daily temperature range [°C], mean daily temperature [°C], tile depth [cm], and stream velocity [m/s]) were used to produce a set of components (PLS loadings) that maximize variance explained for % tensile loss per day and biofilm biomass (chl-*a* accumulation and biofilm growth rate) (Y), constructed using simultaneous decomposition of X and Y matrices (Eriksson et al., 2013). Cross-validated goodness of prediction (Q^2) was used to assess model performance, where goodness of prediction ($Q^2 > 0.097$) is computed as the difference between predicted and observed values using a tenfold cross-validation method with 999 iterations. The total explanatory capacity of the PLS model is defined as the sum of explanatory capacity (R^2 Y) for each component, and only components that account for 10 % or more of the variation in response (Y) variables were retained. Variable importance projection (VIP) scores were used to assess the influence of each predictor (X) variable, and only predictors with a VIP score greater than one were considered important for explaining response (Y) variables. Using a biplot, the direction of association between predictor and response variables was assessed using resultant loadings. PLS analyses were done in R (version 4.0.3) using the *plsdepot* package (Sanchez, 2016).

We used a BIOENV (matching of biotic and environmental patterns; Clarke & Warwick, 1994) to evaluate associations between measured environmental variables (mean daily temperature range [°C], mean daily temperature [°C], tile depth [cm], and stream velocity [m/s], pH, specific conductivity [µS/cm]) and diatom assemblage composition. Using a Spearman rank correlation, the BIOENV computes the extent of the association between two (dis)similarity matrices, resulting in pairs of samples where similar environmental variables are associated with similar diatom assemblage composition (Clarke & Warwick, 1994). To create the biotic matrices for the diatom assemblage composition we used Bray-Curtis distance on Hellinger transformed relative abundance data for taxa that comprised at least 2 % of relative abundance in a minimum of one sample in a given reach. Environmental matrices were constructed using Euclidean distance on normalized environmental variables (Clarke & Warwick, 1994). Analyses were conducted with *bioenv* function and significance was tested using *mantel* function with 999 permutations using environmental distances extracted from *bioenv* results (vegan package, Oksanen et al., 2020).

3.3 Results

3.3.1 Environmental conditions

Subsurface streambed temperatures in both runs and the upper riffle of the HG reach were typically between 16 and 18 °C, with some patches of cooler water (14 – 16 °C; Fig. 3.2a). The lower HG riffle was cooler with temperatures largely between 14 – 16 °C, with small areas as low as 12 °C). The upper run in the MG reach had uniform subsurface streambed temperature of 14 – 16 °C, whereas the two riffles (10 to 18 °C) and more downstream run (12 – 16 °C) had more spatially variable subsurface streambed temperatures (Fig. 3.2b). The LG reach had the warmest subsurface temperatures that were typically greater than 16 °C (Fig. 3. 2c).

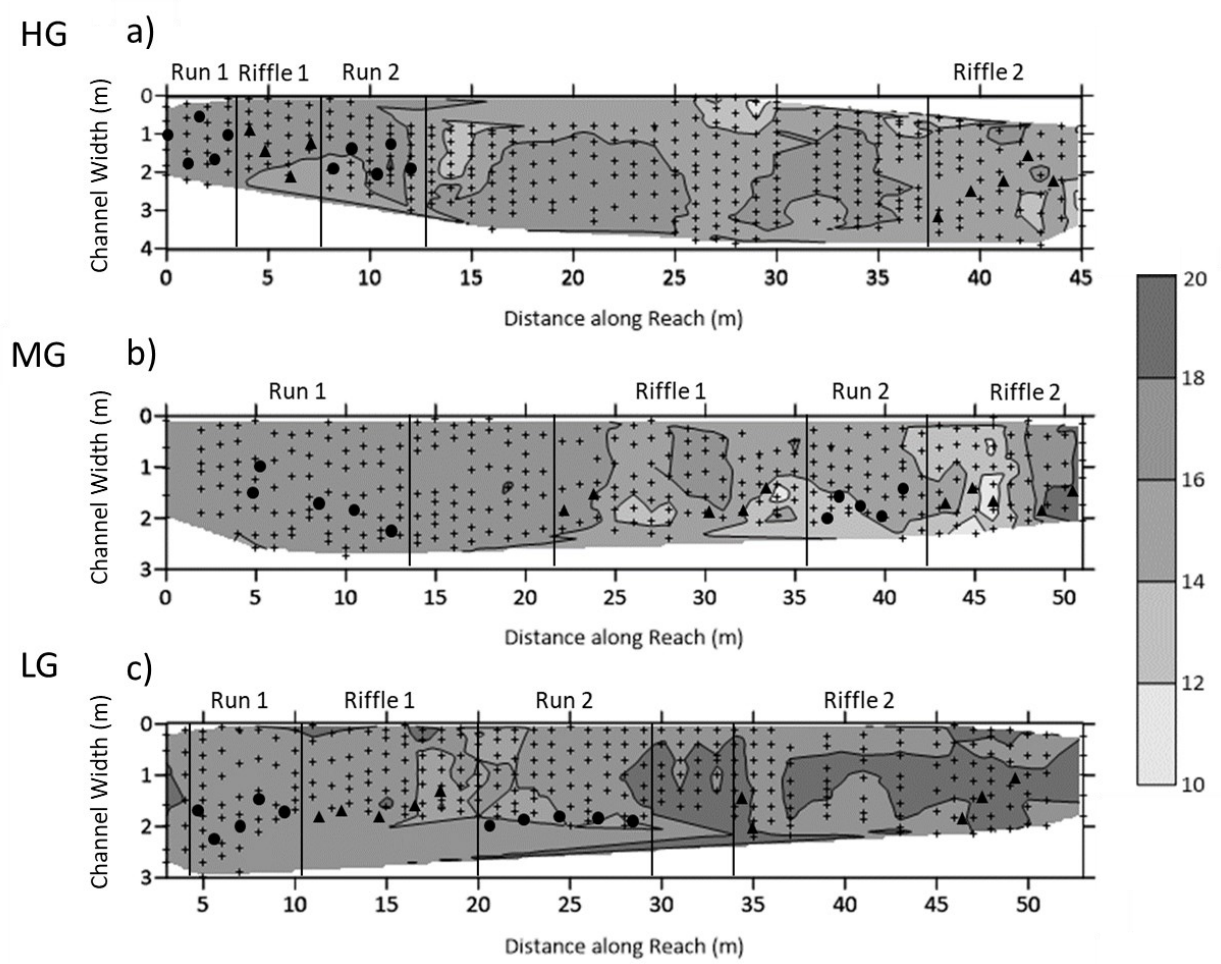

Figure 3.2 Subsurface (10 cm) streambed temperatures (°C) for three reaches in Kintore Creek, Ontario, Canada receiving high (HG, a), moderate (MG, b), and low (LG, c) inputs of groundwater. The temperature surface was generated by kriging interpolation. Cross symbols identify temperature measurement locations. Black circles show tile placement in runs, black triangles show tile placement in riffles.

The temperature gradient (stream surface water temperature – subsurface streambed temperature) in the HG reach increased from the top to bottom of the reach (Fig. 3.3a). The upper run temperature gradients were between 1 and 3 °C, the upper riffle and lower run ranged from 1 to 7 °C, whereas the lower riffle was typically between 5 and 9 °C. The temperature gradient of the upper run in the MG reach was consistently between -1 and 1 °C (Fig. 3.3b). In

contrast, the lower run and both riffles were patchier, exhibiting areas of lower (1 – 3 °C) and higher (5 – 7 °C) temperature gradients. Throughout the LG reach, the temperature gradients were typically between 1 and 3 °C, with small patches of larger temperature gradients (3 – 5 °C) in the upper riffle and lower run (Fig. 3.3a).

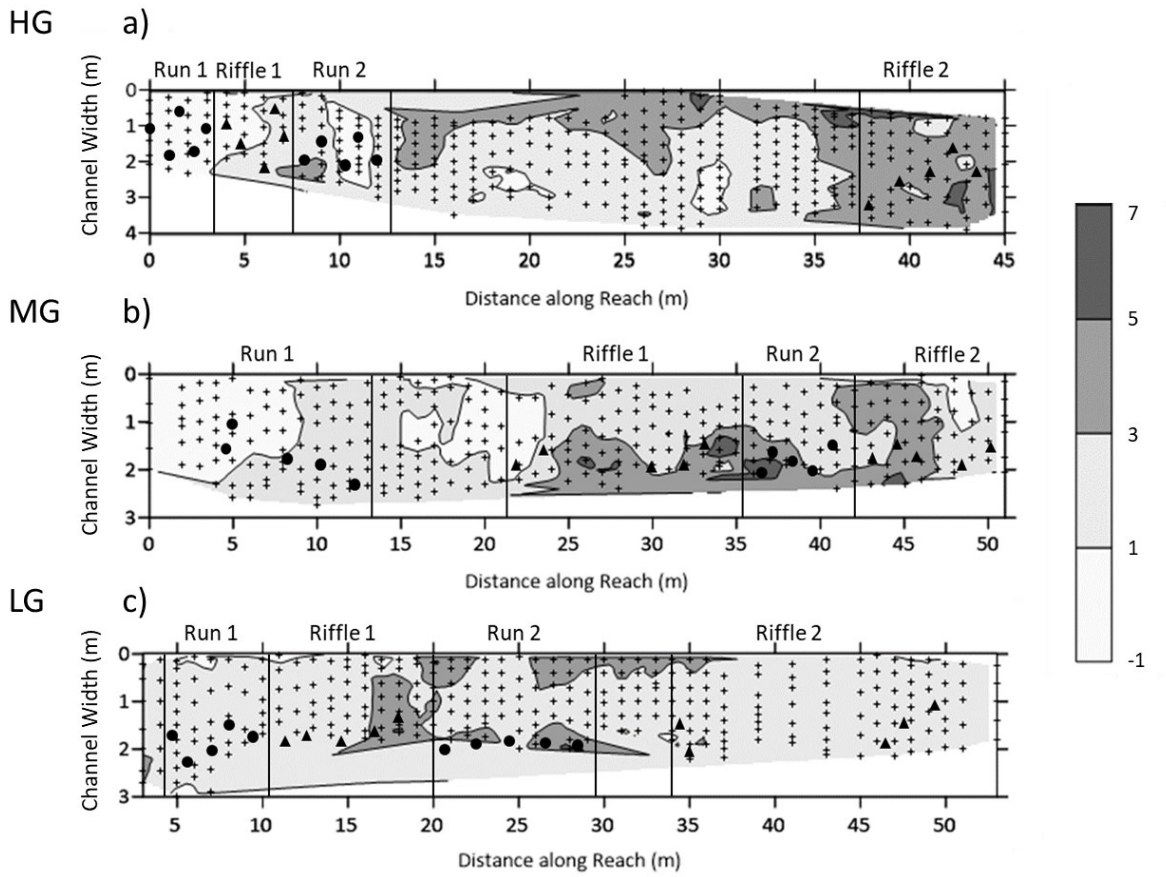

Figure 3.3 Temperature gradient between surface water and subsurface streambed temperature (°C) (i.e., stream surface water temperature - subsurface streambed temperature) for three reaches in Kintore Creek, Ontario, Canada receiving high (HG, a), moderate (MG, b), and low (LG, c) inputs of groundwater. The temperature surface was generated by kriging interpolation. Cross symbols identify temperature measurement locations. Black circles show tile placement in runs, black triangles show tile placement in riffles.

Across all riffle habitats, stream velocity in runs (0.120 ± 0.059 m/s) was about 60 % of that of riffles (0.217 ± 0.096 m/s) (Fig. 3.4a). MG had the fastest mean stream velocity in riffles and slowest in runs. Runs (15.8 ± 5.6 cm) were typically deeper than riffles (11.4 ± 2.5 cm) across all reaches (Fig. 3.4b), with LG having the smallest depths for both habitats and the smallest difference between runs and riffles (~3 cm on average).

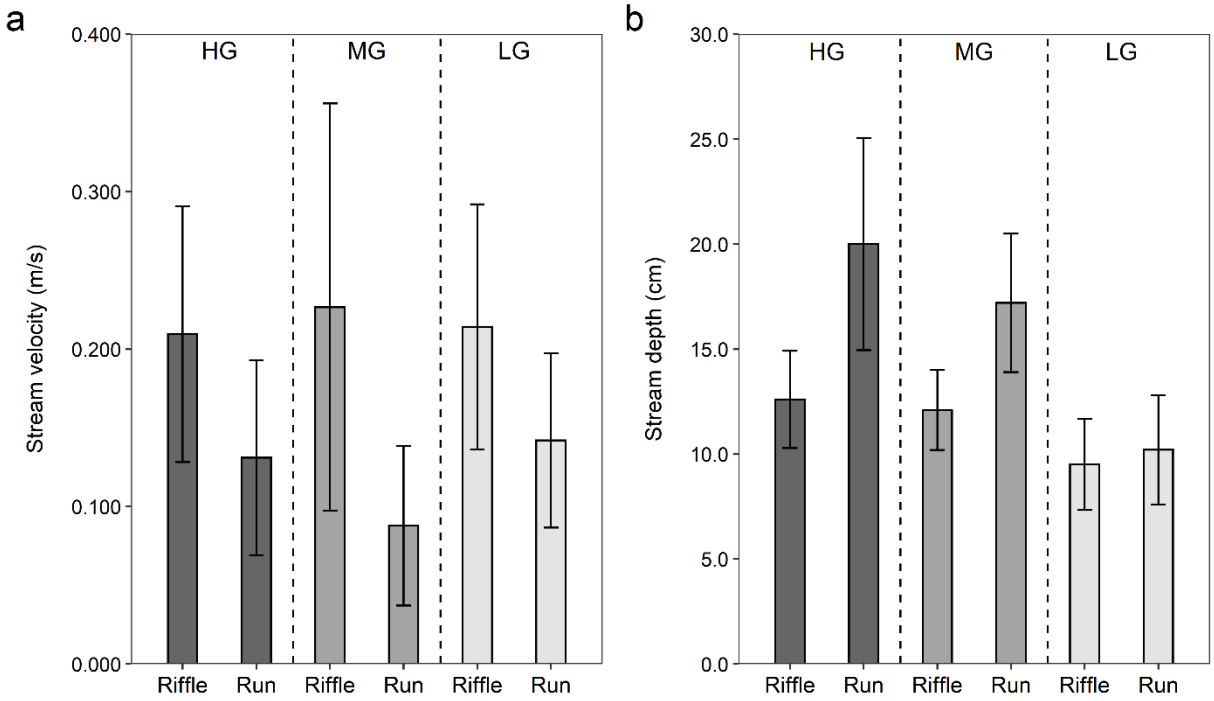

Figure 3.4 Bar plots (mean ± one standard deviation) of (a) stream velocity (m/s) and (b) stream depth (cm) for riffle (n = 10) and run (n = 10) habitats in three sampled stream reaches (high groundwater reach [HG], moderate groundwater reach [MG], and low groundwater reach [LG]) in Kintore Creek, Ontario.

Across all reaches and habitats, mean daily surface water temperature ranges and mean daily surface water temperatures were within approximately 2.5 °C and 2 °C, respectively (Fig. 3.5). The greatest mean daily temperature range for both habitats was observed in HG (Fig. 3.5a). Mean daily temperature was the lowest in HG for both habitats (Fig. 3.5b).

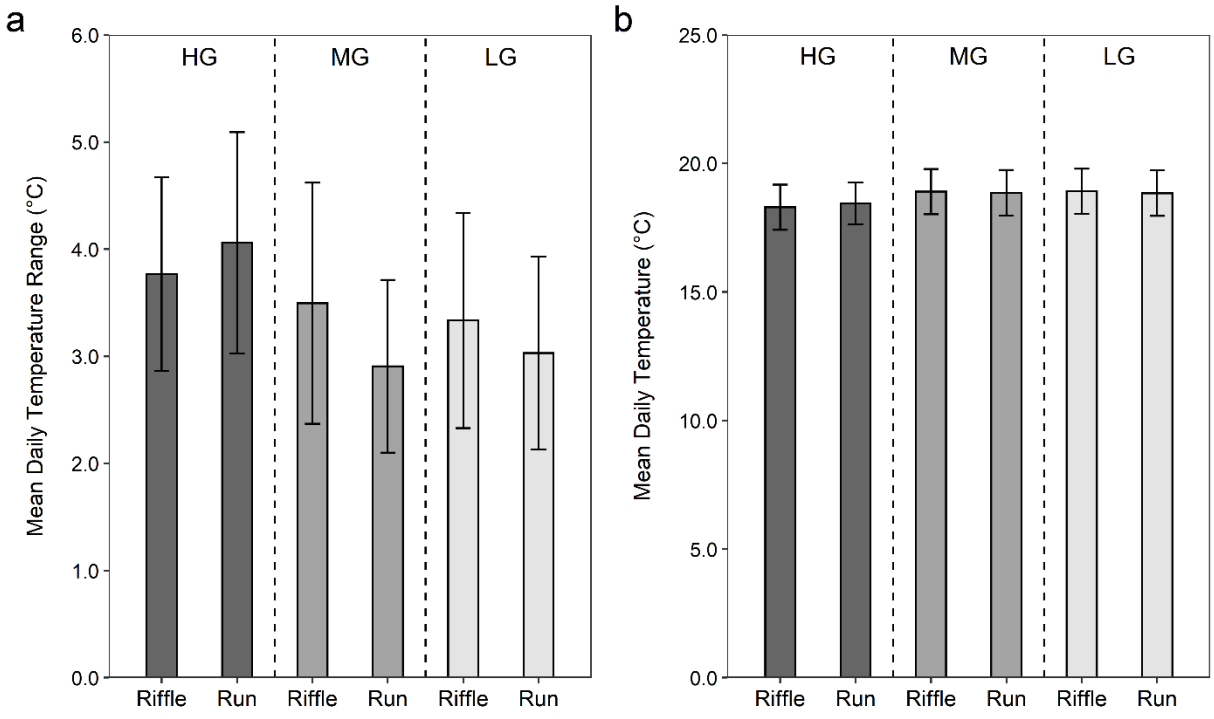

Figure 3.5 Bar plots (mean ± one standard deviation) of (a) mean daily temperature range (°C) and (b) mean daily temperature (°C) of stream water temperature for riffle (n = 10) and run (n = 10) habitats in each study reach (high groundwater reach [HG], moderate groundwater reach [MG], and low groundwater reach [LG]) in Kintore Creek, Ontario.

3.3.2 Reach and habitat effects on biofilms and cellulose decomposition

The GLM assessing spatial patterns in chl-*a* found the interaction of reach and habitat was significant ($F_{2,54} = 2.66$, $p = 0.08$) (Fig. 3.6a). Tukey's post-hoc tests showed three-times greater accumulation in runs than riffles in HG ($p = 0.07$). Similarly, chl-*a* accumulation in runs at MG was approximately five-times greater than in riffles ($p = 0.01$). However, no differences were found between chl-*a* accumulation in riffles and runs at LG ($p = 0.99$).

The GLM on biofilm growth rate identified a significant interaction of groundwater input and habitat ($F_{2,54} = 2.64$, $p = 0.08$) (Fig. 3.6b). Runs in HG had biofilm growth rates more

than double that of riffles (p = 0.04). Similarly, runs in MG had biofilm growth rates more than three-times greater than riffles (p = 0.02). In contrast, runs in LG had biofilm growth rates that were not different than those in riffles (p = 0.99).

The PLS regressions for biomass metrics (chl-*a* accumulation and biofilm growth rate) resulted in an interpretable model (Q^2 = 0.277) with one component. The component explained 45 % of the variance of the environmental variables and 34 % of the variance in biological variables. The component organized sites based on variation in stream velocity (VIP = 1.12) and depth (VIP = 1.38). Depth was positively associated with chl-*a* accumulation and biofilm growth rate. Conversely, stream velocity was negatively associated with chl-*a* accumulation and biofilm growth rate. Run samples from HG were located towards the positive end of the axis. All other samples were clustered in the center-left of the axis.

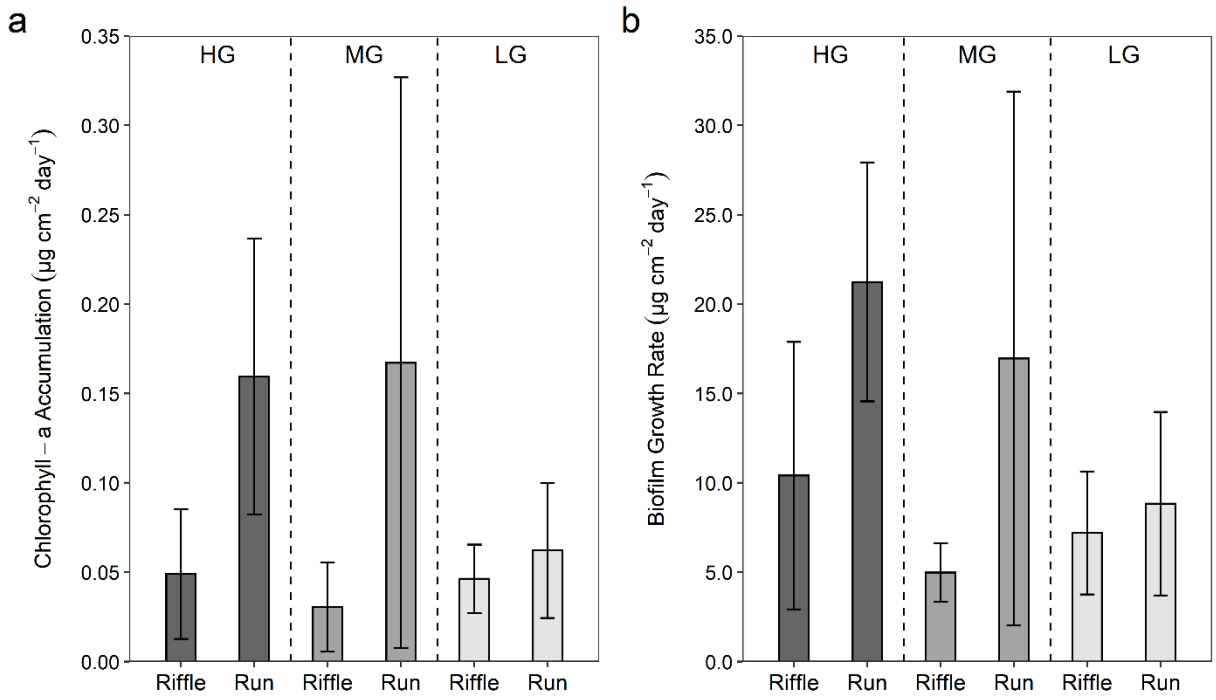

Figure 3.6 Bar plots (mean ± one standard deviation) of (a) chl-*a* accumulation (µg cm^{-2} day^{-1}) and (b) biofilm growth rate (µg cm^{-2} day^{-1}) for riffle (n = 10) and run (n = 10) habitat units in each study reach (high groundwater reach [HG], moderate groundwater reach [MG], and low groundwater reach [LG]) in Kintore Creek, Ontario.

3.3.3 Diatom Assemblages

Fifty-four diatom species were observed across all reaches and habitat units. The three most abundant taxa *Achnanthidium eutrophilum* (Lange-Bertalot 1999) Lange-Bertalot (20 %), *Amphora pediculus* (Kützing) Grunow (14 %), and *Cocconeis placentula* (Ehrenberg) (52 %) accounted for 86 % of total abundance across all reaches. Total taxa richness in HG was 33 in runs and 29 in riffles. At MG, richness was 22 in runs and 22 in riffles. From riffles to runs, *C. placentula* abundance decreased by two-thirds and *A. eutrophilum* abundance increased by about a third. In LG, total taxa richness was 25 in runs and 25 in riffles. Both riffles and runs in LG were dominated by *C. placentula*.

GLM analyses of taxa richness, % dominant, taxa evenness, and density of diatoms showed differing responses to the effects of groundwater input and habitat (Fig. 3.7). For taxa richness, there was a significant interaction of groundwater input and habitat ($F_{1,24} = 5.98$, $p = 0.005$) (Fig. 3.7a). However, there were no differences between habitats in HG ($p = 0.29$), MG ($p = 0.13$), or LG ($p = 0.87$). For % dominant, there was also a significant interaction of groundwater input and habitat ($F_{1,24} = 3.81$, $p = 0.03$) (Fig. 3.7b). There were more % dominant taxa in runs compared to riffles in MG ($p = 0.04$), but no difference in HG ($p = 0.99$) or LG ($p = 0.99$). Analysis of taxa evenness showed a non-significant interaction term ($p = 0.68$), and no effect of habitat ($p = 0.35$), but there was a difference among groundwater input levels ($F_{2,24} = 4.45$, $p = 0.02$) (Fig. 3.7c). Taxa evenness was greater in HG compared to MG ($p = 0.014$), but there were no differences between HG and LG ($p = 0.63$) nor MG and LG ($p = 0.12$). Diatom slide density had a significant interaction of groundwater input and habitat ($F_{1,24} = 4.07$, $p = 0.02$) (Fig. 3.7d). Diatom density was greater in run than in riffle habitats in HG ($p = 0.006$) and MG ($p = 0.06$), but there was no difference between habitats in LG ($p = 0.99$).

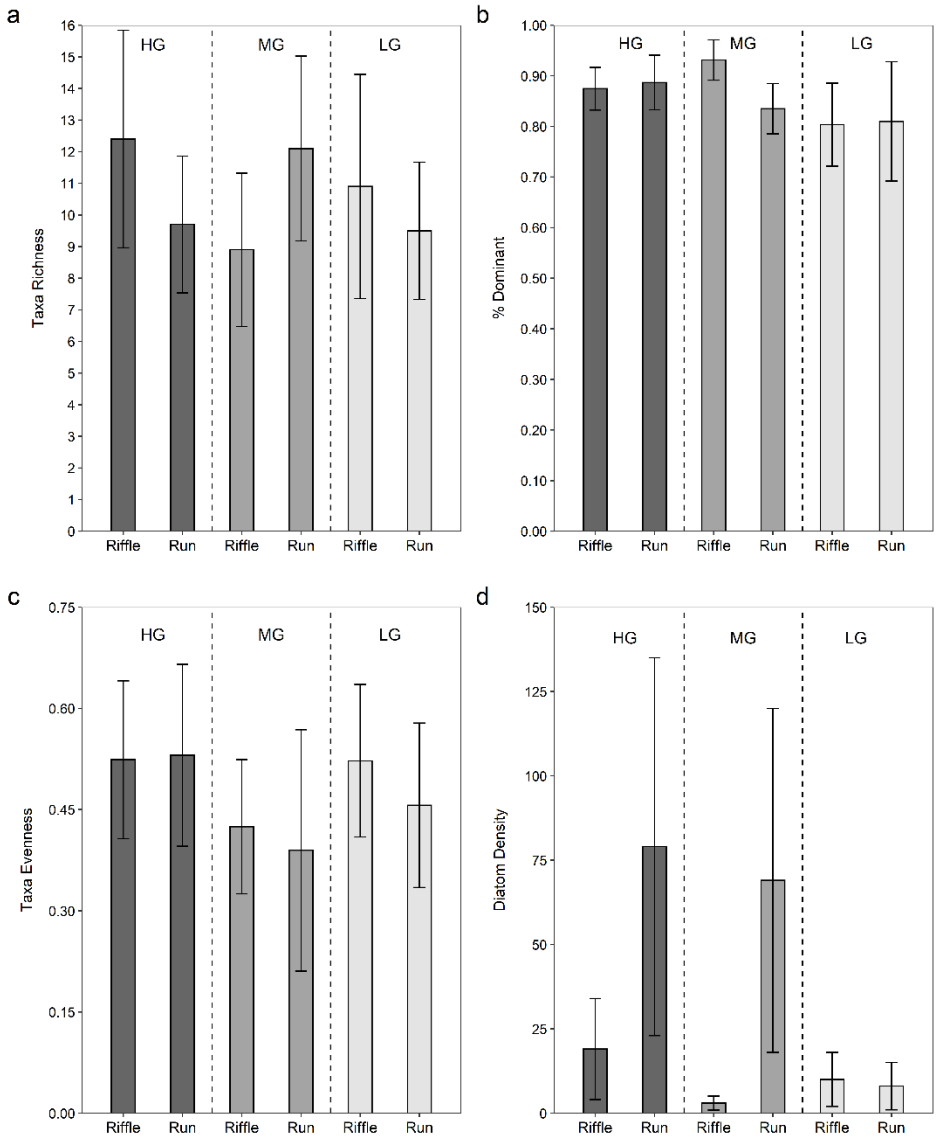

Figure 3.7 Barplots (mean ± one standard deviation) for (a) taxa richness (b) % dominant (c) evenness and (d) density of diatom for riffle (n = 10) and run (n = 10) habitat units in three study (high groundwater reach [HG], moderate groundwater reach [MG], and low groundwater reach [LG]) in Kintore Creek, Ontario.

Ordination of relative abundance of diatom assemblages showed that diatom communities in riffles and runs in HG clustered separately from those in MG and LG (Fig. 3.8). A two factor PERMANOVA showed a significant interaction between reaches of varying groundwater input and habitat (pseudo-$F_{(2,54)}$ = 2.10, p = 0.03). A post-hoc pairwise comparison of habitats with groundwater input showed that diatom assemblages in riffles and runs differed significantly in HG (p = 0.005) and MG (p = 0.006), but not in LG (p = 0.28). *C. placentula* abundance decreased by a third from riffles to runs, whereas *A. eutrophilum* abundance increased from negligible (< 2 %) in riffles to a quarter of total abundance in runs.

SIMPER analysis indicated that nearly three-quarters of total average dissimilarity (32.3 %) between runs and riffles in HG were attributed to six taxa: *C. placentula* (22.3 %), *A. eutrophilum* (14.4 %), *A. pediculus* (14.2 %), *Reimeria sinuata* (W. Gregory) Kociolek & Stoermer (6.0 %), and *Planothidium frequentissimum* (Lange-Bertalot) Lange-Bertalot (5.6 %). In MG, total average dissimilarity between runs and riffles was 36.0 %, with five taxa: *A. eutrophilum* (20.2 %), *C. placentula* (19.0 %), *A. pediculus* (12.5 %), *P. frequentissimum* (9.9 %), and *Cocconeis pediculus* (Ehrenberg 1838) (5.7 %) contributing two-thirds of total average dissimilarity. BIOENV analysis showed that depth and pH were positively correlated (r = 0.504, p = 0.001) with dissimilarity among diatom assemblages (Fig. 3.8).

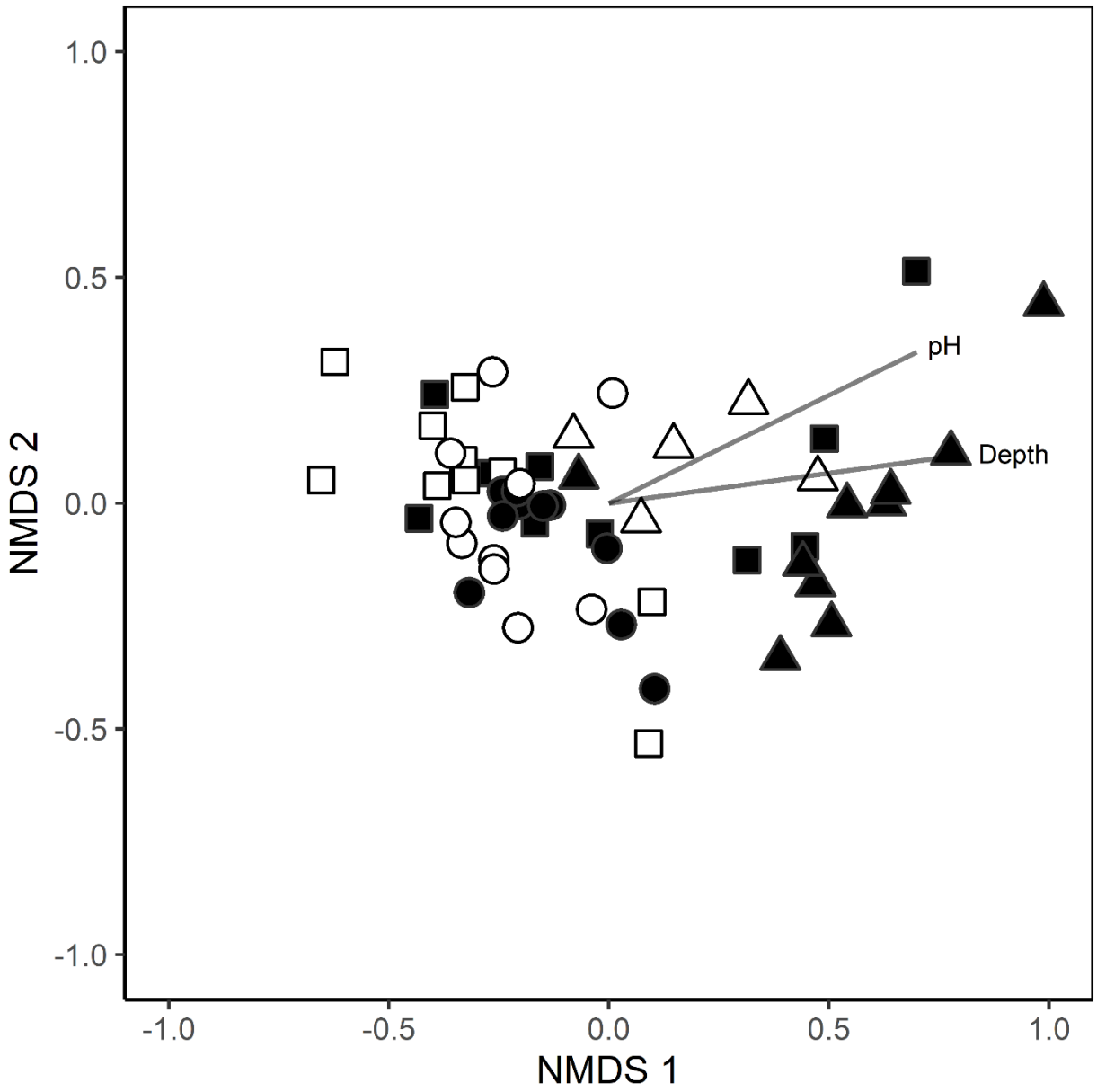

Figure 3.8 nMDS ordination plot using Bray-Curtis dissimilarity index showing separation of diatom assemblage relative abundance based on reach and habitat (stress = 0.12) with significant (r = 0.504, p = 0.001) environmental variables vectors overlaid. Reaches are represented by shape where triangles are high groundwater reach (HG), squares are moderate groundwater reach (MG), and circles are low groundwater reach (LG). Habitats are represented by open shapes for riffles and closed shapes for runs.

3.3.4 Cellulose Decomposition

Across all reaches and habitats, mean % tensile loss per day (% tensile loss day^{-1}) at the streambed surface was 1 to 2 % per day faster than in the subsurface (Fig. 3.9). The LMEM assessing differences in % tensile loss day^{-1} at the streambed surface showed a significant interaction between groundwater input and habitat ($F_{1,24}$ = 12.59, $p < 0.001$). Subsequent GLMs showed that rates of % tensile loss day^{-1} in riffles were 1.15-times faster than runs ($p < 0.001$). Rates of % tensile loss day^{-1} in riffles in HG were 10% faster than runs in HG ($p = 0.002$). Similarly, in MG rates of % tensile loss day^{-1} in riffles a third faster than runs ($p = 0.006$). However, % tensile loss day^{-1} did not differ between riffles and runs in LG ($p = 0.50$).

The PLS analysis for streambed surface % tensile loss produced an interpretable model ($Q^2 = 0.272$) comprised of one component. The component accounted for 44 % of the variance in environmental variables with stream velocity (VIP = 1.01), mean daily temperature range (VIP = 1.22), and mean daily temperature (VIP = 1.18) retained. The component also explained 34 % of the variance in streambed surface % tensile loss day^{-1}. Stream velocity, mean daily temperature range, and mean daily temperature were positively associated with surface % tensile loss day^{-1}. In HG and MG, riffle samples were typically clustered on the positive end of the axis. Runs from all reaches and riffles from LG tended to cluster in the center and center-left of the axis.

The LMEM on subsurface tensile loss showed no interaction between groundwater input and habitat ($F_{2,24} = 0.18$, $p = 0.84$), as well as no effect of habitat ($F_{1,24} = 0.69$, $p = 0.42$) (Fig. 3.9a). There was an effect of groundwater input ($F_{2,24}$ = 3.74, $p = 0.04$), such that subsurface tensile loss was faster at HG than at either MG ($p = 0.02$) and LG ($p = 0.002$) (Fig. 3.9b). There was no difference in subsurface tensile loss between MG and LG ($p = 0.70$).

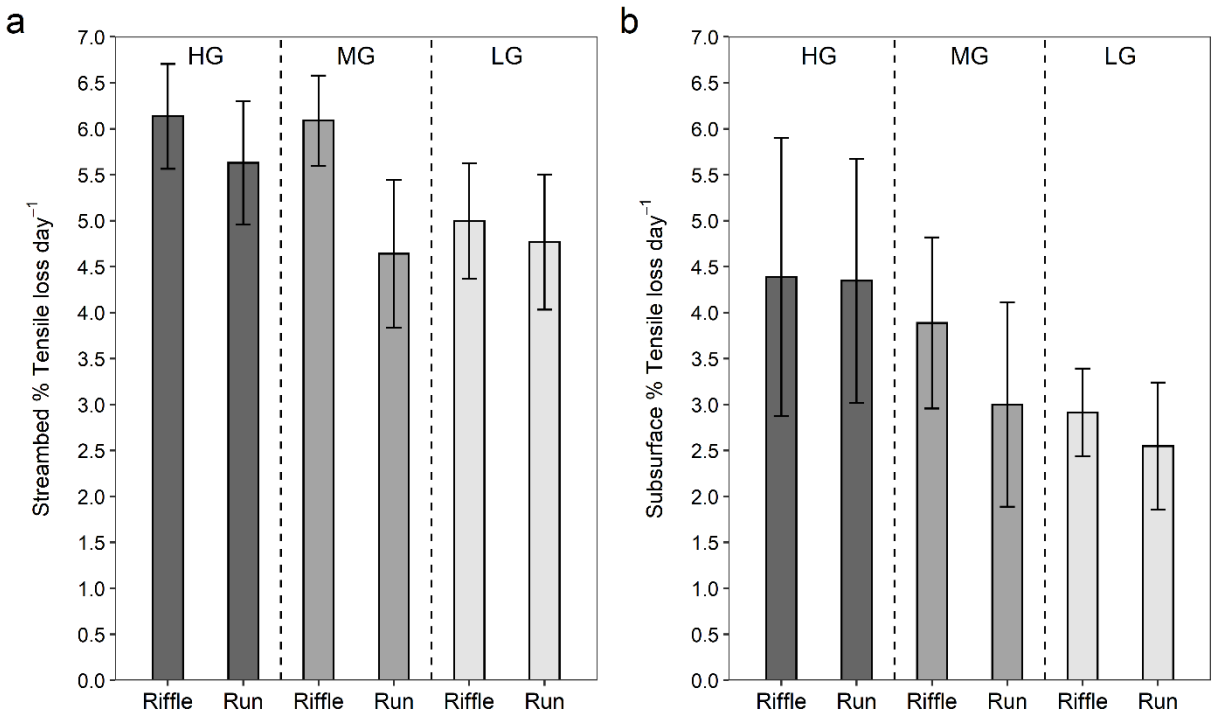

Figure 3.9 Bar plots (mean ± one standard deviation) for (a) surface cellulose decomposition (% tensile loss day^{-1}) for riffle (n = 50) and run (n = 50) habitats, and (b) subsurface cellulose decomposition (% tensile loss day^{-1}) for riffle (n = 30) and run (n = 30) habitat units in three study reaches (high groundwater reach [HG], moderate groundwater reach [MG], and low groundwater reach [LG]) in Kintore Creek, Ontario.

3.4 Discussion

3.4.1 Habitat specificity of groundwater effects on stream biofilms

Biofilm biomass, diatom assemblage composition, and cellulose decomposition differed among reaches in Kintore Creek with greater chl-*a* accumulation and biofilm growth in reaches receiving moderate and high groundwater inputs. Greater biomass in groundwater receiving reaches is consistent with past findings from a range of stream ecosystem types. For example, in an alluvial river in northwestern Montana groundwater input was typically associated with increased chl-*a* concentration and biofilm biomass (Stanford et al., 1994; Wyatt et al., 2008). Similarly, algal biomass in an alpine stream was greater downstream of a

groundwater spring (Roy et al., 2011). Likewise, groundwater inputs promoted algal production in the Fitzroy River, Australia (Burrows et al., 2020). Past work has also found evidence that groundwater inputs influence diatom assemblage composition. Indeed, Roy et al. (2011) and Stevenson et al. (2009) both observed stream reaches with significant groundwater inputs to exhibit compositionally distinct diatom assemblage composition compared to stream reaches not receiving groundwater. Additionally, past work has shown that groundwater inputs are associated with slower cellulose decomposition rates in warmer seasons (Griffiths & Tiegs, 2016; Poisson & Yates, 2022). However, unlike many past studies, our study found that effects of groundwater were habitat specific.

Many of the ecological endpoints assessed in our study were indicative of an interactive effect of groundwater input and habitat. Indeed, we found that runs in reaches with moderate to high groundwater input had 2-3 times greater chl-*a* accumulation and biofilm growth rates, as well as greater diatom density than associated riffles. Likewise, diatom composition shifted in dominant taxa from *C. placentula* in riffles to *A. eutrophilum* in runs. Finally, we found that rates of tensile loss at the streambed surface (but not buried) were greater in the reach with high groundwater inputs. Thus, it appears that stream biofilm communities at the streambed experience effects of groundwater inputs differently based on habitat type.

Habitat specific manifestation of groundwater effects is consistent with known groundwater – surface water exchange patterns (i.e., upwelling and downwelling) in riffles and runs. At the beginning of riffles, downward pressure has been shown to result in surface water downwelling, followed by groundwater upwelling at the end of the riffle or start of the subsequent run (Thibodeaux & Boyle, 1987; Harvey & Bencala, 1993). Thus, groundwater inputs may have been suppressed in riffles but expressed in runs, leading to the habitat specific outcomes we observed. However, as suppression of groundwater inputs to riffles is not fully supported by the subsurface temperature measures, other microscale factors (e.g., chemical constituents, redox) may also be important in determining the observed ecological patterns that manifested at the habitat scale. Future work that directly captures the amount and characteristics (e.g., nutrient concentrations) of upwelling groundwater are thus needed to

validate the role of habitat type as a modifier of groundwater – surface water exchange patterns and provide a mechanistic link between groundwater input and stream biofilm communities.

Although biological patterns matched expected associations between habitat type and effects of groundwater inputs, these differences also corresponded to patterns of stream velocity in the groundwater receiving reaches. As stream velocity has been well-demonstrated to influence algal biomass, diatom assemblage composition, and cellulose decomposition (Horner et al., 1990; Biggs & Gerbeaux, 1993; Biggs & Hickey, 1994; Biggs et al., 1998; Tiegs et al., 2009; Webb et al., 2019), it is possible that velocity may have partially accounted for the patterns we observed. Indeed, a modifying role of stream velocity on groundwater inputs was reported by Burrows et al. (2020) who suggested that greater environmental stability in areas of slower velocity coupled with enhanced delivery of resources (e.g., chemical constituents, nutrients, and thermal effects) via groundwater input cumulatively acted to enhance algal biomass accumulation. Differences in stream velocity may have also impacted diatom community composition, as diatoms have shown varying preferences to velocity (Van Dam et al., 1994; Passy, 2007). Conversely, faster velocities and greater sheer stress in riffles compared to runs may more rapidly dissipate the effects of groundwater inputs close to the streambed surface (Storey et al., 2003). Cumulative effects of stream velocity and moderate to high groundwater input are also consistent with the patterns of cellulose decomposition we observed as the increased velocity and associated enhancement of physical breakdown may have further accelerated decomposition in riffles (Tiegs et al., 2009; Webb et al., 2019). However, it is unlikely that the observed biological patterns were solely because of velocity. We base this conclusion on our finding no biological differences between habitat types in the low groundwater reach, despite this reach exhibiting similar velocity patterns to the moderate and high groundwater reaches. Our results suggest that the role of stream velocity is, at most, subsidiary to that of groundwater, and therefore additional studies are needed to test hypotheses regarding the apparent cumulative effects of groundwater input and stream velocity.

3.4.2 Groundwater modified environmental drivers of stream biofilms

Although we detected a relationship between stream biofilm metrics and groundwater input, we did not observe associations between measured stream environmental parameters that can be modified by groundwater and the observed ecological heterogeneity. The lack of association between ecological endpoints and measured environmental parameters in reaches of Kintore Creek is in contrast with past studies in low nutrient streams (i.e., < 5 μg P L^{-1} SRP, < 0.50 mg N L^{-1} NO_3^--N) that have suggested that groundwater inputs were associated with greater benthic algal biomass and heterotrophic microbial activity (Wyatt et al., 2008; Roy et al., 2011; Fellman et al., 2014; Griffiths & Tiegs, 2016; Mejia et al., 2016; Burrows et al., 2020). The difference in our results compared to past studies may be due to reaches in our study having more or similar amounts of nutrients in the surface water compared to groundwater inputs (C. Robinson, unpublished data). Likewise, we found that mean daily temperature of stream water at the bed was 18 °C and varied by approximately 2 °C across all reaches and habitats, despite indications from temperature mapping of significant groundwater flux in the high and moderate groundwater reaches. As previous work has suggested that differences in temperature need to be at least 3 °C and 4 – 5 °C, to impact chl-*a* and cellulose decomposition, respectively (Godwin & Carrick, 2008; Griffiths & Tiegs, 2016; Delgado et al., 2017; Follstad Shah et al., 2017), it appears groundwater inputs were insufficient to affect stream biota through control of stream temperatures. Indeed, the lack of among reach variation in nutrients and temperature suggests that impacts of groundwater inputs may have been masked by prevailing surface water conditions.

Streambed temperature mapping of the three reaches of Kintore Creek indicated patchiness in groundwater input within the high and moderate groundwater reaches. However, the observed spatial patterns of groundwater inputs were not detectable at the reach or habitat unit scales with the approaches we used to measure to environmental conditions where biofilms were sampled. Thus, it appears that in Kintore Creek, effects of groundwater inputs may have been rapidly dissipated at the streambed – surface water interface. Alternatively, the ecological response observed in groundwater receiving reaches may have been due to unaccounted

environmental differences among reaches rather than groundwater inputs. However, this second explanation is unlikely as we found that reaches with high and moderate groundwater input showed similar ecological patterns. Rather, our findings of biological variation among reaches, without associations to reach scale environmental conditions, suggest that stream biofilm communities and cellulose breakdown may have been more strongly linked to microscale environmental conditions at the stream water – biofilm interface. However, measuring environmental conditions at such microscales is a methodologically challenging endeavor and was beyond the scope of this study. Future studies using novel methods to capture environmental conditions at the stream water – biofilm interface are thus needed to further our understanding of the role of groundwater inputs in structuring stream communities and processes.

3.4.3 Effect of burial on cellulose decomposition

We observed strips on the streambed surface generally had faster breakdown rates than strips buried in the substrate; a finding consistent with past studies (Boulton & Quinn, 2000; Claret et al., 2001; Cornut et al., 2010). Slower subsurface cellulose breakdown in the streambed has been attributed to reduced physical abrasion, as well as lower temperature and dissolved oxygen limiting heterotrophic activity in the hyporheic zone (Strommer & Smock, 1989; Malard & Hervant, 1999; Crenshaw et al., 2002; Cornut et al., 2010). The differences in decomposition between the streambed surface and subsurface highlight the need for measurement of both surface and subsurface decomposition to fully describe rates of organic matter processing in streams.

For subsurface cellulose breakdown, we found that the reach with high groundwater input was associated with faster subsurface cellulose breakdown compared to the moderate and low groundwater reaches. Our results are in contrast to past work that suggest that higher groundwater inputs would slow subsurface decomposition due to cooler water temperatures and lower dissolved oxygen (Štěrba et al., 1992; Boulton & Foster, 1998; Franken et al., 2001). A potential explanation is that greater groundwater – surface water exchange in the high groundwater reach may have stimulated heterotrophic decomposers in the streambed through

greater access to key biogeochemical resources (e.g., DOC, nutrients). However, because we did not sample subsurface conditions (e.g., dissolved oxygen) aside from temperature, our study is limited in explaining the observed patterns. Thus, future studies should focus on investigating the controls of organic matter breakdown in the subsurface when varying amount of groundwater is present.

3.5 Summary

We found that the ecological response to groundwater input manifested in specific habitat types and varied depending on the biological measure. In reaches receiving moderate to high groundwater inputs, biofilm biomass was greater in runs, and streambed cellulose breakdown was faster in riffles. However, ecological patterns were not associated with our measurements of surface water temperature or nutrient availability, suggesting that some controlling factors were not measured (e.g., chemical characteristics of upwelling groundwater), or that impacts of groundwater inputs may have dissipated rapidly at the streambed interface, and thus were not captured by our environmental measurements. Indeed, we suspect that the effect of groundwater inputs may be limited to streambed surface interface, where biofilms experience and interact with the stream environment. Future work on the effect of groundwater inputs on stream biofilm communities and cellulose decomposition in enriched streams should focus on assessments in multiple habitat types and environmental measurements at the stream water – biofilm interface.

3.6 References

Agriculture and Agri-Food Canada (2020) AAFC annual crop inventory 2019. https://open.canada.ca/data/en/dataset/d90a56e8-de27-4354-b8ee-33e08546b4fc. Accessed 13 Feb 2021

Atkinson, A. P., I. Cartwright, B. S. Gilfedder, H. Hofmann, N. P. Unland, D. I. Cendón, & R. Chisari, 2015. A multi-tracer approach to quantifying groundwater inflows to an upland river; assessing the influence of variable groundwater chemistry. Hydrological Processes 29: 1–12, https://doi.org/10.1002/hyp.10122.

Bates, D., M. Mächler, B. M. Bolker, & S. C. Walker, 2015. Fitting linear mixed-effects models using lme4. Journal of Statistical Software. https://doi.org/10.18637/jss.v067.i01.

Battin, T. J., K. Besemer, M. M. Bengtsson, A. M. Romani, & A. I. Packmann, 2016. The ecology and biogeochemistry of stream biofilms. Nature Reviews Microbiology 14: 251–263, https://doi.org/10.1038/nrmicro.2016.15.

Battin, T. J., L. A. Kaplan, J. D. Newbold, & C. M. E. Hansen, 2003. Contributions of microbial biofilms to ecosystem processes in stream mesocosms. Nature 426: 439–442, https://doi.org/10.1038/nature02152.

Benfield, E. F., K. M. Fritz, & S. D. Tiegs, 2017. Leaf-litter breakdown In Lamberti, G. A., & F. R. Hauer (eds), Methods in Stream Ecology, Volume 2: Ecosystem Function. Elsevier, Academic Press: 71–82, https://doi.org/10.1016/B978-0-12-813047-6.00005-X.

Besemer, K., 2015. Biodiversity, community structure and function of biofilms in stream ecosystems. Research in Microbiology 166: 774–781, https://doi.org/10.1016/j.resmic.2015.05.006.

Bey, M., & L. Ector, 2013. Atlas des diatomées des cours d'eau de la région Rhône-Alpes − Tomes 1 à 6. DREAL, Rhône-Alpes.

Biggs, B. J. F., 1995. The contribution of flood disturbance, catchment geology and land use to the habitat template of periphyton in stream ecosystems. Freshwater Biology 33: 419–438, https://doi.org/10.1111/j.1365-2427.1995.tb00404.x.

Biggs, B. J. F., & P. Gerbeaux, 1993. Periphyton development in relation to macro-scale (geology) and micro-scale (velocity) limiters in two gravel-bed rivers, New Zealand. New Zealand Journal of Marine and Freshwater Research 27: 39–53, https://doi.org/10.1080/00288330.1993.9516544.

Biggs, B. J. F., D. G. Goring, & V. I. Nikora, 1998. Subsidy and stress responses of stream periphyton to gradients in water velocity as a function of community growth form. Journal of Phycology 34: 598–607, https://doi.org/10.1046/j.1529-8817.1998.340598.x.

Biggs, B. J. F., & C. W. Hickey, 1994. Periphyton responses to a hydraulic gradient in a regulated river in New Zealand. Freshwater Biology John Wiley & Sons, Ltd 32: 49–59, https://doi.org/https://doi.org/10.1111/j.1365-2427.1994.tb00865.x.

Biggs, B. J. F., V. I. Nikora, & T. H. Snelder, 2005. Linking scales of flow variability to lotic ecosystem structure and function. River Research and Applications 21: 283–298, https://doi.org/10.1002/rra.847.

Boano, F., J. W. Harvey, A. Marion, A. I. Packman, R. Revelli, L. Ridolfi, & A. Wörman, 2014. Hyporheic flow and transport processes. Reviews of Geophysics 52: 603–679, https://doi.org/10.1002/2012RG000417.

Borchardt, M., 1996. Nutrients In Stevenson, R. J., M. Bothwell, & R. Low (eds), Algal ecology: freshwater benthic ecosystems. Academic Press, San Diego, CA, USA: 183–227.

Boulton, A. J., & J. G. Foster, 1998. Effects of buried leaf litter and vertical hydrologic exchange on hyporheic water chemistry and fauna in a gravel-bed river in northern New South Wales, Australia. Freshwater Biology 40: 229–243, https://doi.org/10.1046/j.1365-2427.1998.00345.x.

Boulton, A. J., & P. J. Hancock, 2006. Rivers as groundwater-dependent ecosystems: A review of degrees of dependency, riverine processes and management implications. Australian Journal of Botany 54: 133–144, https://doi.org/10.1071/BT05074.

Boulton, A. J., & J. M. Quinn, 2000. A simple and versatile technique for assessing cellulose decomposition potential in floodplain and riverine sediments. Archiv für Hydrobiologie 150: 133–151, https://doi.org/10.1127/archiv-hydrobiol/150/2000/133.

Brunke, M., & T. Gonser, 1997. The ecological significance of exchange processes between rivers and groundwater. Freshwater Biology 37: 1–33, https://doi.org/10.1046/j.1365-2427.1997.00143.x.

Burrows, R. M., L. Beesley, M. M. Douglas, B. J. Pusey, & M. J. Kennard, 2020. Water velocity and groundwater upwelling influence benthic algal biomass in a sandy tropical river: implications for water-resource development. Hydrobiologia 847: 1207–1219, https://doi.org/10.1007/s10750-020-04176-3.

Carrascal, L. M., I. Galván, & O. Gordo, 2009. Partial least squares regression as an alternative to current regression methods used in ecology. Oikos 118: 681–690, https://doi.org/10.1111/j.1600-0706.2008.16881.x.

Clapcott, J. E., & L. A. Barmuta, 2010. Metabolic patch dynamics in small headwater streams: Exploring spatial and temporal variability in benthic processes. Freshwater Biology 55: 806–824, https://doi.org/10.1111/j.1365-2427.2009.02324.x.

Claret, C., A. J. Boulton, M.-J. Dole-Olivier, & P. Marmonier, 2001. Functional processes versus state variables: interstitial organic matter pathways in floodplain habitats. Canadian Journal of Fisheries and Aquatic Sciences 58: 1594–1602, https://doi.org/10.1139/cjfas-58-8-1594.

Clarke, K. R., & R. N. Gorley, 2015. Primer v7: User manual/tutorial. Primer-E. Plymouth, UK, 93.

Clarke, K. R., & R. M. Warwick, 1994. Similarity-based testing for community pattern: the two-way layout with no replication. Marine Biology 118: 167–176, https://doi.org/10.1007/BF00699231.

Coleman, R. L., & C. N. Dahm, 1990. Stream geomorphology: effects on periphyton standing crop and primary production. Journal of the North American Benthological Society 9: 293–302, https://doi.org/10.2307/1467897.

Conant, B., C. E. Robinson, M. J. Hinton, & H. A. J. Russell, 2019. A framework for conceptualizing groundwater-surface water interactions and identifying potential impacts on water quality, water quantity, and ecosystems. Journal of Hydrology 574: 609–627, https://doi.org/10.1016/j.jhydrol.2019.04.050.

Cook, P. G., 2013. Estimating groundwater discharge to rivers from river chemistry surveys. Hydrological Processes 27: 3694–3707, https://doi.org/10.1002/hyp.9493.

Cornut, J., A. Elger, D. Lambrigot, P. Marmonier, & E. Chauvet, 2010. Early stages of leaf decomposition are mediated by aquatic fungi in the hyporheic zone of woodland streams. Freshwater Biology 55: 2541–2556, https://doi.org/10.1111/j.1365-2427.2010.02483.x.

Crenshaw, C. L., H. M. Valett, & J. L. Tank, 2002. Effects of coarse particulate on fungal biomass and organic matter in invertebrate the of subsurface a headwater stream density. Journal of the North American Benthological Society 21: 28–42, https://doi.org/https://doi.org/10.2307/1468297.

Cummins, K. W., 1974. Structure and function of stream ecosystems. BioScience 24: 631–641, https://doi.org/https://doi.org/10.2307/1296676.

Delgado, C., S. F. P. Almeida, C. L. Elias, V. Ferreira, & C. Canhoto, 2017. Response of biofilm growth to experimental warming in a temperate stream. Ecohydrology 10: 1–9, https://doi.org/10.1002/eco.1868.

Dent, C. L., N. B. Grimm, & S. G. Fisher, 2001. Multiscale effects of surface-subsurface exchange on stream water nutrient concentrations. Journal of the North American Benthological Society 20: 162–181, https://doi.org/10.2307/1468313.

Environment and Climate Change Canada, 2010. Canadian Climate Normals. https://climate.weather.gc.ca/climate_normals/. Accessed 22 March 2021.

Eriksson, L., T. Bryne, E. Johansson, J. Trygg, & C. Wiksröm, 2013. Multi-and megavariate data analysis: part I: basic principles and applications. Umetrics AB, Umeå.

Fellman, J. B., R. G. M. Spencer, P. A. Raymond, N. E. Pettit, G. Skrzypek, P. J. Hernes, & P. F. Grierson, 2014. Dissolved organic carbon biolability decreases along with its modernization in fluvial networks in an ancient landscape. Ecology 95: 2622–2632, https://doi.org/10.1890/13-1360.1.

Follstad Shah, J. J., J. S. Kominoski, M. Ardón, W. K. Dodds, M. O. Gessner, N. A. Griffiths, C. P. Hawkins, et al., 2017. Global synthesis of the temperature sensitivity of leaf litter breakdown in streams and rivers. Global Change Biology 23: 3064–3075, https://doi.org/10.1111/gcb.13609.

Forsyth, D. K., C. M. Riseng, K. E. Wehrly, L. A. Mason, J. Gaiot, T. Hollenhorst, C. M. Johnston, et al., 2016. The Great Lakes hydrography dataset: Consistent, binational watersheds for the Laurentian Great Lakes basin. Journal of the American Water Resources Association 52: 1068–1088, https://doi.org/10.1111/1752-1688.12435.

Franken, R. J. M., R. G. Storey, & D. Dudley Williams, 2001. Biological, chemical and physical characteristics of downwelling and upwelling zones in the hyporheic zone of a north-temperate stream. Hydrobiologia 444: 183–195, https://doi.org/10.1023/A:1017598005228.

Godwin, C. M., & H. J. Carrick, 2008. Spatio-temporal variation of periphyton biomass and accumulation in a temperate spring-fed stream. Aquatic Ecology 42: 583–595, https://doi.org/10.1007/s10452-007-9133-z.

Graça, M. A. S., V. Ferreira, C. Canhoto, A. C. Encalada, F. Guerrero-Bolaño, K. M. Wantzen, & L. Boyero, 2015. A conceptual model of litter breakdown in low order streams. International Review of Hydrobiology 100: 1–12, https://doi.org/10.1002/iroh.201401757.

Griffiths, N. A., & S. D. Tiegs, 2016. Organic-matter decomposition along a temperature gradient in a forested headwater stream. Freshwater Science 35: 518–533, https://doi.org/10.1086/685657.

Harvey, J. W., & E. Bencala, 1993. The effect of streambed topography on surface-subsurface water exchange in mountain catchments. 29: 89–98, https://doi.org/https://doi.org/10.1029/92WR01960.

Horner, R. R., E. B. Welch, M. R. Seeley, & J. M. Jacoby, 1990. Responses of periphyton to changes in current velocity, suspended sediment and phosphorus concentration. Freshwater Biology 24: 215–232, https://doi.org/10.1111/j.1365-2427.1990.tb00704.x.

Jowett, I. G., 1993. A method for objectively identifying pool, run, and riffle habitats from physical measurements. New Zealand Journal of Marine and Freshwater Research 27: 241–248, https://doi.org/10.1080/00288330.1993.9516563.

Kalbus, E., F. Reinstorf, & M. Schirmer, 2006. Measuring methods for groundwater - surface water interactions: A review. Hydrology and Earth System Sciences 10: 873–887, https://doi.org/10.5194/hess-10-873-2006.

Krause, S., D. M. Hannah, & T. Blume, 2011. Transformation ecosystem change and ecohydrology: ushering in a new era for watershed management. Ecohydrology 4: 549–563, https://doi.org/10.1002/eco.199.

Kuznetsova, A., P. B. Brockhoff, & R. H. B. Christensen, 2017. lmerTest Package: Tests in Linear Mixed Effects Models. Journal of Statistical Software 82: 1–26, https://doi.org/10.18637/JSS.V082.I13.

Lavoie, I., S. Campeau, N. Zugic-Drakulic, J. G. Winter, & C. Fortin, 2014. Using diatoms to monitor stream biological integrity in Eastern Canada: An overview of 10 years of index

development and ongoing challenges. Science of the Total Environment 475: 187–200, https://doi.org/10.1016/j.scitotenv.2013.04.092.

Lavoie, I., P. Hamilton, S. Campeau, M. Grenier, & P. J. Dillon, 2008. Guide d'identification des diatomées des rivières de l'Est du Canada. Presses de L'Université du Québec, Québec.

Legendre, P., & E. D. Gallagher, 2001. Ecologically meaningful transformations for ordination of species data. Oecologia 129: 271–280, https://doi.org/10.1007/s004420100716.

Lewandowski, J., S. Arnon, E. Banks, O. Batelaan, A. Betterle, T. Broecker, C. Coll, J. D. et al., 2019. Is the hyporheic zone relevant beyond the scientific community? Water (Switzerland) 11: https://doi.org/10.3390/w11112230.

Malard, F., & F. Hervant, 1999. Oxygen supply and the adaptations of animals in groundwater. Freshwater Biology 41: 1–30, https://doi.org/10.1046/j.1365-2427.1999.00379.x.

Martínez, A., A. Larrañaga, J. Pérez, E. Descals, & J. Pozo, 2014. Temperature affects leaf litter decomposition in low-order forest streams: field and microcosm approaches. Microbiology Ecology 87: 257–267, https://doi.org/10.1111/1574-6941.12221.

Mejia, F. H., C. V. Baxter, E. K. Berntsen, & A. K. Fremier, 2016. Linking groundwater – surface water exchange to food production and salmonid growth. Canadian Journal of Fisheries and Aquatic Sciences 73: 1650–1660, https://doi.org/10.1139/cjfas-2015-0535.

Minshall, G. W., 1978. Autotrophy in stream ecosystems. BioScience 28: 767–771, https://doi.org/10.2307/1307250.

Mulholland, P. J., 1996. Role in nutrient cycling in streams In Stevenson, R. J., M. Bothwell, & R. Lowe (eds), Algal ecology: freshwater benthic ecosystems. Academic Press, San Diego, CA, USA: 609–639.

Oksanen, J., F. G. Blanchet, M. Friendly, R. Kindt, P. Legendre, D. McGlinn, P. R. Minchin, R. B. et al., 2020. vegan: community ecology package.

Ontario Geological Survey, 2010. Surficial geology of southern Ontario; Ontario Geological Survey, Miscellaneous Release Data 128 - Revised.

Passy, S. I., 2007. Diatom ecological guilds display distinct and predictable behavior along nutrient and disturbance gradients in running waters. Aquatic Botany 86: 171–178, https://doi.org/10.1016/j.aquabot.2006.09.018.

Petersen, R. C., & K. W. Cummins, 1974. Leaf processing in a woodland stream. Freshwater Biology 4: 343–368, https://doi.org/https://doi.org/10.1111/j.1365-2427.1974.tb00103.x.

Poisson, R., & A. G. Yates, 2022. Impaired cellulose decomposition in a headwater stream receiving subsurface agricultural drainage. Ecological Processes 11: 1–17, https://doi.org/10.1186/s13717-022-00406-9.

R Core Team, 2020. R: A language and environment for statistical computing. R Foundation for Statistical Computing, Vienna, Austria.

Renard, P., & D. Allard, 2013. Connectivity metrics for subsurface flow and transport. Advances in Water Resources Elsevier Ltd 51: 168–196, https://doi.org/10.1016/j.advwatres.2011.12.001.

Roy, J. W., B. Zaitlin, M. Hayashi, & S. B. Watson, 2011. Influence of groundwater spring discharge on small-scale spatial variation of an alpine stream ecosystem. 670: 661–670, https://doi.org/10.1002/eco.

Royer, T. V, & G. W. Minshall, 2003. Controls on leaf processing in streams from spatial-scaling and hierarchical perspectives. Journal of the North American Benthological Society 22: 352–358, https://doi.org/https://doi.org/10.2307/1468266.

Sanchez, G., 2016. plsdepot: partial least squares data analysis methods. Version 0.1.17.

Stanford, J. A., J. V Ward, & B. K. Ellis, 1994. Ecology of the alluvial aquifers of the Flathead River, Montana In Gibert, J., D. L. Danielopol, & J. A. Stanford (eds), Groundwater Ecology. Academic Press, San Diego, USA: 367–390.

Steinman, A. D., G. A. Lamberti, & P. R. Leavitt, 2007. Biomass and pigments of benthic algae In Hauer, F. R., & G. Lamberti (eds), Methods in Stream Ecology. Academic Press, San

Diego, CA, USA: 357–379, https://doi.org/https://doi.org/10.1016/B978-012332908-0.50024-3.

Štěrba, O., V. Uvíra, P. Mathur, & M. Rulík, 1992. Variations of the hyporheic zone through a riffle in the R. Morava, Czechoslovakia. Regulated Rivers: Research & Management 7: 31–43, https://doi.org/10.1002/rrr.3450070106.

Stevenson, R. J., 1997. Scale-dependent determinants and consequences of benthic algal heterogeneity. Journal of the North American Benthological Society 16: 248–262, https://doi.org/10.2307/1468255.

Stevenson, R.J., Novoveska, L., C.M. Riseng, & M.J., Wiley, 2009. Comparing responses of diatom species composition to natural and anthropogenic factors in streams of glaciated ecoregions. Nova Hedwigia 135: 1–13.

Storey, R. G., K. W. F. Howard, & D. D. Williams, 2003. Factors controlling riffle-scale hyporheic exchange flows and their seasonal changes in a gaining stream : A three-dimensional groundwater flow model. Water Resources Research 39: 1–17, https://doi.org/10.1029/2002WR001367.

Strommer, J. L., & L.A. Smock, 1989. Vertical distribution and abundance of invertebrates within the sandy substrate of a low-gradient headwater stream. Freshwater Biology 22: 263–274, https://doi.org/https://doi.org/10.1111/j.1365-2427.1989.tb01099.x.

Thibodeaux, L., & J. Boyle, 1987. Bedform-generated convective transport in bottom sediment. Nature 325: 341–343, https://doi.org/doi-org/10.1038/325341a0.

Tiegs, S. D., P. O. Akinwole, & M. O. Gessner, 2009. Litter decomposition across multiple spatial scales in stream networks. Oecologia 161: 343–351, https://doi.org/10.1007/s00442-009-1386-x.

Tiegs, S. D., J. E. Clapcott, N. A. Griffiths, & A. J. Boulton, 2013. A standardized cotton-strip assay for measuring organic-matter decomposition in streams. Ecological Indicators 32: 131–139, https://doi.org/10.1016/j.ecolind.2013.03.013.

Tiegs, S. D., D. Costello, M. Isken, G. Woodward, P. McIntyre, M. O. Gessner, E. Chauvet, N. A. Griffiths, A. Flecker, V. Acuña, & R. Albariño, 2019. Global patterns and drivers of ecosystem functioning in rivers and riparian zones. Science Advances 5: 1–8, https://doi.org/10.1126/sciadv.aav0486.

Van Dam, H., A. Mertens, & J. Sinkeldam, 1994. A coded checklist and ecological indicator values of freshwater diatoms from The Netherlands. Netherlands Journal of Aquatic Ecology 28: 117–133, https://doi.org/10.1007/BF02334251.

Vissers, M. A., J. W. Roy, A. G. Yates, K. Robinson, S. Rakhimbekova, & C. E. Robinson, 2023. Spatio-temporal variability of porewater phosphorus concentrations in streambed sediments of an agricultural stream. Journal of Hydrology 617: 129133, https://doi.org/10.1016/j.jhydrol.2023.129133.

Webb, J. R., N. J. T. Pearce, K. J. Painter, & A. G. Yates, 2019. Hierarchical variation in cellulose decomposition in least-disturbed reference streams: a multi-season study using the cotton strip assay. Landscape Ecology 34: 2353–2369, https://doi.org/10.1007/s10980-019-00893-w.

Wold, S., M. Sjöström, & L. Eriksson, 2001. PLS-regression: A basic tool of chemometrics. Chemometrics and Intelligent Laboratory Systems 58: 109–130, https://doi.org/10.1016/S0169-7439(01)00155-1.

Wyatt, K. H., F. R. Hauer, & G. F. Pessoney, 2008. Benthic algal response to hyporheic-surface water exchange in an alluvial river. Hydrobiologia 607: 151–161, https://doi.org/10.1007/s10750-008-9385-1.

4 Influence of groundwater upwelling on patch scale patterns of stream biofilm communities and cellulose decomposition in an agricultural stream reach

4.1 Introduction

Spatial heterogeneity of stream environmental conditions observed at the reach scale can be viewed as an aggregation of heterogeneity at smaller spatial scales, hereafter referred to as patch scale (Pringle et al., 1988; Townsend, 1989). Environmental heterogeneity at the patch scale can result from variations in stream velocity, water temperature, and water chemistry, among other factors (Thorp et al., 2006, 2008). Environmental variation amongst patches can also be driven by groundwater – surface water exchange through the streambed (Brunke & Gonser, 1997; Boano et al., 2014). Indeed, groundwater inputs can modify surface water nutrient availability, water temperature, and water chemistry at centimeter to meter scales (Schilling et al., 2017; Earon et al., 2020). Where differences in physical and chemical properties between groundwater and surface waters are substantive these small-scale variations in environmental conditions may influence spatial patterns in biotic processes and assemblages (Boulton & Hancock, 2006; Boano et al., 2014; Irvine & Lautz, 2015).

Benthic stream biofilm communities consist of microbial autotrophs and heterotrophs, that include algae, bacteria and fungi that are attached to the streambed. Biofilm communities are highly sensitive to changes in local environmental conditions (Besemer, 2015; Battin et al., 2016). Indeed, environmental variability within reaches have been shown to influence biofilm communities and organic matter processing (Gulis & Suberkropp, 2003; Webb et al., 2019; Risse-Buhl et al., 2020; Banks et al., 2023b). Heterogeneity in environmental factors at multiple spatial scales can influence biological patterns in streams (Palmer & Poff, 1997). Within a reach, variability in habitat and microhabitat conditions can influence patch scale heterogeneity in biofilms (Stevenson, 1997; Royer & Minshall, 2003; Graça et al., 2015). Indeed, past work has shown that stream velocity can vary between habitat types (i.e., riffle, runs) and near-bed velocities can generate heterogeneity in biofilms (Biggs et al., 1998, 2005; Battin et al., 2003). Further, Cardinale et al., (2002) showed that within a riffle, physical heterogeneity in streambed sediments had significant impacts on primary productivity and

respiration in biofilms through alteration of stream velocity. However, in a study of diatom community assemblage, Passy, (2001) found only a third of variability in was explained by measured environmental and spatial variables, primarily stream velocity, suggesting that other factors may be contributing to variation in diatom communities. Similarly, unexplained variance in decomposition across multiple spatial scales has been observed. For example, more variance was found to be explained at the litter bag and habitat scale, rather than larger (i.e., watershed, segment, reach) scales (Tiegs et al., 2009; Tonin et al., 2018). Though smaller scales tend to contribute the most variance explained, Tonin et al., (2018) found, while nearly a third of total variance was unexplained. Likewise, Tiegs et al., (2009) over half of the variance remained unexplained by measured environmental variables. The consistent findings of unexplained variation across various components of the biofilm suggest that there are unmeasured environmental factors contributing to heterogeneity in biofilm. Heterogeneity in stream biofilm communities has been associated with groundwater inputs at multiple scales (i.e., spatial and temporal) across stream ecosystems (Valett et al., 1994; Wyatt et al., 2008; Stevenson et al., 2009; Tang et al., 2019; Banks et al., 2023a).

Within reaches, at both habitat and patch scales, groundwater input can alter environmental conditions in receiving surface waters (Brunke & Gonser, 1997; Dent et al., 2001; Boano et al., 2014). Groundwater influenced changes to environmental conditions at smaller (i.e., habitat) scales has been shown to generate heterogeneity in biofilm communities (Pepin & Hauer, 2002; Roy et al., 2011; Mejia et al., 2016; Burrows et al., 2020; Banks et al., 2023b). Locations of groundwater upwelling has been repeatedly associated with greater primary production and differences in algal community composition (Coleman & Dahm, 1990; Roy et al., 2011; Bolpagni & Laini, 2016; Mejia et al., 2016; Burrows et al., 2020). Areas of groundwater upwelling in a reach have also been suggested to enhance organic breakdown by providing nutrient subsidies to heterotrophic microbial decomposers (Griffiths & Tiegs, 2016). Conversely, cooler upwelling groundwater has been associated with reduced activity of heterotrophic microbes and slower cellulose decomposition during warm seasons (Webb et al., 2019, Poisson & Yates, 2022). Slower decomposition rates have also been associated with low

dissolved oxygen where groundwater is upwelling (Cornut et al., 2010). Further, differences in stream velocity within a reach have been shown to modify the effects of groundwater on biofilm communities (Burrows et al., 2020; Banks et al., 2023b). However, to date, there has not been an investigation of the role of groundwater input in influencing biological response at the patch scale. Past work on associations between groundwater input and biofilm heterogeneity have largely been performed at the reach scale, and currently there is limited understanding of how heterogeneity in the biofilm at patch scales may be linked to within reach variation in the amount of groundwater upwelling.

Our study goal was to assess the response of stream biofilm communities (i.e., biomass and diatom composition) and organic matter breakdown (i.e., cellulose decomposition) to a gradient of groundwater upwelling at the patch scale within a reach. We identified locations of groundwater upwelling, and assessed if there was an association between environmental conditions to biofilm communities and cellulose decomposition. We hypothesized that variation in groundwater upwelling and consequent modification of surface water environmental conditions at the patch scale would explain spatial heterogeneity in biofilm communities and cellulose decomposition. Our results further enhance our understanding of patch scale dynamics of environmental heterogeneity generated by groundwater input and the response of stream biofilm communities and organic matter processing.

4.2 Methods

4.2.1 Study area and site selection

The study was conducted in a headwater reach of Kintore Creek, southern Ontario, Canada (Fig. 4.1a, b). The studied reach is characterized by having a straight and entrenched channel with an average channel width of 2.0 m, the presence of habitat features (i.e., riffles and runs), and no canopy cover. Kintore Creek experiences mean annual low and high air temperatures of - 6.0 °C and 20.2 °C, respectively, with an average annual precipitation of 1069.5 mm (Environment and Climate Change Canada, 2010). Land use in the Kintore Creek catchment is primarily agricultural (80 %), with forest (12 %) and residential (4 %) uses

encompassing smaller areas (Agriculture and Agri-Food Canada, 2020). Crop cover is typically row crops of soybean and corn, as well as alfalfa, and many fields have subsurface tile drainage. Surficial geology varies in permeability because of glacial deposits of sand and gravel across the catchment (Ontario Geological Survey, 2010).

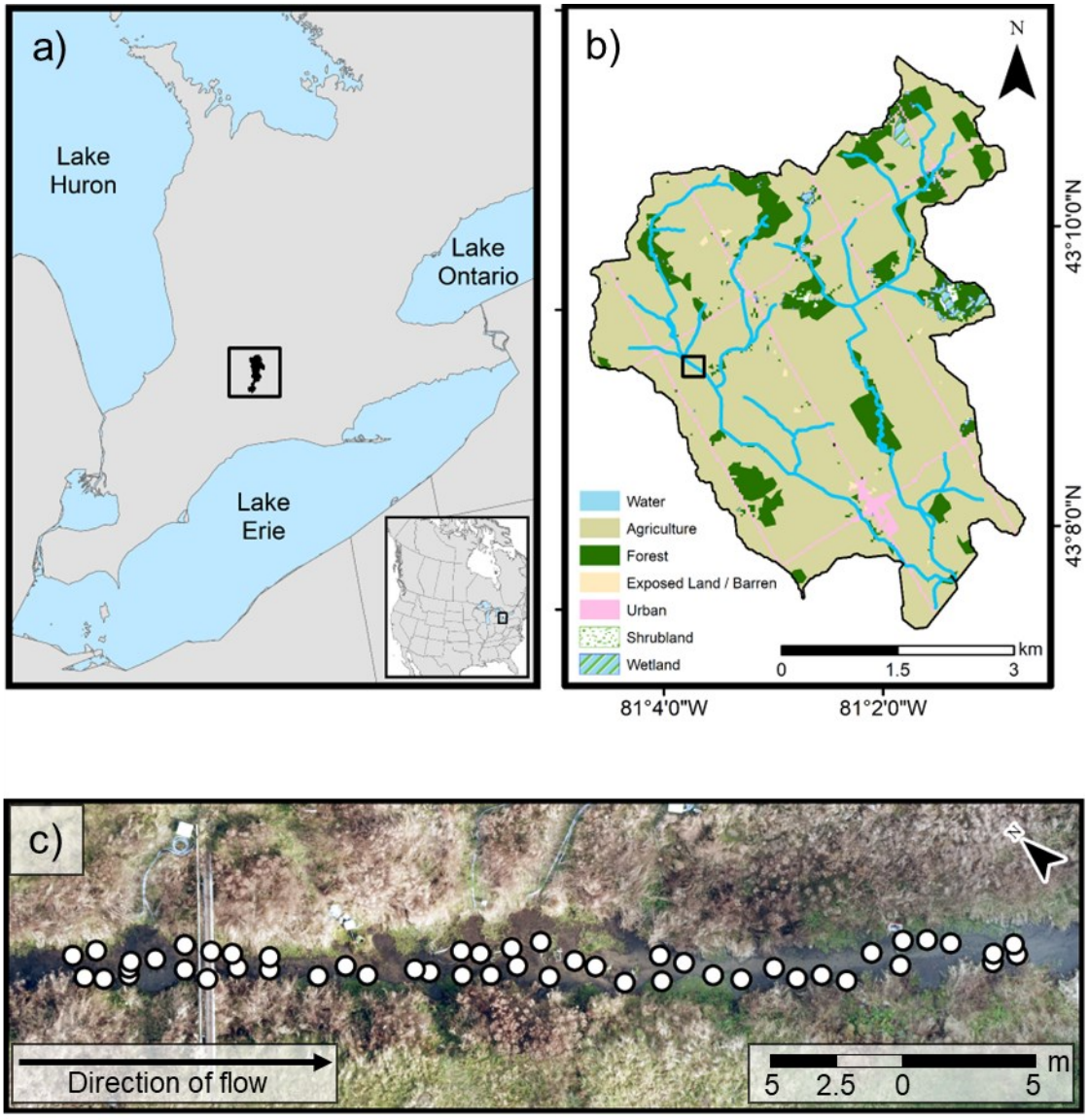

Figure 4.1 Location of study area (a) indicated by a black square in Great Lakes Region of North America (inset). Land use in the Kintore Creek headwaters in southern Ontario (b). Aerial photo of the studied reach (c) in the western headwater branch of Kintore Creek overlaid

with sampling locations (circles) (Catchment boundaries/stream network in Forsyth et al., 2016; Land use/cover in Agricutlure and Agri-Food Canada, 2020)

A 35 m reach of the western branch of Kintore Creek was selected for this study based on existence of high-resolution streambed temperature mapping conducted by Robinson et al. (2022). Spatial streambed temperature mapping is a widely used, quantitative proxy for groundwater flux because groundwater is typically cooler than receiving surface waters in warm seasons (Kalbus et al., 2006). Spatial streambed temperature mapping was conducted during baseflow by Robinson et al. (2022) on July 2nd, 2020 using transects across the stream width at 1 m offsets in the studied reach. At each transect, Robinson et al. (2002) measured subsurface streambed temperature approximately every 0.2 m across the stream width at 0.1 m depth in the streambed subsurface. Stream surface water temperature was measured once in the center of the stream for each transect, allowing for stream water - subsurface temperature gradient (i.e., stream surface water temperature minus subsurface streambed temperature) to be calculated at each point in the transect.

We used the resultant streambed temperature mapping from Robinson et al., (2022) to select 50 sampling locations that captured the full range of subsurface streambed temperature and full range of subsurface temperature gradients (Fig. 4.2a, b). In the studied reach, subsurface (0.1 m) streambed temperature was lowest in the upper section and warmer in the mid- and downstream sections of the reach (Fig. 4.2a). The coldest subsurface temperature was 14.0 °C and the warmest was 20.1 °C, with median temperature of 17.9 °C. Stream water - subsurface temperature gradient (°C) tended to have larger ranges (> 2.0 °C) in the upstream and downstream sections and smaller differences (< 2.5 °C) between the midstream section of the reach (Fig. 4.2b).

A one-year investigation into shallow sediment porewater (0.1 - 0.4 m depth) along this same reach by Vissers et al. (2023) revealed groundwater in upwelling areas was typically under oxic, suboxic or nitrate-reducing redox conditions. These coincided with median SRP concentrations < 30 µg/L and nitrate-N concentrations generally of 5-15 mg/L, which was typically less than and greater than the stream water concentrations, respectively. Porewater in

areas with no upwelling groundwater or with downwelling conditions was generally under more reducing redox conditions and had low nitrate-N and often much higher SRP concentrations than the stream.

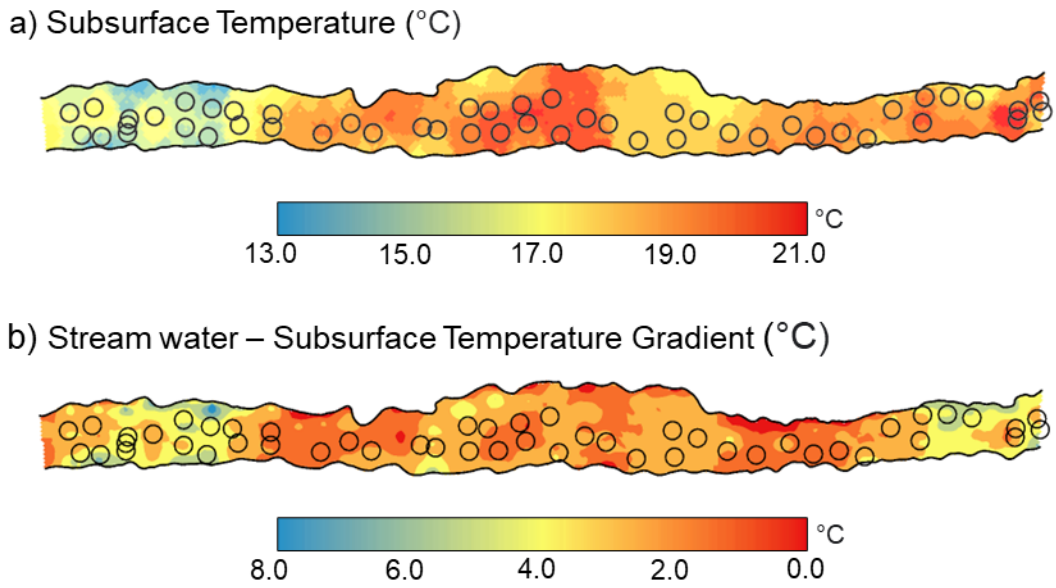

Figure 4.2 (a) Subsurface (0.1 m) streambed temperatures and (b) stream water - subsurface temperature gradient for the 50 sampling locations the studied 35 m headwater reach of Kintore Creek in Ontario, Canada. Direction of flow is left to right. The temperature surface was generated by kriging interpolation using spatial streambed temperature mapping from Robinson et al. (2022)

4.2.2 Sample Collection & Processing

Stream sampling was conducted from August 5th to September 3rd, 2020. At each sampling location, diatom taxonomy, biofilm biomass (chlorophyll-*a* [chl-*a*] and ash-free dry mass [AFDM]), and cellulose decomposition at the streambed surface and buried in the streambed subsurface (0.1 m) were assessed. Environmental variables were also characterized at each sampling location. We measured streambed water temperature continuously and surface water chemistry and nutrients once during our study.

4.2.2.1 Environmental Characterization

We measured streambed water temperature and surface water chemistry at each sampling location (n = 50). Streambed water temperature was measured at 15-minute intervals using temperature loggers (HOBO Pendant, Onset, USA) for the duration of deployment beginning on August 5th and 6th 2020 for 26 or 27 days, respectively. At each location, temperature loggers were anchored on the tile holders using cable binders so that loggers lay flat on the streambed surface. Using the streambed temperature measurements, we calculated mean daily streambed temperature (°C), hereafter streambed temperature, and mean daily streambed temperature range (°C), hereafter streambed temperature range. Streambed temperature was computed using the sum of the mean daily temperature divided by days in the incubation period (*sensu* Benfield et al. 2017). Using daily maximum and minimum temperature for each deployment day, we calculated daily streambed temperature ranges, which were averaged for each location over the deployment period.

Water samples were taken at each sampling location on August 20th, 2020. Samples were collected at the streambed surface for analysis of the dominant bioavailable forms of nitrogen and phosphorus (i.e., nitrate - nitrogen [NO_3^--N]) and Soluble Reactive Phosphorous [SRP], respectively). Both NO_3^--N and SRP samples were filtered using a 0.45-µm cellulose acetate filter. NO_3^--N samples were then frozen until analysed using a liquid chromatography (HPLC) (Thermo Scientific Dionex Aquion Ion Chromatography System with Dionex AS-DV autosampler, LDL 0.25 mg L^{-1} for NO_3^--N). SRP samples were placed in the fridge and analyzed using Flow Injection Analysis automated ion analyzer (FIA) (Lachat QuikChem, QC8500 FIA Automated Ion Analyzer, LDL 1 µg L^{-1} for SRP) within 24 hrs of collection (AWWA, 2004). Using a handheld YSI probe (YSI, Professional Plus), we measured pH and specific conductivity at the streambed for each location at the beginning of deployment.

We measured stream velocity (Hach FH950 Portable Velocity Meter, Hach Ultra Analytics) on three different days (August 12th, 19th, and September 1st, 2020) at the streambed for each of the 50 sampling locations. We then calculated the mean of the stream velocity measurements at each sampling location.

A single instantaneous measurement of photosynthetically active radiation (PAR) (LI-1500, Photometric sensor LI-210R) at each sampling location at the surface of the water on a sunny day with no cloud cover (August 13th, 2020) within a 30-minute span at mid-day. We also measured stream depth at each sampling location on August 5th or 6th using a ruler to determine depth from the center of the tile holder to the stream water surface.

Using a Trimble® Catalyst™ DA2 GNSS (Trimble Geospatial) with centimeter accuracy, we measured the position of sampling locations and marked points every 1 m on the left and right banks of the stream channel to the wetted width. We measured each position for 15 seconds, generating multiple (20 – 50) latitude and longitude points. In post processing, we then averaged the measurements of latitude and longitude to generate a position for each sampling location and the left and right banks stream channel. We generated the stream channel shape by measuring the location of the wetted width of the stream on the left and right banks of the channel (points) and tracing the stream channel (polyline). We then overlaid the point and polyline spatial data with the aerial photo of the reach and interpolated the stream channel shape.

4.2.2.2 Cellulose Decomposition

Cellulose decomposition was measured using the cotton-strip assay (CSA; Tiegs et al. 2013). Cotton strips were produced from Fredrix-brand unprimed 12-oz. heavyweight cotton fabric, Style #548 (Fredrix, Lawrenceville, GA, USA). Each cotton strip was 2.5 cm x 8 cm with 3 mm of frayed 'fuzz' on the length of the fabric strip.

We randomly assigned six cotton strips to each sampling location. Three cotton strips were laid flat on the streambed surface and attached to the tile holder using cable binders. Cotton strips on the streambed surface were deployed on August 5th or 6th 2020 for 13 days. We buried the other three strips at 0.1 m depth in the streambed on August 4th, 2020, and strips were incubated for 28 or 30 days.

After retrieval, strips were sterilized in the field by submersing in a tray containing 70 % ethanol for 7 minutes, stopping microbial activity. After sterilization, strips were gently

brushed to remove sediment and debris. Next, strips were laid flat and folded into aluminum foil and placed in a cooler on ice until return to the lab. In the lab, strips were dried at 40 °C for 24 h. Following drying and cooling to room temperature, tensile strength was measured as an indicator of cellulose decomposition.

Tensile strength is the force required to break the strip, and was measured using a tensiometer and motorized test stand (Force Gauge, Model M3-100), following Tiegs et al. (2013). Equal lengths of the strip were placed in tensiometer grips (Mark-10 brand, Model #MG100) and were pulled at a constant rate of 2 cm/minute until peak tension was reached. Peak tension is defined here as when the strip rips. Percent loss of tensile strength was calculated by comparing mean tensile strength of 50 reference strips to measured tensile strength of incubated sample strips. Reference strips were deployed in a mock field experiment in the lab, which involved strips being saturated in distilled water, and processed as incubated strips. Reference strips were immersed in 70 % ethanol for 7 minutes, followed by gentle brushing and placed in a drying oven for 24 h at 40 °C. Tensile strength of the reference strips were then measured. For each sample strip, tensile loss was measured and then percent tensile loss per day was calculated using Eq.3 (*sensu* Tiegs et al. 2013).

$$\%\ \text{tensile loss per day} = \frac{\left(\frac{\text{Tensile Strength}^{REF} - \text{Tensile Strength}^{SAMP}}{\text{Tensile Strength}^{REF}}\right) \text{x } 100}{\text{Incubation time}}$$

(Eq. 3)

4.2.2.3 Biofilm Sampling

We used standardized artificial substrates (unglazed ceramic tiles; 21.24 cm^2 each) to ensure a consistent surface for stream biofilm accumulation (*sensu* Steinman et al. 2007). Three tiles were placed in a tile holder, then the tile holder was secured to a brick anchor with cable binders. Next, the brick was buried in the stream with the tile holder 'lip' approximately 2 cm above the streambed, securing the brick anchor and tile holder. Tile holders were placed in each sampling location (n = 50) on August 5th and 6th 2020 and incubated for 26 or 27 days. Upon retrieval, tiles were sampled by scraping the entire tile surface with a toothbrush. The

toothbrush was thoroughly rinsed using stream water between each sampling location. Biofilms from one tile was used for each of diatom taxonomy, chlorophyll-*a* (chl-*a*), and ash-free dry mass (AFDM). Diatom taxonomy samples were preserved using Lugol's iodine (~1% v/v), and both chl-*a* and AFDM samples were put on ice immediately after collection, and subsequently stored frozen pending chl-*a* and AFDM analyses.

Diatom taxonomy samples were prepared using acid digestion in 5 mL of 100% (v/v) nitric acid for 15 h, which removed organic matter and ensured visible diatom frustules. To complete the acid digestion process, 1 mL of hydrogen peroxide 30 % (v/v) was added to each sample, followed by immersion of tubes in a hot water bath at 60 °C for 1 h. After incubation in the hot water bath, samples were then cooled to room temperature. Once samples reached room temperature, samples were centrifuged at 5500 rpm for 10 minutes. Following each centrifugation, pellets were retained, and the acid supernatant was discarded. Deionized water was used repeatedly to rinse the pellets until the supernatant had a pH above 6. To mount diatom frustules on microscope slides, Naphrax® (refractive index: 1.74; Brunel microscopes Ltd., Wiltshire, UK) was used. An Olympus BX51 Upright Compound Microscope equipped with differential interference contrast optical components at 1000x magnification was used to enumerate diatom assemblages.

Chl-*a* samples were thawed and filtered through Whatman GF/C filters. 10 mL of 90 % ethanol was then poured into 50 mL centrifuge tubes. Filters were then fully submerged in ethanol in the centrifuge tubes. A hot ethanol, non-acidification extraction method was completed by placing centrifuge tubes in an 80 °C hot water bath for 7 minutes. A Turner Designs Trilogy Fluorometer (Model: 7200e000) was used to measure chl-*a* concentration in each sample. Extracted liquid was diluted if maximum detection limits (> 75 µg/mL) were surpassed. To standardize chl-*a* in each sample, we calculated chl-*a* accumulation by dividing chl-*a* concentration by number of days incubated in the stream.

Frozen AFDM samples were thawed and filtered onto pre-ashed Whatman GF/C filters. After filtering, samples were dried at 105 °C for at least 12 h and weighed. Filters were then ashed at 550 °C for 1 h in a muffle furnace and cooled to room temperature. Ashed filters were

then weighed to determine mass loss on ignition. Our study reach has high levels of silt/clay and were corrected for water loss due to the presence of clay and other minerals by re-wetting and drying for a minimum of 12 h at 105 °C. After cooling to room temperature, samples were re-weighed. Samples were then standardized to biofilm growth rate by dividing AFDM by number of days incubated in the stream.

4.2.3 Data Analysis

Multiple linear regression was used to analyze the association between environmental variables (Table 4.1) and tensile loss (i.e., streambed surface and subsurface cellulose decomposition) and biofilm biomass (i.e., chl-*a* accumulation and biomass growth rate). Prior to regression analysis, we checked statistical assumptions (normality and heteroscedasticity) using standard graphical methods (Quinn & Keough, 2002) and outliers were tested for using Tukey's Interquartile Range (IQR, Dhana 2017). We found that measured environmental variables, tensile loss, and biofilm biomass fit the assumptions of regression analysis. However, two outliers were identified in the chl-*a* accumulation using Tukey's IQR method and were further assessed during model development.

We generated linear models using the function glmmTMB from the *glmmTMB* package (Brooks et al., 2017). For our regression analyses, we excluded some measured environmental variables. We omitted SRP, streambed temperature, stream depth, pH, and specific conductivity because of limited variation amongst sampling locations (Appendix C1.). We also omitted stream water - subsurface temperature gradient because it was highly correlated with subsurface temperature (Appendix C2.). Thus, we conducted our multiple linear regression using the following environmental variables: NO_3^--N, streambed temperature range, subsurface streambed temperature, PAR, and stream velocity. We hypothesized that indicators of groundwater upwelling, such as greater concentrations of NO_3^--N, smaller surface water temperature ranges, and groundwater input would be associated with faster tensile loss and greater biofilm biomass. We also predicted greater values of PAR would be associated with greater biofilm biomass. Lastly, we expected that faster stream velocity would be associated with faster tensile loss and lower biofilm biomass.

For our analysis of chl-*a* accumulation and biofilm growth rate, we used all possible combinations of the retained environmental measures (Table 4.1). For analysis of surface tensile loss, we removed all models that included PAR as the CSA assesses heterotrophic microbial activity. For buried tensile loss, only subsurface streambed temperature was used as it was the only variable measured in the stream subsurface (Table 4.2). We did not include interactions or higher-order terms in our models as we are limited by a relatively small sample size and therefore the number of models we can generate.

We evaluated *a priori* models following an information-theoretical approach outlined by Burnham & Anderson (2002), Anderson (2008), and Burnham et al. (2011). We used model selection by the Akaike Information Criterion corrected for small sample sizes (AICc). AICc is used to identify the best model of a series of candidate models developed *a priori*. In AIC, the model with the smallest AIC_c value is considered the best explanatory model relative to other competing candidate models. However, models within 7 AIC_c units of the best explanatory model are considered plausible, with the predictor variables in those models likely containing relevant information (Richards, 2005; Anderson, 2008). If multiple plausible models were identified, we calculated model-averaged parameter estimates (i.e., slope), unconditional standard errors, and 85% unconditional confidence intervals of each parameter in the models to determine important parameters (Burnham & Anderson, 2002; Anderson, 2008; Arnold, 2010; Mazerolle, 2016). Parameter estimates with 85% unconditional confidence intervals that overlapped zero are considered 'pretending' parameters and all models that included these parameter(s) were removed (*sensu* Anderson, 2008). We then re-ran and re-ranked models by their AIC_c values and model weight using *AICcmodavg* package in R (Mazerolle, 2016).

We conducted visual assessments of residuals from the best models to identify possible spatial autocorrelation. If we found indications of spatial autocorrelation (i.e., clustering of residuals), then we re-ran the regression analysis including spatial position as a predictor variable. To generate the spatial position variable, we used the coordinates (latitude and longitude) of sampling locations to compute distance downstream from all upstream points

using Euclidean distance. We then applied the asymmetric eigenvector mapping (AEM) framework where and used a Principal Components Analysis (PCA) to represent between site distances. Scree plots were used to identify the important components and site scores of those components were considered the metric of spatial position. (Blanchet et al., 2008). The PCA was performed using the *prcomp* function in the *stats* package in R (R Core Team, 2020).

Table 4.1 *A priori* stream biofilm biomass, surface tensile loss, and buried tensile loss models for locations in a reach in Kintore Creek, Ontario. Model parameters are NO_3^--N (NO_3^--N), stream velocity (Velocity), Photosynthetically Active Radiation (PAR), surface water temperature range (°C range), and subsurface streambed temperature (Subsurface °C). The ordinate intercept is indicated by I.

Model No.	Model Parameters	Model Structure
1	NO_3^--N	β1(NO_3^--N) + β2(I)
2	Velocity	β1(Velocity) + β2(I)
3	PAR	β1(PAR) + β2(I)
4	°C range	β1(°C range) + β2(I)
5	Subsurface °C	β1(Subsurface °C) + β2(I)
6	NO_3^--N + Velocity	β1(NO_3^--N) + β2(Velocity) + β3(I)
7	NO_3^--N + PAR	β1(NO_3^--N) + β2(PAR) + β3(I)
8	NO_3^--N + °C range	β1(NO_3^--N) + β2(°C range) + β3(I)
9	NO_3^--N + Subsurface °C	β1(NO_3^--N) + β2(Subsurface °C) + β3(I)
10	Velocity + PAR	β1(Velocity) + β2(PAR) + β3(I)
11	Velocity + °C range	β1(Velocity) + β2(°C range) + β3(I)
12	Velocity + Subsurface °C	β1(Velocity) + β2(Subsurface °C) + β3(I)
13	PAR + °C range	β1(PAR) + β2(°C range) + β3(I)
14	PAR + Subsurface °C	β1(PAR) + β2(Subsurface °C) + β3(I)

15	°C range + Subsurface °C	β1(°C range) + β2(Subsurface °C) + β3(I)
16	NO_3^--N + Velocity + PAR	β1(NO_3^--N) + β2(Velocity) + β3(PAR) + β4(I)
17	NO_3^--N + Velocity + °C range	β1(NO_3^--N) + β2(Velocity) + β3(°C range) + β4(I)
18	NO_3^--N + Velocity + Subsurface °C	β1(NO_3^--N) + β2(Velocity) + β3(Subsurface °C) + β4(I)
19	NO_3^--N + PAR + °C range	β1(NO_3^--N) + β2(PAR) + β3(°C range) + β4(I)
20	NO_3^--N + PAR + Subsurface °C	β1(NO_3^--N) + β2(PAR) + β3(Subsurface °C) + β4(I)
21	NO_3^--N + °C range + Subsurface °C	β1(NO_3^--N) + β2(°C range) + β3(Subsurface °C) + β4(I)
22	Velocity + PAR + °C range	β1(Velocity) + β2(PAR) + β3(°C range) + β4(I)
23	Velocity + PAR + Subsurface °C	β1(Velocity) + β2(PAR) + β3(Subsurface °C) + β4(I)
24	Velocity + °C range + Subsurface °C	β1(Velocity) + β2(°C range) + β3(Subsurface °C) + β4(I)
25	PAR + °C range + Subsurface °C	β1(PAR) + β2(°C range) + β3(Subsurface °C) + β4(I)
26	Velocity + PAR + °C range + Subsurface °C	β1(Velocity) + β2(PAR) + β3(°C range) + β4(Subsurface °C) + β5(I)
27	NO_3^--N + Velocity + PAR + °C range	β1(NO_3^--N) + β2(Velocity) + β3(PAR) + β4(°C range) + β5(I)
28	NO_3^--N + Velocity + PAR + Subsurface °C	β1(NO_3^--N) + β2(Velocity) + β3(PAR) + β4(Subsurface °C) + β5(I)
29	NO_3^--N + Velocity + °C range + Subsurface °C	β1(NO_3^--N) + β2(Velocity) + β3(°C range) + β4(Subsurface °C) + β5(I)
30	NO_3^--N + PAR + °C range + Subsurface °C	β1(NO_3^--N) + β2(Velocity) + β3(°C range) + β4(Subsurface °C) + β5(I)
Null	Intercept only	β1(1)
Global	NO_3^--N + Velocity + PAR + °C range + Subsurface °C	β1(NO_3^--N) + β2(Velocity) + β3(PAR) + β4(°C range) + β5(Subsurface °C) + β6(I)

Table 4.2 *A priori* buried tensile loss for sampling locations in a reach in Kintore Creek, Ontario. Model parameters are subsurface streambed temperature (Subsurface °C). The ordinate intercept is indicated by I.

Model No.	Model Parameters	Model Structure
1	Subsurface °C	β1(Subsurface °C) + β2(I)
Null	Intercept only	β1(1)

Dissimilarity in diatom assemblage composition among sampling locations was assessed using non-metric multidimensional scaling (nMDS) on relative abundance data. Relative abundance data included taxa with a relative abundance of ≥ 2 % in at least one sample and was Hellinger transformed prior to analysis (Legendre & Gallagher, 2001). A two-dimensional nMDS was performed using Bray-Curtis distance with a maximum of 1000 iterations or until two convergent solutions were found. Analyses were completed in R (version 4.0.5, R Core Team, 2020) using the *vegan* package (Oksanen et al., 2020).

We used BIOENV (matching of biotic and environmental patterns; Clarke & Warwick 1994) to evaluate associations between selected environmental variables (i.e., NO_3^--N, surface water temperature range, subsurface streambed temperature, PAR, and stream velocity), and diatom assemblage composition. A BIOENV computes the extent of the association between two dissimilarity matrices, outputting pairs of samples where similar environmental variables are correlated with similar diatom assemblage composition (Clarke & Warwick 1994). We used the Bray-Curtis distance was calculated for the nMDS, construct biotic matrices. Environmental matrices were generated using Euclidean distance normalized environmental variables and the spatial position variable (Clarke & Warwick 1994). For our analysis, we used a Spearman rank correlation to evaluate the association between biotic and environmental matrices. Analyses were conducted using *bioenv* function and the *mantel* function with 999

permutations using environmental distances extracted from *bioenv* results was used to test for significance (vegan package, Oksanen et al., 2020).

4.3 Results

4.3.1 Environmental conditions

Median SRP was 42.2 µg P L^{-1} and varied between 40 µg P L^{-1} and 44.5 µg P L^{-1} across the reach, (Fig. 4.3a). Median NO_3^--N was 8.1 mg N L^{-1}, with about half of sampling locations were within ± 1 mg N L^{-1} (i.e., 7.0 – 9.0 N L^{-1}) with minimum NO_3^--N concentration was 2.1 mg N L^{-1} (Fig. 4.3b). We did not observe a spatial pattern for either SRP or NO_3^--N (Fig. 3a, 3b)

Streambed temperatures and streambed temperature ranges had ranges of 1.2 °C and 5.1 °C, respectively (Fig. 4.3c, d). The lowest mean streambed temperature (17.2 °C) was in the upper section of the reach and warmer temperatures (18.5 to 19.0 °C) were throughout the mid- and downstream sections of the reach (Fig. 4.3c). Throughout the reach streambed temperature ranges were typically between 2.5 and 3.5 °C with greater ranges generally found in the downstream portion of the reach (Fig. 4.3d).

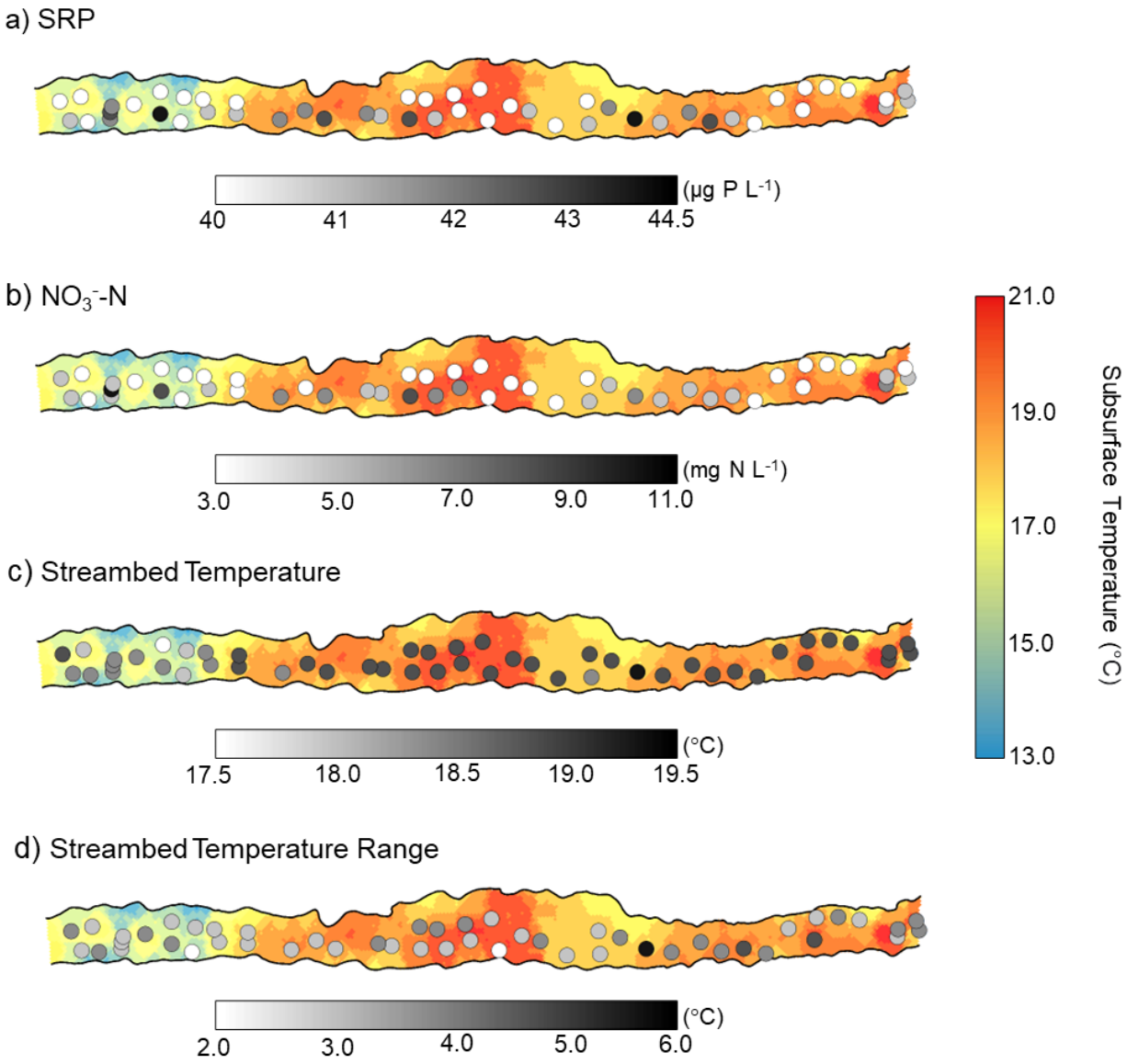

Figure 4.3 Sampling locations (n = 50) of (a) SRP, (b) NO_3^--N, (c) streambed temperature, and (d) streambed temperature range of the studied reach in Kintore Creek, Ontario, Canada. Circles indicate sampling locations, and shading corresponds to measured value. Direction of stream flow is left to right. Sampling locations are overlaid on the subsurface (0.1 m) streambed temperature. The subsurface (0.1 m) streambed temperature surface was generated by kriging interpolation using spatial streambed temperature mapping from Robinson et al. (2022)

Stream velocity showed sequences of faster and slower velocity across the reach, where areas of faster velocity corresponded to riffles and areas of slower velocity corresponded to runs (Fig. 4.4a). Median stream velocity was 0.078 m/s and ranged from 0.002 m/s to 0.205 m/s. Stream depth ranged from 5.0 to 17.5 cm (median = 11.7 cm) and was generally shallower in the upper section of the reach (i.e., 5.0 – 10.0 cm), and deeper in the lower section (i.e., 10.0 – 15.0 cm) (Fig. 4.4b). We observed little variability in pH (median = 8.1; range = 0.37) and specific conductivity (median = 615 µS/cm; range = 36 µS/cm) across the sampling locations (Fig. 4.4c, d). Median PAR was 1691 µmol/s/m^2 with a range of 314 µmol/s/m^2 with no clear spatial pattern (Fig. 4.4e).

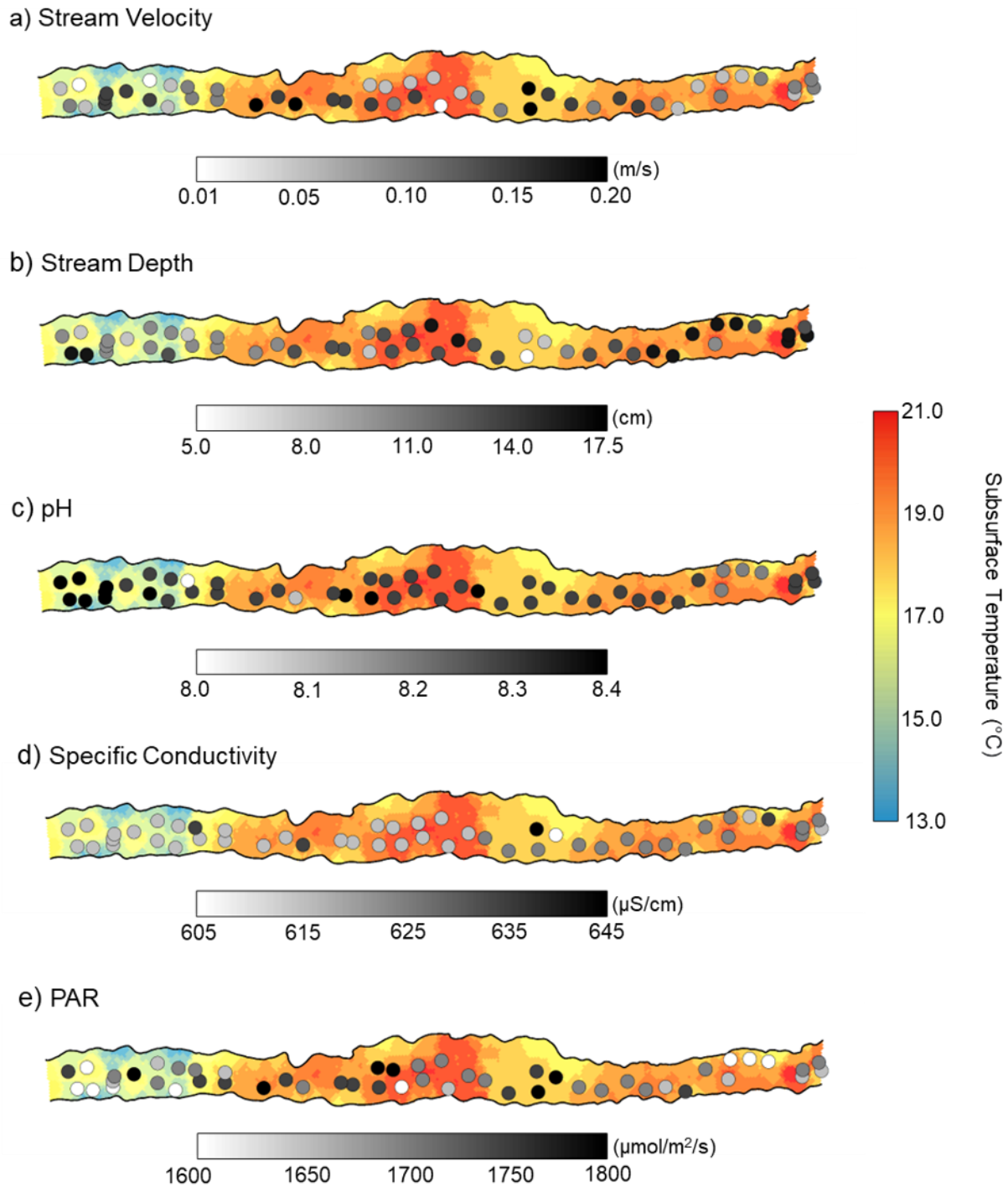

Figure 4.4 Sampling locations (n = 50) of the studied reach in Kintore Creek, Ontario (a) stream velocity, (b) stream depth, (c) pH, (d) specific conductivity, and (e) photosynthetically active

radiation (PAR) overlaying subsurface (0.1 m) temperature. Circles indicate sampling locations, and shading corresponds to measured value. Direction of stream flow is left to right. Sampling locations are overlaid on the subsurface (0.1 m) streambed temperature. The subsurface (0.1 m) streambed temperature surface was generated by kriging interpolation using spatial streambed temperature mapping from Robinson et al. (2022)

4.3.2 Tensile loss and algal biomass

Mean % tensile loss per day at the streambed surface was approximately 2-times faster than in the subsurface (Fig. 4.5a, b). Tensile loss on the streambed had a median % tensile loss day^{-1} of 5.2, with a range of 2.8 % tensile loss day^{-1} (Fig. 4.5a). Subsurface tensile loss was slower in the upper section of the reach where subsurface streambed temperature was lower. In the upper section, subsurface tensile loss was typically below 2 % tensile loss day^{-1}, with a slowest rate of 0.9 % tensile loss day^{-1} (Fig. 4.5b). Subsurface tensile loss in the downstream section was generally greater than 2.5 % tensile loss day^{-1}, with a maximum rate of 6.1 % tensile loss day^{-1}.

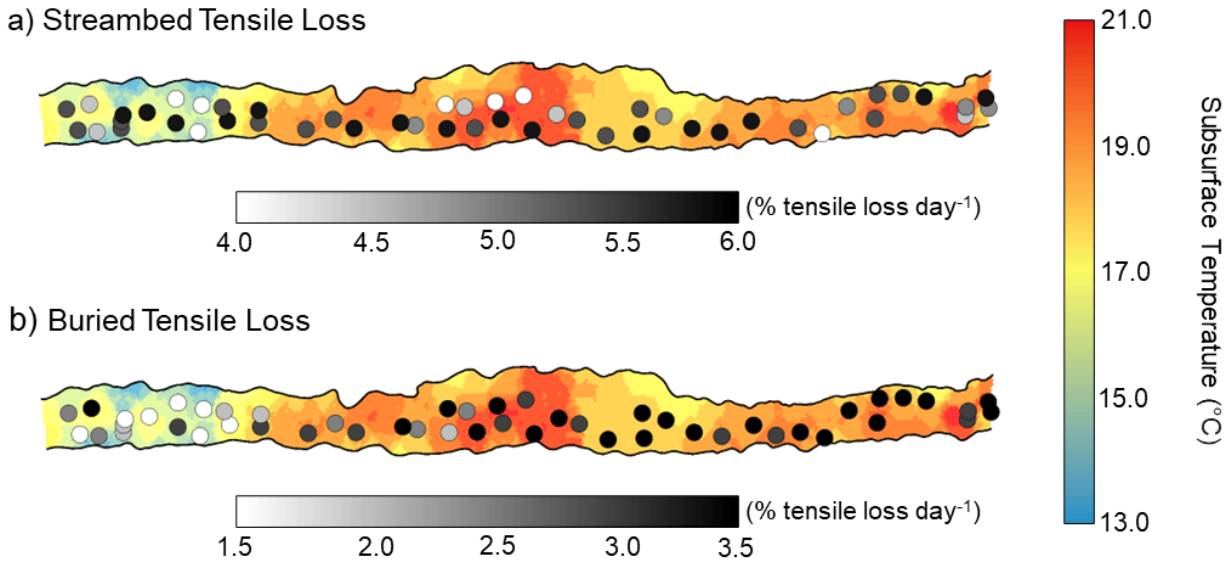

Figure 4.5 Sampling locations (n = 50) of (a) streambed surface tensile loss, (b) buried tensile loss overlaying subsurface (0.1 m) streambed temperature of the studied reach in Kintore

Creek, Ontario, Canada. Circles indicate sampling locations, and shading corresponds to measured value. Direction of stream flow is left to right. Sampling locations are overlaid on the subsurface (0.1 m) streambed temperature. The subsurface (0.1 m) streambed temperature surface was generated by kriging interpolation using spatial streambed temperature mapping from Robinson et al. (2022)

Streambed surface tensile loss was best predicted by a model consisting of stream velocity (Model 2; Table 4.3). Although more complex models (Models 12, 11, 6, 18, 24, 17, Global) had support (i.e., within 7 AIC_c units), model-averaging results showed that standard errors for the additional parameter estimates had 85% confidence intervals that overlapped zero and were thus discarded. Stream velocity was positively associated with streambed surface tensile loss (model-averaged parameter estimates ± SE: 8.79 ± 0.02) that explained 38% of variation ($R^2_{adj} = 0.38$).

Table 4.3 Comparison of *a priori* models predicting streambed surface tensile loss for 50 sampling locations in a reach of Kintore Creek, Ontario, using corrected Akaike Information Criteria corrected for small sample sizes (AIC_c). Only models within 7 AIC_c units of the best model are shown. Supporting variables for model selection included change in AIC_c (ΔAIC_c), log-likelihood (Log[L]), and model weight (ω_i).

Model number	**AIC_c**	**ΔAIC_c**	**Log(L)**	**ω_i**
2	88.3	0.0	-40.91	0.37
12	89.8	1.4	-40.45	0.18
11	90.3	2.0	-40.70	0.14
6	90.5	2.2	-40.82	0.12
18	91.8	3.5	-40.24	0.06
24	92.0	3.7	-40.32	0.06
17	92.6	4.2	-40.59	0.04

Global Model	94.2	5.8	-40.10	0.02
Null Model	111.3	23.0	-53.52	< 0.01

We found that the regression of buried tensile loss and subsurface temperature had support and the null model has little support (Table 4.4). Visual assessment of the residuals of the top model for buried tensile loss indicated that there was spatial autocorrelation in sampling location and buried tensile loss. Therefore, we re-ran models with the spatial position (i.e., site scores) included in the analysis. In our spatially corrected modeling (Table 4.4), we found that Model 1, which only contained spatial position (site scores), was the best model. However, the corrected global model (site scores + Subsurface °C) was less than 2 AIC_c units from Model 1, and therefore could not be excluded (Table 4.4). Model-averaging results indicated that subsurface streambed temperature and spatial position (site scores) were both informative parameters. Spatial position (site scores) was negatively associated with buried tensile loss (spatial position model-averaged parameter estimates ± SE: -0.01 ± 0.002) and subsurface streambed temperature was positively associated with buried tensile loss (subsurface streambed temperature model-averaged parameter estimates ± SE: 0.09 ± 0.06) which explained 59 % of variation ($R^2_{adj} = 0.59$).

Table 4.4 Comparison of tested models for predicting buried tensile loss for 50 sampling locations in a reach of Kintore Creek, Ontario, using corrected Akaike Information Criteria corrected for small sample sizes (AIC_c) showing models within 7 AIC_c units of the best model. Supporting variables for model selection included change in AIC_c (Δ AIC_c), log-likelihood (Log[L]), and model weight (ω_i).

Model number	**AIC_c**	**Δ AIC_c**	**Log(L)**	**ω_i**
1	73.7	0.0	-33.61	0.53
Global Model	74.0	0.2	-32.54	0.47
Null Model	115.7	42.0	-55.72	< 0.01

Chl-*a* accumulation (µg cm^{-2} day^{-1}) and biofilm growth rate (µg cm^{-2} day^{-1}) both showed no clear pattern across the studied reach (Fig. 4.6a, b). Further, we generally observed chl-*a* accumulation to positively correspond to biofilm growth rates. Median chl-*a* accumulation was 0.05 µg cm^{-2} day^{-1} with minimum and maximum accumulation of 0.001 and 0.27 µg cm^{-2} day^{-1}, respectively (Fig. 4.6a). We found that two locations were outliers, one in the upstream (0.27 µg cm^{-2} day^{-1}) and one further downstream (0.25 µg cm^{-2} day^{-1}), which was over 40 % greater than the next highest location. Biofilm growth rate ranged from 0.0002 to 0.0315 µg cm^{-2} day^{-1} with a median rate of 0.0063 µg cm^{-2} day^{-1} (Fig. 4.6b).

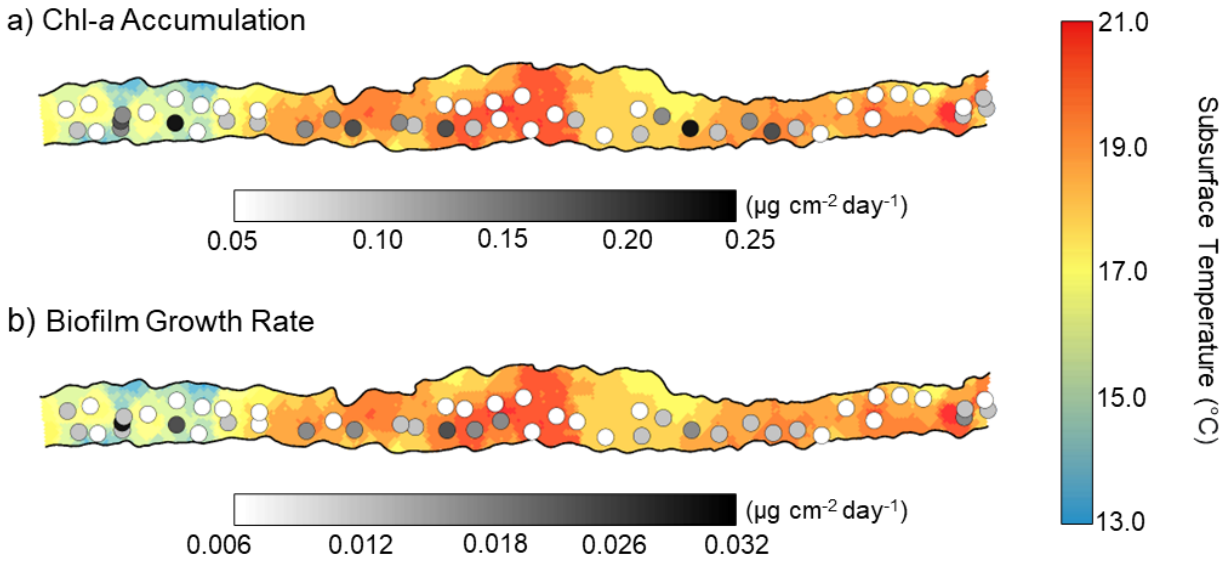

Figure 4.6 Sampling locations (n = 50) of (a) chl-*a* accumulation (µg cm^{-2} day^{-1}), and (b) biofilm growth rate (µg cm^{-2} day^{-1}) overlaying subsurface (0.1 m) streambed temperature (°C) of the studied reach in Kintore Creek, Ontario, Canada. Circles indicate sampling locations, and shading corresponds to measured value. Direction of stream flow is left to right. Sampling locations are overlaid on the subsurface (0.1 m) streambed temperature. The subsurface (0.1 m) streambed temperature surface was generated by kriging interpolation using spatial streambed temperature mapping from Robinson et al. (2022)

We used all measured locations for chl-*a* accumulation in our initial modelling. However, we found that the two locations with high levels of chl-*a* accumulation (0.27 and 0.25 μg cm^{-2} day^{-1}), that were identified as outliers based on Tukey's IQR method, appeared to be having a strong influence on modelling results. We found that chl-*a* accumulation was best predicted by a model that included stream velocity, streambed temperature range, and subsurface streambed temperature. We found that streambed temperature range and subsurface streambed temperature were positively and negatively associated with chl-*a* accumulation, respectively. We predicted that streambed temperature range would be negatively associated with chl-*a* accumulation, thus our model is contrary to our prediction. Further investigation revealed that the locations of high chl-*a* accumulation two locations with the largest streambed temperature range. Further, these locations were outlying points with respect to subsurface temperature, our proxy of groundwater input (Appendix C3.). Therefore, we excluded these two locations from our modelling.

Chl-*a* accumulation was best predicted by *a priori* Model 2 (Table 5), which included one environmental variable, NO_3^--N. The model with the second highest support (Model 6) also had one environmental variable, stream velocity. More complex models (Model 24) and models with single environmental variables (Model 10, 12, 13) models had support (i.e., within 7 AIC_c units; Table 5). Using model averaging, we found that NO_3^--N, PAR, streambed temperature range, and subsurface streambed temperature had 85% confidence intervals that overlapped zero and were thus discarded. Based on our analysis of best and competing models, we found the most support for Model 6, which explains 53% of variation and included stream velocity as an environmental driver. Stream velocity was positively associated with chl-*a* accumulation (model-averaged parameter estimates ± SE: 0.79 ± 0.11 and 0.64 ± 0.94, respectively).

Table 4.5 Comparison of tested models for predicting chl-*a* accumulation for 48 sampling locations in a reach of Kintore Creek, Ontario, using corrected Akaike Information Criteria corrected for small sample sizes (AIC_c) showing models within 7 AIC_c units of the best model.

Supporting variables for model selection included change in AIC_c (Δ AIC_c), log-likelihood (Log[L]), model weight (ω_i), and the adjusted R^2 (R^2_{adj}).

Model Number	**AIC_c**	**Δ AIC_c**	**Log(L)**	**ω_i**
2	-176.6	0.0	91.59	0.25
6	-175.1	1.5	92.02	0.12
10	-174.9	1.8	91.89	0.10
12	-174.8	1.8	91.88	0.10
11	-174.6	2.0	91.78	0.09
18	-173.8	2.8	92.63	0.06
16	-173.2	3.4	92.32	0.05
24	-173.0	3.7	92.20	0.04
22	-172.9	3.7	92.18	0.04
17	-172.9	3.7	92.15	0.04
23	-172.7	3.9	92.07	0.04
28	-171.7	4.9	92.87	0.02
27	-171.5	5.2	92.76	0.02
26	-171.0	5.6	92.52	0.01
30	-170.8	5.8	91.59	0.01
Null	-134.7	41.9	74.39	< 0.01
Global	-135.0	41.7	73.20	< 0.01

Our evaluation of *a priori* models for biofilm growth rate indicated that Model 2 (Table 4.6), consisting of stream velocity, was the best model. We also found support for models (10,

6, 16, 12, 23 18 and 27 where Δ AIC_c differed by < 2 AIC_c units per additional parameter (Table 4.6). However, NO_3^--N, PAR, surface water temperature range, and subsurface streambed temperature all had 85 % confidence intervals overlapping zero. Thus, all candidate models containing these parameters were discarded, and Model 2 containing stream velocity was retained. Stream velocity was positively associated with biofilm growth rate (model-averaged parameter estimates ± SE: 0.09 ± 0.02) and explained 39% (R^2_{adj} = 0.39) of the variation in biofilm growth rate.

Table 4.6 Comparison of tested models for predicting biofilm growth rate for 50 sampling locations in a reach of Kintore Creek, Ontario, using corrected Akaike Information Criteria corrected for small sample sizes (AIC_c) showing models within 7 AIC_c units of the best model. Supporting variables for model selection included change in AIC_c (Δ AIC_c), log-likelihood (Log[L]), model weight (ω_i), and the adjusted R^2 (R^2_{adj}).

Model Number	AIC_c	Δ AIC_c	Log(L)	ω_i
2	-378.3	0.0	192.39	0.21
10	-377.6	0.7	193.23	0.15
6	-377.0	1.3	192.95	0.11
11	-376.3	1.9	192.62	0.08
16	-376.2	2.1	193.78	0.08
12	-375.9	2.3	192.40	0.07
22	-375.8	2.5	193.58	0.06
23	-375.1	3.1	193.25	0.04
17	-374.9	3.3	193.14	0.04
18	-374.7	3.6	193.02	0.04
27	-374.2	4.0	194.09	0.03

24	-373.9	4.3	192.66	0.02
28	-373.6	4.6	193.78	0.02
26	-373.2	5.0	193.58	0.02
29	-372.6	5.7	193.26	0.01
Global	-371.5	6.7	194.11	0.01
Null	-354.5	23.8	179.4	< 0.01

4.3.3 Diatom assemblage patterns and drivers

Fifty-one diatom taxa (most identified to the species level) were enumerated across all sampling locations. Taxa richness varied among locations, with minimum and maximum taxonomic richness of 6 and 25, respectively. Four taxa contributed 86 % of total relative abundance: *Achnanthidium eutrophilum* (Lange-Bertalot) Lange-Bertalot (10 %), *Amphora pediculus* (Kützing) Grunow (36 %), and *Cocconeis placentula* Ehrenberg (30 %), and *Planothidium frequentissimum* (Lange-Bertalot) Lange-Bertalot (10 %).

Ordination of the diatom assemblages showed no clear trend based on location within the reach (Fig. 4.7a). BIOENV analysis showed that stream velocity was positively correlated with dissimilarity among diatom assemblages ($r = 0.336$, $p = 0.001$; Fig. 4.7a). We found that *Nitzschia dissipata* (Kützing) Rabenhorst (NDIS), *Nitzschia amphibia* (Grunlow) (NAMP), *Rhoicosphenia abbreviata* (Agardh) Lange-Bertalot (RABB), *Gomphonema parvulum* (Kützing) (GPAR) were associated with faster velocity, and *A. pediculus* (APED), *Navicula lanceolata* (Agardh) Ehrenberg (NLAN), and *Sellaphora pupula* (Kützing) Mereschkowksy (SPUP) were associated with slower velocity (Fig. 4.7b).

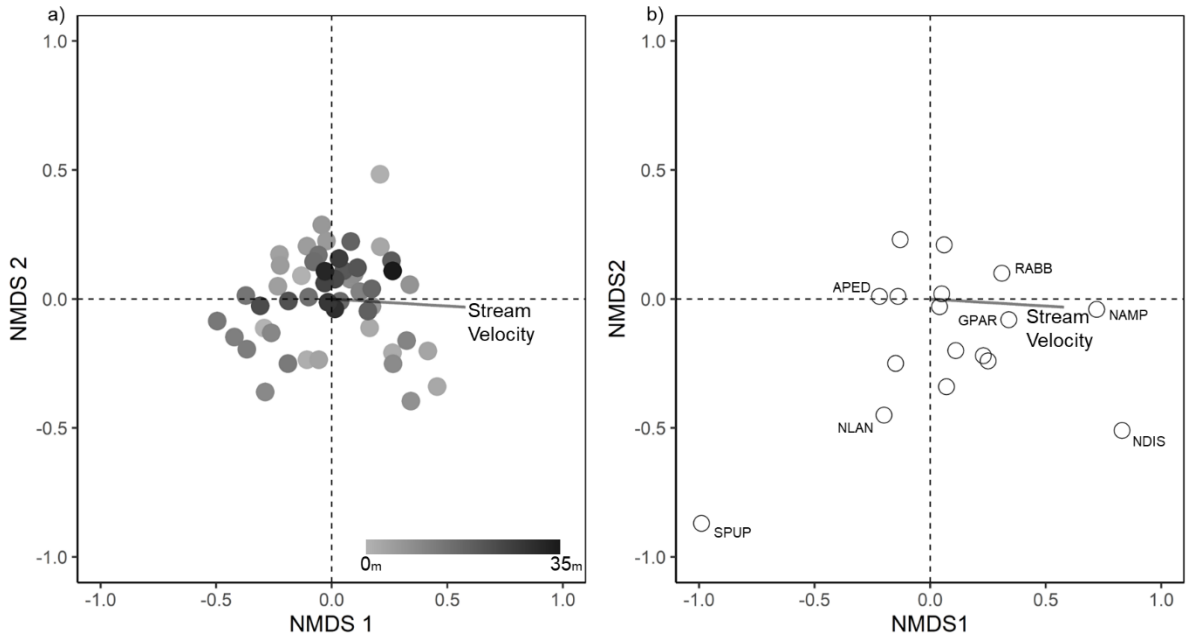

Figure 4.7 nMDS ordination plot using Bray-Curtis dissimilarity index for the relative abundance of diatom assemblages for each sampling location in a reach of Kintore Creek, Ontario, Canada (stress = 0.14) with stream velocity vector overlaid (r = 0.336, p = 0.001). (a) Shows site scores, which are represented by circles. Shading of circles darkens with increasing distance to downstream. (b) Species scores are shown with selected diatom taxa labelled

4.4 Discussion

4.4.1 Lack of groundwater modified environmental conditions

We predicted that groundwater input would generate patch scale variation in surface water temperature and nutrient availability at the streambed in the headwater reach of Kintore Creek. Indeed, the groundwater template in the studied reach showed differences in subsurface temperature and stream water - subsurface temperature gradient (Robinson et al., 2022). However, we did not find variability in environmental drivers modified by groundwater inputs. Our findings are in contrast to past work has shown that underlying patterns in subsurface temperature is a robust predictor of shallow groundwater flux into the streambed (Conant, 2004; Kalbus et al., 2006; Fleckenstein et al., 2010; Boano et al., 2014; Rau et al., 2014; Irvine

& Lautz, 2015). This discrepancy may be due to low amounts of groundwater input entering the surface water at the patch scale in our study. In the studied reach, Robinson et al., (2022) found that vertical hydraulic head differences, a direct measurement of direction, but not magnitude, of groundwater flux (Conant et al., 2019), suggest patterns in groundwater flux consistent with patterns shown by subsurface temperature. Our findings suggest that there was likely variation in groundwater flux throughout the reach, however, groundwater inputs may have been rapidly diluted by greater volumes of surface water, thus any environmental variation generated by groundwater may have been overwhelmed. For example, in areas of groundwater upwelling in the studied reach, porewater SRP was typically approximately 14 μg P L^{-1} (mean = 14 ± 6 μg P L^{-1}), which is about a third of surface water SRP (~ 42 μg P L^{-1}), though we observed little variation in surface water P concentrations (i.e., < 5 μg P L^{-1}). Alternatively, there may not have been a substantial variability between water temperature and nutrient availability between surface water and groundwater, thus no variation in environmental conditions was generated. Indeed, we found that, across all sampling locations, streambed temperatures varied by approximately 1.2 °C, suggesting limited thermal effects of groundwater inputs. Similarly, during our study we found that areas of groundwater flux had concentrations of porewater NO_3^--N was similar to NO_3^--N in the surface water (~8.0 mg N L^{-1}). Our findings suggest that the amount of and/or chemical and physical properties (i.e., nutrients, temperature) of groundwater entering the stream was likely insufficient to generate patch scale environmental variation of any magnitude.

4.4.2 Groundwater effects on stream biofilms at the streambed

In our study, the lack of environmental variation likely explains the lack of biological association with patterns in groundwater input. Our findings are in contrast to past work that have shown that groundwater inputs can alter surface water conditions, and subsequently generate heterogeneity in biofilm communities. For example, greater algal biomass has been consistently associated with point measurements of groundwater inputs (Wyatt et al., 2008; Mejia et al., 2016). Likewise, the composition of diatom assemblages have been shown to be altered by differences in groundwater inputs at the reach scale, where habitat type may be a

modifying factor (Roy et al., 2011; Burrows et al., 2020; Banks et al., 2023b). Differences in cellulose decomposition at the streambed have been associated with groundwater inputs, however the directionality of the association varies. Cooler groundwater inputs have been shown to slow decomposition (Webb et al., 2019; Poisson & Yates, 2022). However, additional resource subsidies from groundwater inputs throughout a reach may stimulate heterotrophic microbial activity (Griffiths & Tiegs, 2016; Banks et al., 2023b). In our study, the lack of response of biofilm communities at the streambed to groundwater inputs was likely driven by no observed variation in environmental variables modified by groundwater.

We found that the ecological heterogeneity we observed at the streambed in the studied reach in Kintore Creek was primarily associated with variation in stream velocity. Stream velocity has been regularly associated with patterns in stream biofilm communities and organic matter processing at the patch scale (Poff, 1997; Stevenson, 1997; Graça et al., 2015). For example, consistent with past work, we found that faster velocity was associated with faster streambed cellulose decomposition, likely attributed to increased physical abrasion (Tiegs et al., 2009; Webb et al., 2019; Banks et al., 2023b). We also found that faster biofilm growth rate and greater chl-*a* accumulation were both associated with faster stream velocity. In our study, the fastest velocity was 0.2 m/s, which is within the range where there is enhanced delivery of resources (e.g., surface water nutrients) to the biofilm with limited sloughing due to shear stress (Biggs et al., 1998; Battin et al., 2003; Arnon et al., 2010). Similarly, we found that diatom community composition differed based on stream velocity, a finding consistent with past studies (Biggs et al., 1998; Passy, 2001, 2007; Jamoneau et al., 2018). In line with past work, we found that most taxa co-occurring with faster velocities tended to be motile or low profile, likely due to the greater shear stress associated with faster stream velocity (Pringle, 1990; Passy, 2007). Conversely, we found that taxa at slower velocities tended to be motile or high profile, which may be due to the mobility of the taxa moving to more suitable habitats, high profile taxa accessing resources (light, nutrients) above the biofilm matrix, or exclusion from locations with faster velocity (Dodds, 1992; Larned et al., 2004; Passy, 2007). The lack of variation in environmental factors modified by groundwater and the variation in stream

velocity likely resulted in our findings that biofilm communities at the streambed were driven by stream velocity.

4.4.3 Groundwater effects on subsurface cellulose decomposition

We found that groundwater upwelling was associated with slower subsurface cellulose breakdown. Our findings are consistent with past work showing slower organic matter processing in the streambed substratum has been attributed to lower temperature, which slows heterotrophic activity (Strommer & Smock, 1989; Malard & Hervant, 1999; Crenshaw et al., 2002; Cornut et al., 2010). In our study, we used cooler subsurface temperatures as an indicator of groundwater upwelling. In the studied reach, we found slower subsurface decomposition in areas of cooler subsurface temperatures, suggesting that during warmer seasons carbon processing in the substratum may be slowed. As our study was conducted in summer when groundwater is typically cooler than surface water, future work should assess if patterns in subsurface breakdown reverse in cooler seasons, as surface water is typically cooler than groundwater in cold temperate seasons (Kalbus et al., 2006). Furthering our understanding of controls on organic matter processing in the streambed substrate will provide greater insights into environmental drivers of carbon cycling in shallow streambeds.

4.5 Summary

We found that ecological response at the streambed did not consistently match the groundwater template in the studied reach in Kintore Creek and we did not observe an association with biofilm communities and groundwater input, with the exception of chl-*a* accumulation. Rather, we found that environmental variation generated by stream velocity across the sampling locations emerged as the main factor in determining biofilm communities and cellulose decomposition at the streambed. We did find greater benthic chl-*a* biomass was associated cooler subsurface temperatures, our indicator of groundwater upwelling. Our findings may be due to rapid dilution of groundwater effects by surface water conditions, or because of limited differences in nutrient concentration between the groundwater and surface water. In the subsurface, slower cellulose decomposition was associated with cooler subsurface

temperatures, suggesting that carbon cycling may be slowed in the cooler subsurface patches. areas where there are patches of cooler subsurface. Future work assessing the effect of groundwater inputs on stream biofilm communities and cellulose decomposition at the patch scale should include a more extensive gradient of groundwater flux and environmental measurements at the stream water – biofilm interface.

4.6 References

Agriculture and Agri-Food Canada (2020) AAFC annual crop inventory 2019. https://open.canada.ca/data/en/dataset/d90a56e8-de27-4354-b8ee-33e08546b4fc. Accessed 10 April 2023

Anderson, D. R., 2008. Model based inference in the life sciences: A primer on evidence. Model Based Inference in the Life Sciences: A Primer on Evidence. Springer Science and Business Media, New York, USA, https://doi.org/10.1007/978-0-387-74075-1.

Arnold, T. W., 2010. Uninformative Parameters and Model Selection Using Akaike's Information Criterion. Journal of Wildlife Management 74: 1175–1178, https://doi.org/10.2193/2009-367.

Arnon, S., L. P. Marx, K. E. Searcy, & A. I. Packman, 2010. Effects of overlying velocity, particle size, and biofilm growth on stream – subsurface exchange of particles. Hydrologi 24: 108–114, https://doi.org/10.1002/hyp.

American Water Works Association, AWWA (2004) Flow injection analysis for orthophosphate. Standard methods for the examination of water and wastewater, 22nd edn. American Public Health Association, American Water Works Association, Water Environment Federation, 4500-P-G

Banks, L. K., I. Lavoie, M. P. Boreux, S. L. Kroeze, N. Gotkowski, C. E. Robinson, J. W. Roy, & A. G. Yates, 2023a. Intra-annual patterns in biofilm communities and cellulose decomposition in a headwater stream network with spatially variable groundwater inputs. Aquatic Ecology Springer Netherlands, https://doi.org/10.1007/s10452-023-10038-6.

Banks, L. K., I. Lavoie, C. E. Robinson, J. W. Roy, & A. G. Yates, 2023b. Effects of groundwater inputs on algal assemblages and cellulose decomposition differ based on habitat type in an agricultural stream. Hydrobiologia Springer International Publishing, https://doi.org/10.1007/s10750-023-05251-1.

Battin, T. J., K. Besemer, M. M. Bengtsson, A. M. Romani, & A. I. Packmann, 2016. The ecology and biogeochemistry of stream biofilms. Nature Reviews Microbiology 14: 251–263, https://doi.org/10.1038/nrmicro.2016.15.

Battin, T. J., L. A. Kaplan, J. D. Newbold, X. Cheng, & C. Hansen, 2003. Effects of current velocity on the nascent architecture of stream microbial biofilms. Applied and Environmental Microbiology 69: 5443–5452, https://doi.org/10.1128/AEM.69.9.5443.

Benfield, E. F., K. M. Fritz, & S. D. Tiegs, 2017. Leaf-Litter Breakdown In Lamberti, G. A., & F. R. Hauer (eds), Methods in Stream Ecology, Volume 2: Ecosystem Function. Elsevier, Academic Press: 71–82, https://doi.org/10.1016/B978-0-12-813047-6.00005-X.

Besemer, K., 2015. Biodiversity, community structure and function of biofilms in stream ecosystems. Research in Microbiology 166: 774–781, https://doi.org/10.1016/j.resmic.2015.05.006.

Biggs, B. J. F., D. G. Goring, & V. I. Nikora, 1998. Subsidy and stress responses of stream periphyton to gradients in water velocity as a function of community growth form. Journal of Phycology 34: 598–607, https://doi.org/10.1046/j.1529-8817.1998.340598.x.

Biggs, B. J. F., V. I. Nikora, & T. H. Snelder, 2005. Linking scales of flow variability to lotic ecosystem structure and function. River Research and Applications 21: 283–298, https://doi.org/10.1002/rra.847.

Blanchet, F. G., P. Legendre, & D. Borcard, 2008. Modelling directional spatial processes in ecological data. Ecological Modelling 215: 325–336, https://doi.org/10.1016/j.ecolmodel.2008.04.001.

Boano, F., J. W. Harvey, A. Marion, A. I. Packman, R. Revelli, L. Ridolfi, & A. Wörman, 2014. Hyophreic flow and transport processes. Reviews of Geophysics 52: 603–679, https://doi.org/10.1002/2012RG000417.

Bolpagni, R., & A. Laini, 2016. Microhabitat patterns of soft-bodied benthic algae in a lowland river largely fed by groundwater. Fottea 16: 244–254, https://doi.org/10.5507/fot.2016.007.

Brooks, M. E., K. Kristensen, K. J. van Benthem, A. Magnusson, C. W. Berg, A. Nielsen, H. J. Skaug, M. Maechler, & B. M. Bolker, 2017. glmmTMB Balances Speed and Flexibility Among Packages for Zero-inflated Generalized Linear Mixed Modeling. The R Journal 9: 378–400, https://doi.org/10.32614/RJ-2017-066.

Brunke, M., & T. Gonser, 1997. The ecological significance of exchange processes between rivers and groundwater. Freshwater Biology 37: 1–33, https://doi.org/10.1046/j.1365-2427.1997.00143.x.

Burnham, K. P., & D. R. Anderson, 2002. Model Selection and Multimodel Inference: A practical information-theoretic approach. Angewandte Chemie International Edition, 6(11), 951–952. Springer-Verlag, New York.

Burnham, K. P., D. R. Anderson, & K. P. Huyvaert, 2011. AIC model selection and multimodel inference in behavioral ecology: Some background, observations, and comparisons. Behavioral Ecology and Sociobiology 65: 23–35, https://doi.org/10.1007/s00265-010-1029-6.

Burrows, R. M., L. Beesley, M. M. Douglas, B. J. Pusey, & M. J. Kennard, 2020. Water velocity and groundwater upwelling influence benthic algal biomass in a sandy tropical river: implications for water-resource development. Hydrobiologia 847: 1207–1219, https://doi.org/10.1007/s10750-020-04176-3.

Cardinale, B. J., M. A. Palmer, C. M. Swan, S. Brooks, & N. LeRoy Poff, 2002. The influence of substrate heterogeneity on biofilm metabolism in a stream ecosystem. Ecology 83: 412–422, https://doi.org/10.1890/0012-9658(2002)083[0412:TIOSHO]2.0.CO;2.

Clarke, K. R., & R. M. Warwick, 1994. Similarity-based testing for community pattern: the two-way layout with no replication. Marine Biology 118: 167–176, https://doi.org/10.1007/BF00699231.

Coleman, R. L., & C. N. Dahm, 1990. Stream geomorphology: effects on periphyton standing crop and primary production. Journal of the North American Benthological Society 9: 293–302, https://doi.org/10.2307/1467897.

Conant, B., 2004. Delineating and quantifying ground water discharge zones using streambed temperatures. Ground Water 42: 243–257.

Conant, B., C. E. Robinson, M. J. Hinton, & H. A. J. Russell, 2019. A framework for conceptualizing groundwater-surface water interactions and identifying potential impacts on water quality, water quantity, and ecosystems. Journal of Hydrology 574: 609–627, https://doi.org/10.1016/j.jhydrol.2019.04.050.

Cornut, J., A. Elger, D. Lambrigot, P. Marmonier, & E. Chauvet, 2010. Early stages of leaf decomposition are mediated by aquatic fungi in the hyporheic zone of woodland streams. Freshwater Biology 55: 2541–2556, https://doi.org/10.1111/j.1365-2427.2010.02483.x.

Crenshaw, C. L., H. M. Valett, & J. L. Tank, 2002. Effects of coarse particulate on fungal biomass and organic matter in invertebrate the of subsurface a headwater stream density. Journal of the North American Benthological Society 21: 28–42, https://doi.org/https://doi.org/10.2307/1468297.

Dent, C. L., N. B. Grimm, & S. G. Fisher, 2001. Multiscale effects of surface-subsurface exchange on stream water nutrient concentrations. Journal of the North American Benthological Society 20: 162–181, https://doi.org/10.2307/1468313.

Dhana, K., 2017. Outlier removal by the Tukey rules on quartiles +/- 1.5 IQR.

Dodds, W. K., 1992. A modified fiber-optic light microprobe to measure spherically integrated photosynthetic photon flux density: Characterization of periphyton photosynthesis-irradiance patterns. Limnology and Oceanography 37: 871–878, https://doi.org/10.4319/lo.1992.37.4.0871.

Earon, R., J. Riml, L. Wu, & B. Olofsson, 2020. Insight into the influence of local streambed heterogeneity on hyporheic-zone flow characteristics. Hydrogeology Journal 28: 2697–2712.

Environment and Climate Change Canada, 2010. Canadian Climate Normals. https://climate.weather.gc.ca/climate_normals/. Accessed 13 March 2023.

Fleckenstein, J. H., S. Krause, D. M. Hannah, & F. Boano, 2010. Groundwater-surface water interactions: New methods and models to improve understanding of processes and dynamics. Advances in Water Resources Elsevier Ltd 33: 1291–1295, https://doi.org/10.1016/j.advwatres.2010.09.011.

Forsyth, D. K., C. M. Riseng, K. E. Wehrly, L. A. Mason, J. Gaiot, T. Hollenhorst, C. M. Johnston, C. Wyrzykowski, G. Annis, C. Castiglione, K. Todd, M. Robertson, D. M. Infante, L. Wang, J. E. McKenna, & G. Whelan, 2016. The Great Lakes hydrography dataset: Consistent, binational watersheds for the Laurentian Great Lakes basin. Journal of the American Water Resources Association 52: 1068–1088, https://doi.org/10.1111/1752-1688.12435.

Graça, M. A. S., V. Ferreira, C. Canhoto, A. C. Encalada, F. Guerrero-Bolaño, K. M. Wantzen, & L. Boyero, 2015. A conceptual model of litter breakdown in low order streams. International Review of Hydrobiology 100: 1–12, https://doi.org/10.1002/iroh.201401757.

Griffiths, N. A., & S. D. Tiegs, 2016. Organic-matter decomposition along a temperature gradient in a forested headwater stream. Freshwater Science 35: 518–533, https://doi.org/10.1086/685657.

Gulis, V., & K. Suberkropp, 2003. Leaf litter decomposition and microbial activity in nutrient-enriched and unaltered reaches of a headwater stream. Freshwater Biology 48: 123–134, https://doi.org/10.1046/j.1365-2427.2003.00985.x.

Irvine, D. J., & L. K. Lautz, 2015. High resolution mapping of hyporheic fluxes using streambed temperatures: Recommendations and limitations. Journal of Hydrology Elsevier B.V. 524: 137–146, https://doi.org/10.1016/j.jhydrol.2015.02.030.

Jamoneau, A., S. I. Passy, J. Soininen, T. Leboucher, & J. Tison-Rosebery, 2018. Beta diversity of diatom species and ecological guilds: Response to environmental and spatial mechanisms along the stream watercourse. Freshwater Biology 63: 62–73, https://doi.org/10.1111/fwb.12980.

Kalbus, E., F. Reinstorf, & M. Schirmer, 2006. Measuring methods for groundwater - Surface water interactions: A review. Hydrology and Earth System Sciences 10: 873–887, https://doi.org/10.5194/hess-10-873-2006.

Larned, S. T., V. I. Nikora, & B. J. F. Biggs, 2004. Mass-transfer-limited nitrogen and phosphorus uptake by stream periphyton: A conceptual model and experimental evidence. Limnology and Oceanography 49: 1992–2000, https://doi.org/10.4319/lo.2004.49.6.1992.

Legendre, P., & E. D. Gallagher, 2001. Ecologically meaningful transformations for ordination of species data. Oecologia 129: 271–280, https://doi.org/10.1007/s004420100716.

Malard, F., & F. Hervant, 1999. Oxygen supply and the adaptations of animals in groundwater. Freshwater Biology 41: 1–30, https://doi.org/10.1046/j.1365-2427.1999.00379.x.

Mazerolle, M. J., 2016. AICcmodavg: Model selection and multimodel inference based on (Q) AIC (c).

Mejia, F. H., C. V. Baxter, E. K. Berntsen, & A. K. Fremier, 2016. Linking groundwater – surface water exchange to food production and salmonid growth. Canadian Journal of Fisheries and Aquatic Sciences 73: 1650–1660, https://doi.org/10.1139/cjfas-2015-0535.

Oksanen, J., F. G. Blanchet, M. Friendly, R. Kindt, P. Legendre, D. McGlinn, P. R. Minchin, R. B. O'Hara, G. L. Simpson, P. Solymos, M. H. H. Stevens, E. Szoecs, & H. Wagner, 2020. vegan: community ecology package.

Ontario Geological Survey, 2010. Surficial geology of southern Ontario; Ontario Geological Survey, Miscellaneous Release Data 128 - Revised. .

Palmer, M. A., & N. L. Poff, 1997. The influence of heterogeneity on patterns and processes in streams. Journal of the North American Benthological Society 16: 169–173.

Passy, S. I., 2001. Spatial paradigms of lotic diatom distribution: A landscape ecology perspective. Journal of Phycology 37: 370–378, https://doi.org/10.1046/j.1529-8817.2001.037003370.x.

Passy, S. I., 2007. Diatom ecological guilds display distinct and predictable behavior along nutrient and disturbance gradients in running waters. Aquatic Botany 86: 171–178, https://doi.org/10.1016/j.aquabot.2006.09.018.

Pepin, D. M., & F. R. Hauer, 2002. Benthic responses to groundwater-surface water exchange in 2 alluvial rivers in northwestern Montana. Journal of the North American Benthological Society 21: 370–383, https://doi.org/10.2307/1468476.

Poff, N. L., 1997. Landscape Filters and Species Traits : Towards Mechanistic Understanding and Prediction in Stream Ecology. Journal of the North American Benthological Society 16: 391–409.

Poisson, R., & A. G. Yates, 2022. Impaired cellulose decomposition in a headwater stream receiving subsurface agricultural drainage. Ecological Processes 11: 1–17, https://doi.org/10.1186/s13717-022-00406-9.

Pringle, C., 1990. Nutrient Spatial Heterogeneity: Effects on Community Structure, Physiognomy, and Diversity of Stream Algae. Ecology 71: 905–920.

Pringle, C. M., R. J. Naiman, G. Bretschko, J. R. Karr, M. W. Oswood, J. R. Webster, R. L. Welcomme, & M. J. Winterbourn, 1988. Patch Dynamics in Lotic Systems: The Stream as a Mosaic. Journal of the North American Benthological Society 7: 503–524, https://doi.org/10.2307/1467303.

Quinn, G. P., & M. J. Keough, 2002. Experimental Design and Data Analysis for Biologists. Cambridge University Press, New York, USA.

R Core Team, 2020. R: A language and environment for statistical computing. R Foundation for Statistical Computing, Vienna, Austria.

Rau, G. C., M. S. Andersen, A. M. McCallum, H. Roshan, & R. I. Acworth, 2014. Heat as a tracer to quantify water flow in near-surface sediments. Earth-Science Reviews Elsevier B.V. 129: 40–58, https://doi.org/10.1016/j.earscirev.2013.10.015.

Richards, S. A., 2005. Testing ecological theory using the information-theoretic approach: Examples and cautionary results. Ecology 86: 2805–2814, https://doi.org/10.1890/05-0074.

Risse-Buhl, U., C. Anlanger, A. Chatzinotas, C. Noss, A. Lorke, & M. Weitere, 2020. Near streambed flow shapes microbial guilds within and across trophic levels in fluvial biofilms. Limnology and Oceanography 65: 2261–2277, https://doi.org/10.1002/lno.11451.

Robinson, K., C. E. Robinson, J. W. Roy, M. Vissers, A. Almpanis, U. Schneidewind, & C. Power, 2022. Improved interpretation of groundwater-surface water interactions along a stream reach using 3D high-resolution combined DC resistivity and induced polarization (DC-IP) geoelectrical imaging. Journal of Hydrology Elsevier B.V. 613: 128468, https://doi.org/10.1016/j.jhydrol.2022.128468.

Roy, J. W., B. Zaitlin, M. Hayashi, & S. B. Watson, 2011. Influence of groundwater spring discharge on small-scale spatial variation of an alpine stream ecosystem. 670: 661–670, https://doi.org/10.1002/eco.

Royer, T. V, & G. W. Minshall, 2003. Controls on leaf processing in streams from spatial-scaling and hierarchical perspectives. Journal of the North American Benthological Society 22: 352–358, https://doi.org/https://doi.org/10.2307/1468266.

Schilling, O. S., D. J. Irvine, & P. Hendricks Franssen, H.-J., Brunner, 2017. Estimating the Spatial Extent of Unsaturated Zones in Heterogeneous River-Aquifer Systems. Water Resources Research 50: 583–602, https://doi.org/10.1002/2017WR020409.

Steinman, A. D., G. A. Lamberti, & P. R. Leavitt, 2007. Biomass and pigments of benthic algae In Hauer, F. R., & G. Lamberti (eds), Methods in Stream Ecology. Academic Press, San Diego, CA, USA: 357–379, https://doi.org/https://doi.org/10.1016/B978-012332908-0.50024-3.

Stevenson, R. J., 1997. Scale-dependent determinants and consequences of benthic algal heterogeneity. Journal of the North American Benthological Society 16: 248–262, https://doi.org/10.2307/1468255.

Stevenson, R.J., Novoveska, L., C.M. Riseng, & M.J., Wiley, 2009. Comparing responses of diatom species composition to natural and anthropogenic factors in streams of glaciated ecoregions. Nova Hedwigia 135: 1–13.

Strommer, J. L., & L. A. Smock, 1989. Vertical distribution and abundance of invertebrates within the sandy substrate of a low-gradient headwater stream. Freshwater Biology 22: 263–274, https://doi.org/https://doi.org/10.1111/j.1365-2427.1989.tb01099.x.

Tang, T., S. Guo, L. Tan, T. Li, R. M. Burrows, & Q. Cai, 2019. Temporal effects of groundwater on physical and biotic components of a karst stream. Water (Switzerland) 11:, https://doi.org/10.3390/w11061299.

Thorp, J. H., M. C. Thoms, & M. D. Delong, 2006. The riverine ecosystem synthesis: Biocomplexity in river networks across space and time. River Research and Applications 22: 123–147, https://doi.org/10.1002/rra.901.

Thorp, J. H., M. C. Thoms, & M. D. Delong, 2008. The Riverine Ecosystem Synthesis. The Riverine Ecosystem Synthesis, https://doi.org/10.1016/B978-0-12-370612-6.X0001-0.

Tiegs, S. D., P. O. Akinwole, & M. O. Gessner, 2009. Litter decomposition across multiple spatial scales in stream networks. Oecologia 161: 343–351, https://doi.org/10.1007/s00442-009-1386-x.

Tiegs, S. D., J. E. Clapcott, N. A. Griffiths, & A. J. Boulton, 2013. A standardized cotton-strip assay for measuring organic-matter decomposition in streams. Ecological Indicators 32: 131–139, https://doi.org/10.1016/j.ecolind.2013.03.013.

Tonin, M. A., L. Ubiratan Hepp, & J. F. Gonçalves, 2018. Spatial Variability of Plant Litter Decomposition in Stream Networks: from Litter Bags to Watersheds. Ecosystems 21: 567–581, https://doi.org/10.1007/s10021-017-0169-1.

Townsend, C. R., 1989. The Patch Dynamics Concept of Stream Community Ecology. Journal of the North American Benthological Society 8: 36–50, https://doi.org/10.2307/1467400.

Valett, H. M., S. G. Fisher, N. B. Grimm, & P. Camill, 1994. Vertical hydrologic exchange and ecological stability of a desert stream ecosystem. Ecology 75: 548–560, https://doi.org/10.2307/1939557.

Webb, J. R., N. J. T. Pearce, K. J. Painter, & A. G. Yates, 2019. Hierarchical variation in cellulose decomposition in least-disturbed reference streams: a multi-season study using the cotton strip assay. Landscape Ecology 34: 2353–2369, https://doi.org/10.1007/s10980-019-00893-w.

Wyatt, K. H., F. R. Hauer, & G. F. Pessoney, 2008. Benthic algal response to hyporheic-surface water exchange in an alluvial river. Hydrobiologia 607: 151–161, https://doi.org/10.1007/s10750-008-9385-1.

5 General Conclusion

5.1 Thesis Overview

5.1.1 Summary

This thesis used a multi-scaled approach to assess the role of groundwater input as a driver of spatial and temporal heterogeneity in stream biofilm communities (i.e., biomass and diatom composition) and organic matter processing (i.e., cellulose decomposition). At the largest scale in this study, I assessed if variability in the magnitude of groundwater input influenced patterns of biofilm communities and cellulose decomposition among reaches over four temperate seasons (Chapter 2). At the within reach scale, I compared biofilms in riffle and run habitats among reaches with high, moderate, and low groundwater inputs to determine if the effects of groundwater input on stream biofilm communities and cellulose decomposition were habitat dependent. Additionally, I assessed if environmental drivers modified by groundwater input were associated with patterns in biofilm communities and cellulose decomposition at the habitat scale (Chapter 3). At the smallest scale in this thesis, the patch scale, I assessed the response of stream biofilm communities and cellulose decomposition at patches exhibiting a gradient of groundwater upwelling. I further tested whether there was an association between environmental conditions to biofilm communities and cellulose decomposition (Chapter 4).

5.1.2 Chapter 2: Intra-annual patterns in biofilm communities and cellulose decomposition in a headwater stream network with spatially variable groundwater inputs.

The role of groundwater in modifying surface water environmental conditions and the associations to heterogeneity in stream biofilm communities and organic matter processing at large spatiotemporal scales in nutrient-rich streams is not well-understood. Few studies have examined groundwater influence among reaches in a nutrient-rich stream network through all temperate seasons in streams (but see Griffiths and Tiegs 2016; Tang et al. 2019). Further, in temperate regions, groundwater is often the primary contributor to streamflow to baseflow in the winter and summer months, therefore groundwater influence is likely to vary over an annual cycle (Boulton & Hancock, 2006; Bertrand et al., 2012). Additionally, past work in low nutrient and/or alluvial streams have regularly identified the influence of groundwater on primary productivity and organic matter processing (e.g., Pepin & Hauer, 2002; Wyatt et al., 2008; Griffiths & Tiegs, 2016; Mejia et al., 2016). My work addresses this key knowledge gap by assessing the role of groundwater in influencing spatial and temporal patterns of biofilm communities and organic matter processing in a nutrient-rich headwater stream network.

To assess how variation in the magnitude of groundwater input among reaches in a nutrient-rich stream network in may influence patterns in stream biofilm communities and cellulose decomposition, I measured biofilm communities (i.e., biomass and diatom assemblage composition) and organic matter processing (i.e., cellulose decomposition) in reaches over four temperate seasons. The results showed a lack of association between groundwater input and biofilm communities and organic matter processing in each of the

temperate seasons assessed (autumn, winter, spring, summer). These results suggest that at the reach scale, any nutrient or temperature effect of groundwater input may have been masked by surface water conditions. The findings of this study suggest that regardless of magnitude of groundwater inputs, cumulative upstream mixing of groundwater and surface water likely masked any reach scale environmental heterogeneity associated with groundwater input. Seasonality was found to be the primary factor driving diatom assemblage composition and rates of organic matter processing. Dominant taxa in the diatom assemblage composition shifted with season, following ecological preferences of the taxa. Organic matter processing was slower in winter compared to warmer seasons, however, I found spring had the fastest breakdown rates. These findings highlight the value of multiple season assessments of stream biofilm communities and cellulose decomposition to identify recurring seasonal shifts in ecosystem conditions of temperate streams.

5.1.3 Chapter 3: Effects of groundwater inputs on algal assemblages and cellulose decomposition differ based on habitat type in an agricultural stream.

The modifying role that habitat type (i.e., runs, riffles) may have in altering groundwater input, and subsequent effects on stream biofilm communities and organic matter processing can provide insights into stream ecosystem functioning. Currently, there is a lack of work that explicitly assesses the modifying role of habitat type on groundwater input to nutrient-rich streams, and how this may alter stream environmental conditions, biota, and ecological processes (but see Burrows et al., 2020).

My research addresses this gap by comparing biofilm communities (i.e., biomass and diatom assemblage composition) and organic matter processing (i.e., cellulose decomposition) in riffle and run habitats in reaches with high, moderate, and low groundwater inputs, and identifying if effects of groundwater input were dependent on habitat type. I further assessed the association of environmental variables modified by groundwater inputs to habitat scale patterns in biofilm communities and cellulose decomposition. The results of the study showed that in reaches with moderate and high groundwater inputs algal biomass, and different density and composition of diatom assemblages in runs and riffles, however there was no difference between habitats in the low groundwater reach. Likewise, faster streambed cellulose decomposition in riffles than in runs was observed in reaches with moderate and high groundwater input, with no difference in streambed cellulose decomposition in the reach with low groundwater input. Subsurface cellulose decomposition in both habitat types was significantly faster in the high groundwater reach. This result is in contrast to past work, suggesting that cooler groundwater and lower dissolved oxygen concentrations would slow subsurface decomposition (Štěrba et al., 1992; Boulton & Foster, 1998; Franken et al., 2001). This may be due to groundwater resources (e.g., DOC, nutrients) stimulating heterotrophic activity in the streambed, however, this result suggests that future studies should investigate the role of varying amounts of groundwater have in controlling subsurface organic matter breakdown. These findings suggest that groundwater input may have been rapidly dissipated or overwhelmed by surface water conditions. Thus, future efforts should focus on characterizing upwelling groundwater (e.g., nutrient concentrations, temperature) to mechanistically link habitat type as a modifier of groundwater – surface water exchange

patterns to patterns observed in stream biofilm communities. Overall, the results of this study highlight the co-varying effects of groundwater input and habitat type have in influencing in-stream ecological response in nutrient-rich streams.

5.1.4 Chapter 4: Effects of groundwater input on patch scale patterns in stream biofilm communities and cellulose decomposition.

Within a reach, environmental conditions can vary among habitat types, and at smaller spatial scales within habitats, referred to here as patches (Pringle et al., 1988; Townsend, 1989). Among patches, variation in surface water environmental conditions such as stream velocity, water temperature, and nutrient availability can create a mosaic of patch habitat quality (Thorp et al., 2006, 2008). Environmental heterogeneity at the patch scale has been found to influence biofilm communities and organic matter processing (Stevenson, 1997; Royer & Minshall, 2003; Graça et al., 2015). Groundwater inputs can also contribute to heterogeneity in environmental conditions where there are different physical and chemical properties between groundwater and surface waters, where changes to surface water environmental conditions due to groundwater input has also been associated with changes in biological response (Brunke & Gonser, 1997; Boano et al., 2014). However, there is currently no work that has investigated the patch scale association of groundwater input to biological response at the patch scale.

The findings of this work indicate that groundwater inputs among patches within the studied reach did not generate environmental heterogeneity, despite the groundwater template suggesting variation in groundwater inputs based on variation in subsurface temperature and stream water – subsurface temperature gradient (Robinson et al., 2022). Rather than

environmental drivers modified by groundwater input, this study found that environmental variation among patches was driven by differences in stream velocity, further indicating the lack of environmental heterogeneity driven by groundwater input. Indeed, biofilm biomass, diatom composition, and streambed cellulose decomposition followed expected associations with varying stream velocity at the patch scale (Poff, 1997; Stevenson, 1997; Graça et al., 2015).

Subsurface cellulose decomposition was slower in patches with groundwater upwelling, indicating that where there are groundwater flows in the shallow subsurface during warmer seasons, carbon processing may be decreased. This work represents an initial investigation into patch scale association of groundwater inputs to biological response. The results of this study suggest that additional work, such as using a wider ranging gradient of groundwater – surface water exchange and measuring environmental conditions at the stream water – biofilm interface, will allow for further insights into the patch scale dynamics of environmental variation and associated heterogeneity in biological response.

5.2 Research Implications and Future Work

This thesis presents a comprehensive, multi-scale approach to assessing the role of groundwater inputs in generating heterogeneity in biofilm communities in nutrient-rich streams. By integrating concepts of spatial and temporal scale from stream ecosystems (Vannote et al., 1980; Frissell et al., 1986; Poff, 1997), stream biofilm communities (Stevenson, 1997; Royer & Minshall, 2003), and groundwater – surface water exchange (Dent et al., 2001; Kalbus et al., 2006; Boano et al., 2014; Conant et al., 2019), my work provides

insight into the spatial scaling of the relationship of groundwater – surface water exchange and stream biofilm community character. The results of this work highlight the: 1) importance of landscape context of the stream ecosystem; 2) role of scale in detecting groundwater influence, and; 3) implications for stream ecosystem monitoring.

5.2.1 Landscape Context

My work demonstrates that groundwater input may not necessarily lead to ecological heterogeneity in an enriched agricultural stream ecosystem. An important finding from my studies in an agricultural stream network is that when nutrients are higher in the surface water than the groundwater, there will likely be heterogeneity in assemblages or increases in productivity by stream biofilm communities. My findings are in contrast to previous work in nutrient-poor streams where nutrient-rich groundwater has been shown to stimulate biofilm productivity (e.g., Wyatt et al., 2008; Roy et al., 2011; Mejia et al., 2016; Burrows et al., 2020). The discrepancy between the influence of groundwater input in the enriched surface waters in agricultural stream network presented in this thesis compared to previous work in nutrient-poor streams suggests that in enriched agricultural there may be a lack of groundwater effects because nutrient thresholds for biota are met by surface waters, and/or that groundwater may have lower nutrient availability than surface waters. Agricultural streams are often enriched due to land use, combined with factors such as field run off, tile drainage, and shallow groundwater – surface water exchange may contribute to the dichotomy between the consistent results across scales in the agricultural stream network in this thesis compared with past studies in nutrient-poor streams.

5.2.2 Role of Scale

My work was the first to use multiple, hierarchical spatial scales to assess the role of groundwater on patterns in stream biofilm communities. The multi-scale approach taken in my work in an enriched agricultural stream network showed that stream biofilm community response to groundwater input was scale dependent. At the largest scale in this thesis, among reaches in the stream network over four temperate seasons, groundwater inputs were likely masked by prevailing surface water conditions because there was no biologically meaningful environmental variation among reaches within a given season. Similarly, at the smallest scale in this thesis, the patch scale, environmental variation was driven by stream velocity, rather than environmental variables that can be modified by groundwater (e.g., nutrients and temperature). At the intermediate scale, among reaches with different levels of groundwater inputs, I found that groundwater effects on biofilm communities were expressed in run habitats; however, I was unable to associate heterogeneity in biofilm communities to measured environmental variables. My work across multiple spatial scales in an enriched agricultural stream network suggests that any potential environmental variation driven by groundwater may not be readily detectable through conventional measures of water chemistry, although there may be a biological response to groundwater input (i.e., observed at the habitat scale). My findings are in contrast with past work in nutrient-poor streams which has been conducted at individual scales in differing stream ecosystems (e.g., reach: Tang et al., 2019, Burrows et al., 2020; habitat: Pepin & Hauer 2002; and patch: Wyatt et al., 2008, Mejia et al., 2016) which have consistently observed effects of groundwater on biological response that were associated with environmental variation driven by

groundwater. The results of my work highlight both the importance of stream ecosystem type (i.e., nutrient status) and spatial scale of measurement in detecting an association of groundwater to ecological response.

5.2.3 Stream Monitoring

The multi-scale approach taken in this thesis can inform use or development of monitoring tools. Although not the focus of this work, Chapter 2 highlights the important role of seasonality on driving recurring seasonal shifts in diatom assemblage composition in temperate stream ecosystems. Our findings suggest that if monitoring is done on an annual basis, then monitoring should be conducted in a single season (e.g., late summer, Lavoie et al., 2014) because otherwise the effects of watershed management activities/practices may be masked by natural seasonal variation. Consideration of timing for biomonitoring should be prioritized due to increasingly changing and unpredictable seasonal conditions as a result of climate change.

^{222}Rn concentrations were used to estimate groundwater inflows within a stream reach based on a mass balance model, allowing for categorization of reaches (i.e., high, moderate, and low) for a relative comparison based on groundwater input. Thus, ^{222}Rn concentration as a part of a mass balance approach to generate relative categorical comparisons to assess stream biofilm communities may be a stronger tool for identification of reaches with groundwater input than a gradient of ^{222}Rn concentrations across reaches within a network.

The results of my studies also emphasized the key role of stream velocity as a modifier of groundwater input, where groundwater influence is expressed in areas of slow velocity. My

work is an important addition to the well-understood patterns in hydrogeomorphic features of a stream, where patchiness in groundwater input is has been shown to be influenced by differences in hydraulic head (Harvey & Bencala, 1993; Brunke & Gonser, 1997). However, my work is the first to explicitly assess the role of habitat type (i.e., differing stream velocities) in modifying stream biofilm community response to groundwater input (but see Burrows et al., 2020). The findings of this study indicate that future studies are required to further explore the relationship between stream velocity and groundwater input, and the association to stream biofilm communities across a range of stream ecosystems.

5.3 Concluding Remarks

My work demonstrates that groundwater input may not necessarily manifest in environmental heterogeneity that drives variation in biofilm communities in an enriched agricultural stream ecosystem. In nutrient-poor stream ecosystems, groundwater has been shown to be a modifier of surface water environmental conditions, which are associated with variation biofilm community assemblages and processes. My work shows that groundwater input does not necessarily influence surface water conditions in the same way across stream ecosystem types, highlighting the importance of stream landcape context. These results will contribute to improving our understanding of the role of groundwater in influencing biofilm communities in differing stream ecosytems types and across spatial scales.

References

Allan, J. D., & M. Castillo, 2007a. Primary producers In Allan, D. J., & M. Castillo (eds), Stream Ecology: Structure and function of running waters, 2nd Edition. Springer, Dordrecht, Netherlands: 105–133.

Allan, J. D., & M. Castillo, 2007b. Streamwater chemistry In Allan, D. J., & M. Castillo (eds), Stream Ecology: Structure and function of running waters, 2nd Edition. Springer, Dordrecht, The Netherlands: 57–74.

Allan, J. D., & M. Castillo, 2007c. The abiotic environment In Allan, D. J., & M. Castillo (eds), Stream Ecology: Structure and function of running waters, 2nd Edition. Springer, Dordrecht, The Netherlands: 75–103.

Allan, J. D., & M. M. Castillo, 2007d. Stream ecosystem metabolism In Allan, D. J., & M. Castillo (eds), Stream Ecology: Structure and function of running waters, 2nd Edition. Springer, Dordrecht, The Netherlands: 287–315.

Anderson-Glenna, M. J., V. Bakkestuen, & N. J. W. Clipson, 2008. Spatial and temporal variability in epilithic biofilm bacterial communities along an upland river gradient. FEMS Microbiology Ecology 64: 407–418, https://doi.org/10.1111/j.1574-6941.2008.00480.x.

Atkinson, A. P., I. Cartwright, B. S. Gilfedder, H. Hofmann, N. P. Unland, D. I. Cendón, & R. Chisari, 2015. A multi-tracer approach to quantifying groundwater inflows to an upland river; assessing the influence of variable groundwater chemistry. Hydrological Processes 29: 1–12, https://doi.org/10.1002/hyp.10122.

Aumen, N. G., P. J. Bottomley, G. M. Ward, & S. V Gregory, 1983. Microbial decomposition of wood in streams: Distribution of microflora and factors affecting [14C] lignocellulose mineralization. Applied and Environmental Microbiology 46: 1409–1416, https://doi.org/0099-2240/83/121409-08$02.00/0.

Bailet, B., A. Bouchez, A. Franc, J.-M. Frigerio, F. Keck, S.-M. Karjalainen, F. Rimet, S. Schneider, & M. Kahlert, 2019. Molecular versus morphological data for benthic diatoms

biomonitoring in Northern Europe freshwater and consequences for ecological status. Metabarcoding and Metagenomics 3: 21–35, https://doi.org/10.3897/mbmg.3.34002.

Battin, T. J., K. Besemer, M. M. Bengtsson, A. M. Romani, & A. I. Packmann, 2016. The ecology and biogeochemistry of stream biofilms. Nature Reviews Microbiology 14: 251–263, https://doi.org/10.1038/nrmicro.2016.15.

Battin, T. J., L. A. Kaplan, J. D. Newbold, & C. M. E. Hansen, 2003a. Contributions of microbial biofilms to ecosystem processes in stream mesocosms. Nature 426: 439–442, https://doi.org/10.1038/nature02152.

Battin, T. J., L. A. Kaplan, J. D. Newbold, X. Cheng, & C. Hansen, 2003b. Effects of current velocity on the nascent architecture of stream microbial biofilms. Applied and Environmental Microbiology 69: 5443–5452, https://doi.org/10.1128/AEM.69.9.5443.

Battin, T. J., A. Wille, B. Sattler, & R. Psenner, 2001. Phylogenetic and functional heterogeneity of sediment biofilms along environmental gradients in a glacial stream. Applied and Environmental Microbiology 67: 799–807, https://doi.org/10.1128/AEM.67.2.799-807.2001.

Baxter, C. V., & F. R. Hauer, 2000. Geomorphology, hyporheic exchange, and selection of spawning habitat by bull trout (*Salvelinus confluentus*). Canadian Journal of Fisheries and Aquatic Sciences 57: 1470–1481, https://doi.org/10.1139/f00-056.

Bertrand, G., N. Goldscheider, J. M. Gobat, & D. Hunkeler, 2012. Review: From multi-scale conceptualization to a classification system for inland groundwater-dependent ecosystems. Hydrogeology Journal 20: 5–25, https://doi.org/10.1007/s10040-011-0791-5.

Besemer, K., 2015. Biodiversity, community structure and function of biofilms in stream ecosystems. Research in Microbiology 166: 774–781, https://doi.org/10.1016/j.resmic.2015.05.006.

Biggs, B. J. F., 1990. Periphyton communities and their environments in New Zealand rivers. New Zealand Journal of Marine and Freshwater Research 24: 367–386, https://doi.org/10.1080/00288330.1990.9516431.

Biggs, B. J. F., 1996. Patterns in benthic algae of streams In Stevenson, R. J., M. L. Bothwell, & R. L. Lowe (eds), Algal ecology: freshwater benthic ecosystems. Academic Press, San Diego, CA, USA: 31–56.

Biggs, B. J. F., 2000. Eutrophication of streams and rivers: dissolved nutrient-chlorophyll relationships for benthic algae. Journal of the American Water Resources Association 19: 17–31.

Biggs, B. J. F., & P. Gerbeaux, 1993. Periphyton development in relation to macro-scale (geology) and micro-scale (velocity) limiters in two gravel-bed rivers, New Zealand. New Zealand Journal of Marine and Freshwater Research 27: 39–53, https://doi.org/10.1080/00288330.1993.9516544.

Biggs, B. J. F., D. G. Goring, & V. I. Nikora, 1998. Subsidy and stress responses of stream periphyton to gradients in water velocity as a function of community growth form. Journal of Phycology 34: 598–607, https://doi.org/10.1046/j.1529-8817.1998.340598.x.

Biggs, B. J. F., & C. W. Hickey, 1994. Periphyton responses to a hydraulic gradient in a regulated river in New Zealand. Freshwater Biology John Wiley & Sons, Ltd 32: 49–59, https://doi.org/https://doi.org/10.1111/j.1365-2427.1994.tb00865.x.

Biggs, B. J. F., & H. A. Thomsen, 1995. Disturbance of stream periphyton by perturbations in shear stress: Time to structural failure and differences in community resistance. Journal of Phycology 31: 233–241. https://doi.org/10.1111/j.0022-3646.1995.00233.x.

Boano, F., J. W. Harvey, A. Marion, A. I. Packman, R. Revelli, L. Ridolfi, & A. Wörman, 2014. Hyporheic flow and transport processes. Reviews of Geophysics 52: 603–679, https://doi.org/10.1002/2012RG000417.

Borchardt, M., 1996. Nutrients In Stevenson, R. J., M. Bothwell, & R. Low (eds), Algal ecology: freshwater benthic ecosystems. Academic Press, San Diego, CA, USA: 183–227.

Boulton, A. J., & P. I. Boon, 1991. A review of methodology used to measure leaf litter decomposition in lotic environments: Time to turn over an old leaf?. Australian Journal of Marine and Freshwater Research 42: 1–43, https://doi.org/10.1071/MF9910001.

Boulton, A. J., S. Findlay, P. Marmonier, E. H. Stanley, & H. M. Valett, 1998. The functional significance of the hyporheic zone in streams and rivers. Annual Review of Ecology and Systematics 29: 59–81, https://doi.org/10.1146/annurev.ecolsys.29.1.59.

Boulton, A. J., & P. J. Hancock, 2006. Rivers as groundwater-dependent ecosystems: A review of degrees of dependency, riverine processes and management implications. Australian Journal of Botany 54: 133–144, https://doi.org/10.1071/BT05074.

Boulton, A. J., & J. M. Quinn, 2000. A simple and versatile technique for assessing cellulose decomposition potential in floodplain and riverine sediments. Archiv für Hydrobiologie 150: 133–151.

Brown, J. H., J. F. Gillooly, A. P. Allen, Van. M. Savage, & G. B. West, 2004. Toward a metabolic theory of ecology. Ecology 85: 1771–1789, https://doi.org/10.1890/03-9000.

Brunke, M., & T. Gonser, 1997. The ecological significance of exchange processes between rivers and groundwater. Freshwater Biology 37: 1–33, https://doi.org/10.1046/j.1365-2427.1997.00143.x.

Burkholder, J. M., 1996. Interactions of benthic algae with their substrata In Stevenson, R. J., M. L. Bothwell, & R. L. Lowe (eds), Algal ecology: freshwater benthic ecosystems. San Diego, California: 253–297.

Burrows, R. M., L. Beesley, M. M. Douglas, B. J. Pusey, & M. J. Kennard, 2020. Water velocity and groundwater upwelling influence benthic algal biomass in a sandy tropical river: implications for water-resource development. Hydrobiologia 847: 1207–1219, https://doi.org/10.1007/s10750-020-04176-3.

Cao, Y., D. Larsen, & R. Thorne, 2001. Rare species in multivariate analysis for bioassessment. Journal of the North American Benthological Society 20: 144–153.

Carayon, D., J. Tison-Rosebery, & F. Delmas, 2019. Defining a new autoecological trait matrix for French stream benthic diatoms. Ecological Indicators Elsevier 103: 650–658, https://doi.org/10.1016/j.ecolind.2019.03.055.

Cardenas, M. B., J. L. Wilson, & V. A. Zlotnik, 2004. Impact of heterogeneity, bed forms, and stream curvature on subchannel hyporheic exchange. Water Resources Research 40: 1–14, https://doi.org/10.1029/2004WR003008.

Cardinale, B. J., M. A. Palmer, C. M. Swan, S. Brooks, & N. LeRoy Poff, 2002. The influence of substrate heterogeneity on biofilm metabolism in a stream ecosystem. Ecology 83: 412–422, https://doi.org/10.1890/0012-9658(2002)083[0412:TIOSHO]2.0.CO;2.

Cey, E. E., D. L. Rudolph, G. W. Parkin, & R. Aravena, 1998. Quantifying groundwater discharge to a small perennial stream in southern Ontario, Canada. Journal of Hydrology Elsevier 210: 21–37, https://doi.org/10.1016/S0022-1694(98)00172-3.

Chambers, P. A., D. J. McGoldrick, R. B. Brua, C. Vis, J. M. Culp, & G. A. Benoy, 2012. Development of environmental thresholds for nitrogen and phosphorus in streams. Journal of Environmental Quality 41: 7–20, https://doi.org/10.2134/jeq2010.0273.

Cherry, D. S., & R. K. Guthrie, 1973. Temperature influence on bacterial populations in three aquatic systems. Water Research 8: 149–155, https://doi.org/10.1016/0043-1354(74)90037-2.

Clapcott, J. E., & L. A. Barmuta, 2010a. Metabolic patch dynamics in small headwater streams: exploring spatial and temporal variability in benthic processes. Freshwater Biology (2010) 55: 806–824, https://doi.org/10.1111/j.1365-2427.2009.02324.x.

Conant, B., C. E. Robinson, M. J. Hinton, & H. A. J. Russell, 2019. A framework for conceptualizing groundwater-surface water interactions and identifying potential impacts on water quality, water quantity, and ecosystems. Journal of Hydrology 574: 609–627, https://doi.org/10.1016/j.jhydrol.2019.04.050.

Cook, P. G., G. Favreau, J. C. Dighton, & S. Tickell, 2003. Determining natural groundwater influx to a tropical river using radon, chlorofluorocarbons and ionic environmental tracers. Journal of Hydrology 277: 74–88, https://doi.org/10.1016/S0022-1694(03)00087-8.

Cook, P. G., 2013. Estimating groundwater discharge to rivers from river chemistry surveys. Hydrological Processes 27: 3694–3707, https://doi.org/10.1002/hyp.9493.

Cornut, J., A. Elger, D. Lambrigot, P. Marmonier, & E. Chauvet, 2010. Early stages of leaf decomposition are mediated by aquatic fungi in the hyporheic zone of woodland streams. Freshwater Biology 55: 2541–2556, https://doi.org/10.1111/j.1365-2427.2010.02483.x.

Costello, D. M., S. D. Tiegs, L. Boyero, C. Canhoto, K. A. Capps, M. Danger, P. C. Frost, M. O. Gessner, N. A. Griffiths, H. M. Halvorson, K. et al., 2022. Global Patterns and Controls of Nutrient Immobilization on Decomposing Cellulose in Riverine Ecosystems. Global Biogeochemical Cycles 36: 1–15, https://doi.org/10.1029/2021GB007163.

Costerton, J. W., Z. Lewandowski, D. E. Caldwell, D. R. Korber, & H. M. Lappin-Scott, 1995. Microbial biofilms. Annual Review of Microbiology 49: 711–745, https://doi.org/10.1201/9780203500224.

Crenshaw, C. L., H. M. Valett, & J. L. Tank, 2002. Effects of coarse particulate on fungal biomass and organic matter in invertebrate the of subsurface a headwater stream density. Journal of the North American Benthological Society 21: 28–42, https://doi.org/https://doi.org/10.2307/1468297.

Cummins, K. W., 1974. Structure and Function of Stream Ecosystems. BioScience 24: 631–641, https://doi.org/https://doi.org/10.2307/1296676.

Dang, C. K., M. Schindler, E. Chauvet, & M. O. Gessner, 2009. Temperature oscillation coupled with fungal community shifts can modulate warming effects on litter decomposition. Ecology 90: 122–131.

Dang, H., & C. R. Lovell, 2015. Microbial Surface Colonization and Biofilm Development in Marine Environments. Microbiology and Molecular Biology Reviews 80: 91–138, https://doi.org/10.1128/MMBR.00037-15.

Danger, M., J. Cornut, E. Chauvet, P. Chavez, A. Elger, & A. Lecerf, 2013. Benthic algae stimulate leaf litter decomposition in detritus-based headwater streams: a case of aquatic priming effect?. Ecology 94: 1604–1613.

Delgado, C., S. F. P. Almeida, C. L. Elias, V. Ferreira, & C. Canhoto, 2017. Response of biofilm growth to experimental warming in a temperate stream. Ecohydrology 10: 1–9, https://doi.org/10.1002/eco.1868.

DeNicola, D., 1996. Periphyton responses to temperature at different ecological levels In Stevenson, R. J., M. L. Bothwell, & R. L. Lowe (eds), Algal ecology: freshwater benthic ecosystems. Academic Press, San Diego, CA, USA.: 149–181.

Dent, C. L., N. B. Grimm, & S. G. Fisher, 2001. Multiscale effects of surface-subsurface exchange on stream water nutrient concentrations. Journal of the North American Benthological Society 20: 162–181, https://doi.org/10.2307/1468313.

Dodds, W. K., V. H. Smith, & K. Lohman, 2002. Nitrogen and phosphorus relationships to benthic algal biomass in temperate streams. Canadian Journal of Fisheries and Aquatic Sciences 59: 865–874, https://doi.org/10.1139/F02-063.

Dodds, W. K., & E. B. Welch, 2000. Establishing nutrient criteria in streams. Journal of the North American Benthological Society 19: 186–196.

Egglishaw, H. J., 1972. An experimental study of the breakdown of cellulose in fast-flowing streams. Mem. Ist. Ital. Idrobiol. Suppl. 29 405–428.

Enríquez, S., C. M. Duarte, & K. Sand-Jensen, 1993. Patterns in decomposition rates among photosynthetic organisms: the importance of detritus C:N:P content. Oecologia 94: 457–471, https://doi.org/10.1007/BF00566960.

Fernandes, I., C. Pascoal, H. Guimarães, R. Pinto, I. Sousa, & F. Cássio, 2012. Higher temperature reduces the effects of litter quality on decomposition by aquatic fungi. Freshwater Biology John Wiley & Sons, Ltd 57: 2306–2317, https://doi.org/https://doi.org/10.1111/fwb.12004.

Ferreira, V., B. Castagneyrol, J. Koricheva, V. Gulis, E. Chauvet, & M. A. S. Graça, 2015. A meta-analysis of the effects of nutrient enrichment on litter decomposition in streams. Biological Reviews 90: 669–688, https://doi.org/10.1111/brv.12125.

Ferreira, V., & E. Chauvet, 2011. Future increase in temperature more than decrease in litter quality can affect microbial litter decomposition in streams. Oecologia 167: 279–291, https://doi.org/10.1007/s00442-011-1976-2.

Ferreira, V., V. Gulis, & M. A. S. Graça, 2006. Whole-stream nitrate addition affects litter decomposition and associated fungi but not invertebrates. Oecologia 149: 718–729, https://doi.org/10.1007/s00442-006-0478-0.

Findlay, S. E. G., & T. L. Arsuffi, 1989. Microbial growth and detritus transformations during decomposition of leaf litter in a stream. Freshwater Biology 21: 261–269, https://doi.org/10.1111/j.1365-2427.1989.tb01364.x.

Fleckenstein, J. H., S. Krause, D. M. Hannah, & F. Boano, 2010. Groundwater-surface water interactions: New methods and models to improve understanding of processes and dynamics. Advances in Water Resources Elsevier Ltd 33: 1291–1295, https://doi.org/10.1016/j.advwatres.2010.09.011.

Flinders, C. A., R. L. Ragsdale, J. Ikoma, W. J. Arthurs, & J. Kidd, 2019. Spatial and temporal patterns of diatom assemblages, and their drivers, in four US streams: evidence from a long-term dataset. Hydrobiologia 846: 159–179, https://doi.org/10.1007/s10750-019-04061-8.

Follstad Shah, J. J., J. S. Kominoski, M. Ardón, W. K. Dodds, M. O. Gessner, N. A. Griffiths, C. P. Hawkins, S. L. Johnson, A. Lecerf, C. J. LeRoy, D. W. P. Manning, A. D. Rosemond, R. L. Sinsabaugh, C. M. Swan, J. R. Webster, & L. H. Zeglin, 2017. Global synthesis of the

temperature sensitivity of leaf litter breakdown in streams and rivers. Global Change Biology 23: 3064–3075, https://doi.org/10.1111/gcb.13609.

Frissell, C. A., W. J. Liss, C. E. Warren, & M. D. Hurley, 1986. A hierarchical framework for stream habitat classification: Viewing streams in a watershed context. Environmental Management 10: 199–214, https://doi.org/10.1007/BF01867358.

Frost, P. C., & J. J. Elser, 2002. Effects of light and nutrients on the net accumulation and elemental composition of epilithon in boreal lakes. Freshwater Biology 47: 173–183, https://doi.org/10.1046/j.1365-2427.2002.00796.x.

Geraldes, P., C. Pascoal, & F. Cássio, 2012. Effects of increased temperature and aquatic fungal diversity on litter decomposition. Fungal Ecology 5: 734–740, https://doi.org/10.1016/j.funeco.2012.05.007.

Gessner, M., & E. Chauvet, 2002. A case for using litter breakdown to assess functional stream integrity. Ecological Applications 12: 498–510.

Gessner, M. O., E. Chauvet, & M. Dobson, 1999. A Perspective on Leaf Litter Breakdown in Streams. Oikos 85: 377–384.

Graça, M. A. S., V. Ferreira, C. Canhoto, A. C. Encalada, F. Guerrero-Bolaño, K. M. Wantzen, & L. Boyero, 2015. A conceptual model of litter breakdown in low order streams. International Review of Hydrobiology 100: 1–12, https://doi.org/10.1002/iroh.201401757.

Greenwood, J. L., & A. D. Rosemond, 2005. Periphyton response to long-term nutrient enrichment in a shaded headwater stream. Canadian Journal of Fisheries and Aquatic Sciences 62: 2033–2045, https://doi.org/10.1139/F05-117.

Griffith, M. B., & S. A. Perry, 1994. Fungal biomass and leaf litter processing in streams of different water chemistry. Hydrobiologia 294: 51–60, https://doi.org/10.1007/BF00017625.

Griffiths, N. A., & S. D. Tiegs, 2016. Organic-matter decomposition along a temperature gradient in a forested headwater stream. Freshwater Science 35: 518–533, https://doi.org/10.1086/685657.

Gulis, V., V. Ferreira, & M. A. S. Graça, 2006. Stimulation of leaf litter decomposition and associated fungi and invertebrates by moderate eutrophication: Implications for stream assessment. Freshwater Biology 51: 1655–1669, https://doi.org/10.1111/j.1365-2427.2006.01615.x.

Gulis, V., & K. Suberkropp, 2003. Leaf litter decomposition and microbial activity in nutrient-enriched and unaltered reaches of a headwater stream. Freshwater Biology 48: 123–134, https://doi.org/10.1046/j.1365-2427.2003.00985.x.

Guo, F., M. J. Kainz, F. Sheldon, & S. E. Bunn, 2016. The importance of high-quality algal food sources in stream food webs - current status and future perspectives. Freshwater Biology 61: 815–831, https://doi.org/10.1111/fwb.12755.

Hanrahan, B. R., J. L. Tank, A. F. Aubeneau, & D. Bolster, 2018. Substrate-specific biofilms control nutrient uptake in experimental streams. Freshwater Science 37: 456–471, https://doi.org/10.1086/699004.

Harvey, J. W., & E. Bencala, 1993. The Effect of Streambed Topography on Surface-Subsurface Water Exchange in Mountain Catchments. 29: 89–98, https://doi.org/https://doi.org/10.1029/92WR01960.

Harvey, J. W., & M. Gooseff, 2015. River corridor science: Hydrologic exchange and ecological consequences from bedforms to basins. Water Resources Research 51: 6893–6922, https://doi.org/10.1002/2015WR017617.

Hill, W., 1996. Effects of light In Stevenson, R. J., L. M. Bothwell, & L. R. Lowe (eds), Algal ecology: freshwater benthic ecosystems. Academic Press, San Diego, CA, USA: 121–148, https://doi.org/10.1017/CBO9781107415324.004.

Horner, R. R., E. B. Welch, M. R. Seeley, & J. M. Jacoby, 1990. Responses of periphyton to changes in current velocity, suspended sediment and phosphorus concentration. Freshwater Biology 24: 215–232, https://doi.org/10.1111/j.1365-2427.1990.tb00704.x.

Howard-Parker, B., B. White, H. M. Halvorson, & M. A. Evans-White, 2020. Light and dissolved nutrients mediate recalcitrant organic matter decomposition via microbial priming in experimental streams. Freshwater Biology 65: 1189–1199, https://doi.org/10.1111/fwb.13503.

Hynes, H. B. N., 1983. Groundwater and stream ecology. Hydrobiologia 100: 93–99, https://doi.org/10.1007/BF00027424.

Irvine, D. J., & L. K. Lautz, 2015. High resolution mapping of hyporheic fluxes using streambed temperatures: Recommendations and limitations. Journal of Hydrology 524: 137–146, https://doi.org/10.1016/j.jhydrol.2015.02.030.

Jones, J. B., S. G. Fisher, & N. B. Grimm, 1995. Vertical Hydrologic Exchange and Ecosystem Metabolism in a Sonoran Desert Stream. Ecology John Wiley & Sons, Ltd 76: 942–952, https://doi.org/10.2307/1939358.

Kaandorp, V. P., P. J. Doornenbal, H. Kooi, H. Peter Broers, & P. G. B. de Louw, 2019. Temperature buffering by groundwater in ecologically valuable lowland streams under current and future climate conditions. Journal of Hydrology X 3: 1–16, https://doi.org/10.1016/j.hydroa.2019.100031.

Kalbus, E., F. Reinstorf, & M. Schirmer, 2006. Measuring methods for groundwater - Surface water interactions: A review. Hydrology and Earth System Sciences 10: 873–887, https://doi.org/10.5194/hess-10-873-2006.

Korbel, K. L., & G. C. Hose, 2015. Habitat, water quality, seasonality, or site? Identifying environmental correlates of the distribution of groundwater biota. Freshwater Science 34: 329–342, https://doi.org/10.1086/680038.

Krause, S., D. M. Hannah, J. H. Fleckenstein, C. M. Heppel, D. Kaeser, R. Pickup, G. Pinay, A. L. Robertson, & P. J. Wood, 2011. Inter-disciplinary perspectives on processes in the hyporheic zone. Ecohydrology 481–499, https://doi.org/10.1002/eco.

Lange, K., C. R. Townsend, & C. D. Matthaei, 2016. A trait-based framework for stream algal communities. Ecology and Evolution 6: 23–36, https://doi.org/10.1002/ece3.1822.

Lavoie, I., S. Campeau, N. Zugic-Drakulic, J. G. Winter, & C. Fortin, 2014. Using diatoms to monitor stream biological integrity in Eastern Canada: An overview of 10 years of index development and ongoing challenges. Science of the Total Environment 475: 187–200, https://doi.org/10.1016/j.scitotenv.2013.04.092.

Lavoie, I., & S. Campeau, 2016. Assemblage diversity, cell density and within-slide variability: Implications for quality assurance/quality control and uncertainty assessment in diatom-based monitoring. Ecological Indicators Elsevier Ltd 69: 415–421, https://doi.org/10.1016/j.ecolind.2016.05.001.

Lavoie, I., S. Campeau, M. Grenier, & P. J. Dillon, 2006. A diatom-based index for the biological assessment of eastern Canadian rivers: an application of correspondence analysis (CA). Canadian Journal of Fisheries and Aquatic Sciences 63: 1793–1811, https://doi.org/10.1139/F06-084.

Lavoie, I., S. Campeau, N. Zugic-Drakulic, J. G. Winter, & C. Fortin, 2014. Using diatoms to monitor stream biological integrity in Eastern Canada: An overview of 10 years of index development and ongoing challenges. Science of the Total Environment 475: 187–200, https://doi.org/10.1016/j.scitotenv.2013.04.092.

Lavoie, I., P. J. Dillon, & S. Campeau, 2009. The effect of excluding diatom taxa and reducing taxonomic resolution on multivariate analyses and stream bioassessment. Ecological Indicators 9: 213–225, https://doi.org/10.1016/j.ecolind.2008.04.003.

Lavoie, I., K. M. Somers, A. M. Paterson, & P. J. Dillon, 2005. Assessing scales of variability in benthic diatom community structure. Journal of Applied Phycology 17: 509–513, https://doi.org/10.1007/s10811-005-9001-y.

Lavoie, I., W. F. Vincent, R. Pienitz, & J. Painchaud, 2004. Benthic algae as bioindicators of agricultural pollution in the streams and rivers of southern Québec (Canada). Aquatic Ecosystem Health and Management 7: 43–58, https://doi.org/10.1080/14634980490281236.

Lowe, R., & Y. Pan, 1996. Benthic algal communities as biological monitors In Bothwell, M. L., & R. Lowe (eds), Algal Ecology: Freshwater Benthic Ecosystems. Academic Press, San Diego, CA, USA: 705–739.

Malard, F., & F. Hervant, 1999. Oxygen supply and the adaptations of animals in groundwater. Freshwater Biology 41: 1–30, https://doi.org/10.1046/j.1365-2427.1999.00379.x.

Malard, F., K. Tockner, M. J. Dole-Olivier, & J. V. Ward, 2002. A landscape perspective of surface-subsurface hydrological exchanges in river corridors. Freshwater Biology 47: 621–640, https://doi.org/10.1046/j.1365-2427.2002.00906.x.

Mejia, F. H., C. V. Baxter, E. K. Berntsen, & A. K. Fremier, 2016. Linking groundwater – surface water exchange to food production and salmonid growth. Canadian Journal of Fisheries and Aquatic Sciences 73: 1650–1660, https://doi.org/10.1139/cjfas-2015-0535.

Minshall, G. W., S. A. Thomas, J. D. Newbold, M. T. Monaghan, & C. E. Cushing, 2017. Physical factors influencing fine organic particle transport and deposition in streams. Journal of the North American Benthological Society 19: 1–16. http://www.jstor.org/stable/1468278.

Mulholland, P. J., J. D. Newbold, J. W. Elwood, L. A. Ferren, & J. R. Webster, 1985. Phosphorus Spiralling in a Woodland Stream: Seasonal Variations. Ecology 66: 1012–1023, https://doi.org/10.2307/1940562.

Mullinger, N.J., Binley, A.M., Pates, J.M., & N.P. Crook, 2007. Radon in Chalk streams: Spatial and temporal variation of groundwater sources in the Pang and Lambourn catchments, UK. Journal of Hydrology 339(3-4): 172–182, https://doi.org/10.1016/j.jhydrol.2007.03.010

Munn, M. D., L. L. Osborne, & M. J. Wiley, 1989. Factors influencing periphyton growth in agricultural streams of central Illinois. Hydrobiologia 174: 89–97, https://doi.org/10.1007/BF00014057.

Munn, M.D., J. Frey, & A. Tesoriero, 2010. The influence of nutrients and physical habitat in regulating algal biomass in agricultural streams. Environmental Management 45: 603–615, https://doi.org/10.1007/s00267-010-9435-0.

Negulescu, M., & V. Rojanski, 1969. Recent research to determine reaeration coefficient. Water Research, 3(3): 189-202, https://doi.org/10.1016/0043-1354(69)90058-X

Nogaro, G., T. Datry, F. Mermillod-Blondin, S. Descloux, & B. Montuelle, 2010. Influence of streambed sediment clogging on microbial processes in the hyporheic zone. Freshwater Biology 55: 1288–1302, https://doi.org/10.1111/j.1365-2427.2009.02352.x.

O'Connor, D., & W.E. Dobbins, 1958. Mechanism of Reaeration in Natural Streams. Transactions of the American Society of Civil Engineers, 123: 641-666, https://doi.org/10.1061/TACEAT.0007609

Palmer, M. A., & N. L. Poff, 1997. The influence of heterogeneity on patterns and processes in streams. Journal of the North American Benthological Society 16: 169–173, https://www.jstor.org/stable/1468249.

Pan, Y., R. J. Stevenson, B. H. Hill, A. T. Herlihy, B. Gary, Y. Pan, R. J. A. N. Stevenson, B. H. Hill, A. T. Herlihy, & G. B. Collins, 1996. Using diatoms as indicators of ecological conditions in lotic systems: A regional assessment. Journal of the North American Benthological Society 15: 481–495, http://www.jstor.org/stable/1467800

Passy, S. I., 2001. Spatial paradigms of lotic diatom distribution: A landscape ecology perspective. Journal of Phycology 37: 370–378, https://doi.org/10.1046/j.1529-8817.2001.037003370.x.

Passy, S. I., 2007. Diatom ecological guilds display distinct and predictable behavior along nutrient and disturbance gradients in running waters. Aquatic Botany 86: 171–178, https://doi.org/10.1016/j.aquabot.2006.09.018.

Passy, S. I., & C. A. Larson, 2011. Succession in Stream biofilms is an environmentally driven gradient of stress tolerance. Microbial Ecology 62: 414–424, https://doi.org/10.1007/s00248-011-9879-7.

Pepin, D. M., & F. R. Hauer, 2002. Benthic responses to groundwater – surface water exchange in 2 alluvial rivers in northwestern Montana. Journal of the North American Benthological Society 21: 370–383, https://doi.org/10.2307/1468476.

Petersen, R. C., & K. W. Cummins, 1974. Leaf processing in a woodland stream. Freshwater Biology 4: 343–368, https://doi.org/https://doi.org/10.1111/j.1365-2427.1974.tb00103.x.

Poff, N. L., 1997. Landscape filters and species traits: Towards mechanistic understanding and prediction in stream ecology. Journal of the North American Benthological Society 16: 391–409, https://doi.org/10.2307/1468026

Poff, N. L., J. D. Allan, M. B. Bain, J. R. Karr, K. L. Prestegaard, B. D. Richter, R. E. Sparks, & J. C. Stromberg, 1997. The natural flow regime. BioScience 47: 769–784, https://doi.org/10.2307/1313099.

Poisson, R., & A. G. Yates, 2022. Impaired cellulose decomposition in a headwater stream receiving subsurface agricultural drainage. Ecological Processes 11: 1–17, https://doi.org/10.1186/s13717-022-00406-9.

Pu, S., F. Zhang, Y. Shu, & W. Fu, 2023. Microscopic image recognition of diatoms based on deep learning. Journal of Phycology 59: 1166–1178, https://doi.org/10.1111/jpy.13390.

Pringle, C. M., R. J. Naiman, G. Bretschko, J. R. Karr, M. W. Oswood, J. R. Webster, R. L. Welcomme, & M. J. Winterbourn, 1988. Patch dynamics in lotic systems: The stream as a mosaic. Journal of the North American Benthological Society 7: 503–524, https://doi.org/10.2307/1467303.

Rau, G. C., M. S. Andersen, A. M. McCallum, H. Roshan, & R. I. Acworth, 2014. Heat as a tracer to quantify water flow in near-surface sediments. Earth-Science Reviews 129: 40–58, https://doi.org/10.1016/j.earscirev.2013.10.015.

Renard, P., & D. Allard, 2013. Connectivity metrics for subsurface flow and transport. Advances in Water Resources 51: 168–196, https://doi.org/10.1016/j.advwatres.2011.12.001.

Rimet, F., E. Gusev, M. Kahlert, M. G. Kelly, M. Kulikovskiy, Y. Maltsev, D. G. Mann, M. Pfannkuchen, R. Trobajo, V. Vasselon, J. Zimmermann, & A. Bouchez, 2019. Diat.barcode, an open-access curated barcode library for diatoms. Scientific Reports 9: 15116, https://doi.org/10.1038/s41598-019-51500-6.

Rinehart, A. J., J. B. Jones, & T. K. Harms, 2015. Hydrologic and biogeochemical influences on carbon processing in the riparian zone of a subarctic stream. Freshwater Science 34: 222–232, https://doi.org/10.1086/679595.

Robbins, C. J., D. W. P. Manning, B. C. Norman, R. A. Eckert, A. Pastor, A. K. Dodd, J. Jabiol, E. Bastias, A. Gossiaux, & A. S. Mehring, 2023. Nutrient and stoichiometry dynamics of decomposing litter in stream ecosystems: A global synthesis. Ecology 104: 1–14, https://doi.org/10.1002/ecy.4060.

Robinson, K., C. E. Robinson, J. W. Roy, M. Vissers, A. Almpanis, U. Schneidewind, & C. Power, 2022. Improved interpretation of groundwater-surface water interactions along a stream reach using 3D high-resolution combined DC resistivity and induced polarization (DC-IP) geoelectrical imaging. Journal of Hydrology Elsevier B.V. 613: 128468, https://doi.org/10.1016/j.jhydrol.2022.128468.

Rosemond, A. D., C. M. Pringle, A. Ramírez, M. J. Paul, & J. L. Meyer, 2002. Landscape variation in phosphorus concentration and effects on detritus-based tropical streams. Limnology and Oceanography 47: 278–289, https://doi.org/10.4319/lo.2002.47.1.0278.

Roy, J. W., B. Zaitlin, M. Hayashi, & S. B. Watson, 2011. Influence of groundwater spring discharge on small-scale spatial variation of an alpine stream ecosystem. 670: 661–670, https://doi.org/10.1002/eco.

Royer, T. V., & W. G. Minshall, 2001. Effects of nutrient enrichment and leaf quality on the breakdown of leaves in a hardwater stream. Freshwater Biology 46: 603–610, https://doi.org/10.1046/j.1365-2427.2001.00694.x.

Royer, T. V, & G. W. Minshall, 2003. Controls on leaf processing in streams from spatial-scaling and hierarchical perspectives. Journal of the North American Benthological Society 22: 352–358, https://doi.org/https://doi.org/10.2307/1468266.

Sabater, S., V. Acuña, A. Giorgi, E. Guerra, I. Muñoz, & A. M. Romaní, 2005. Effects of nutrient inputs in a forested Mediterranean stream under moderate light availability. Archiv fur Hydrobiologie 163: 479–496, https://doi.org/10.1127/0003-9136/2005/0163-0479.

Sand-Jensen, K., N. L. Pedersen, & M. Søndergaard, 2007. Bacterial metabolism in small temperate streams under contemporary and future climates. Freshwater Biology 52: 2340–2353, https://doi.org/10.1111/j.1365-2427.2007.01852.x.

Sear, D. A., P. D. Armitage, & F. H. Dawson, 1999. Groundwater dominated rivers. Hydrological Processes 13: 255–276, https://doi.org/10.1002/(SICI)1099-1085(19990228)13:3<255::AID-HYP737>3.0.CO;2-Y.

Snell, M. A., P. A. Barker, B. W. J. Surridge, C. M. W. H. Benskin, N. Barber, S. M. Reaney, W. Tych, D. Mindham, A. R. G. Large, S. Burke, & P. M. Haygarth, 2019. Strong and recurring seasonality revealed within stream diatom assemblages. Scientific Reports 9: 1–7, https://doi.org/10.1038/s41598-018-37831-w.

Soininen, J., 2007. Environmental and spatial control of freshwater diatoms—a review. Diatom Research 22: 473–490, https://doi.org/10.1080/0269249X.2007.9705724.

Sophocleous, M., 2002. Interactions between groundwater and surface water: The state of the science. Hydrogeology Journal 10: 52–67, https://doi.org/10.1007/s10040-001-0170-8.

Sridhar, K. R., & F. Bärlocher, 1993. Effect of temperature on growth and survival of five aquatic hyphomycetes. Sydowia 45: 377–387.

Steinman, A. D., G. A. Lamberti, & P. R. Leavitt, 2007. Biomass and pigments of benthic algae In Hauer, F. R., & G. Lamberti (eds), Methods in Stream Ecology. Academic Press, San Diego, CA, USA: 357–379, https://doi.org/https://doi.org/10.1016/B978-012332908-0.50024-3.

Stevenson, R.J., Novoveska, L., C.M. Riseng, & M.J., Wiley, 2009. Comparing responses of diatom species composition to natural and anthropogenic factors in streams of glaciated ecoregions. Nova Hedwigia 135: 1–13.

Stevenson, R. J., 1997. Scale-dependent determinants and consequences of benthic algal heterogeneity. Journal of the North American Benthological Society 16: 248–262, https://doi.org/10.2307/1468255.

Stevenson, R. J., & Y. Pan, 2010. Assessing environmental conditions in rivers and streams with diatoms In Smol, J. P., & E.F. Stoermer (eds), The diatoms: Applications for the environmental and earth sciences. Cambridge University Press: 11–40, https://doi.org/10.1017/cbo9780511613005.003.

Stoodley, P., K. Sauer, D. G. Davies, & J. W. Costerton, 2002. Biofilms as complex differentiated Communities. Annual Review of Microbiology 56: 187–209, https://doi.org/10.1146/annurev.micro.56.012302.160705.

Strommer, J. L., & L. A. Smock, 1989. Vertical distribution and abundance of invertebrates within the sandy substrate of a low-gradient headwater stream. Freshwater Biology 22: 263–274, https://doi.org/https://doi.org/10.1111/j.1365-2427.1989.tb01099.x.

Suberkropp, K., 1984. Effect of temperature of seasonal occurrence of aquatic hyphomycetes. Transactions of the British Mycological Society British Mycological Society 82: 53–62, https://doi.org/10.1016/S0007-1536(84)80211-9.

Suberkropp, K., 1992. Interactions with invertebrates In Barlocher, F. (ed), The Ecology of Aquatic Hyphomycetes. Springer-Verlag, Berlin: 118–134.

Suberkropp, K., & E. Chauvet, 1995. Regulation of leaf breakdown by fungi in streams influences of water chemistry. Ecology 21: 1433–1445, https://doi.org/10.2307/1938146.

Suberkropp, K., & H. Weyers, 1996. Application of fungal and bacterial production methodologies to decomposing leaves in streams. Applied and Environmental Microbiology 62: 1610–1615.

Tang, T., S. Guo, L. Tan, T. Li, R. M. Burrows, & Q. Cai, 2019. Temporal effects of groundwater on physical and biotic components of a karst stream. Water (Switzerland) 11:1–17, https://doi.org/10.3390/w11061299.

Tank, J. L., & W. K. Dodds, 2003. Nutrient limitation of epilithic and epixylic biofilms in ten North American streams. Freshwater Biology 48: 1031–1049, https://doi.org/10.1046/j.1365-2427.2003.01067.x.

Tank, J. L., & M. J. Winterbourn, 1995. Biofilm development and invertebrate colonization of wood in four New Zealand streams of contrasting pH. Freshwater Biology 34: 303–315, https://doi.org/10.1111/j.1365-2427.1995.tb00890.x.

Thorp, J. H., M. C. Thoms, & M. D. Delong, 2006. The riverine ecosystem synthesis: Biocomplexity in river networks across space and time. River Research and Applications 22: 123–147, https://doi.org/10.1002/rra.901.

Thorp, J. H., M. C. Thoms, & M. D. Delong, 2008. The riverine ecosystem synthesis. The riverine ecosystem synthesis, https://doi.org/10.1016/B978-0-12-370612-6.X0001-0.

Tiegs, S. D., P. O. Akinwole, & M. O. Gessner, 2009. Litter decomposition across multiple spatial scales in stream networks. Oecologia 161: 343–351, https://doi.org/10.1007/s00442-009-1386-x.

Tiegs, S. D., J. E. Clapcott, N. A. Griffiths, & A. J. Boulton, 2013. A standardized cotton-strip assay for measuring organic-matter decomposition in streams. Ecological Indicators 32: 131–139, https://doi.org/10.1016/j.ecolind.2013.03.013.

Tiegs, S. D., D. Costello, M. Isken, G. Woodward, P. McIntyre, M. O. Gessner, E. Chauvet, N. A. Griffiths, A. Flecker, V. Acuña, & R. Albariño, 2019. Global patterns and drivers of ecosystem functioning in rivers and riparian zones. Science Advances 5: 1–8, https://doi.org/10.1126/sciadv.aav0486.

Tiegs, S. D., S. D. Langhans, K. Tockner, & M. O. Gessner, 2007. Cotton strips as a leaf surrogate to measure decomposition in river floodplain habitats. Journal of the North American

Benthological Society 26: 70–77, https://doi.org/doi.org/10.1899/0887-3593(2007)26[70:CSAALS]2.0.CO;2.

Townsend, C. R., 1989. The patch dynamics concept of stream community ecology. Journal of the North American Benthological Society 8: 36–50, https://doi.org/10.2307/1467400.

Valett, H. M., C. N. Dahm, M. E. Campana, J. A. Morrice, M. A. Baker, & C. S. Fellows, 1997. Hydrologic influences on groundwater-surface water ecotones: Heterogeneity in nutrient composition and retention. Journal of the North American Benthological Society 16: 239–247, https://doi.org/10.2307/1468254.

Valett, H. M., S. G. Fisher, N. B. Grimm, & P. Camill, 1994. Vertical hydrologic exchange and ecological stability of a desert stream ecosystem. Ecology 75: 548–560, https://doi.org/10.2307/1939557.

Van Dam, H., A. Mertens, & J. Sinkeldam, 1994. A coded checklist and ecological indicator values of freshwater diatoms from The Netherlands. Netherlands Journal of Aquatic Ecology 28: 117–133, https://doi.org/10.1007/BF02334251.

Vannote, R. L., G. W. Minshall, K. W. C. Cummins, J. R. S. Sedell, & C. E. Cushing, 1980. River continuum concept. Canadian Journal of Fisheries and Aquatic Sciences 37: 130–137, https://doi.org/10.1139/f80-017.

Vissers, M. A., J. W. Roy, A. G. Yates, K. Robinson, S. Rakhimbekova, & C. E. Robinson, 2023. Spatio-temporal variability of porewater phosphorus concentrations in streambed sediments of an agricultural stream. Journal of Hydrology 617: 129133, https://doi.org/10.1016/j.jhydrol.2023.129133.

Webb, J. R., N. J. T. Pearce, K. J. Painter, & A. G. Yates, 2019. Hierarchical variation in cellulose decomposition in least-disturbed reference streams: a multi-season study using the cotton strip assay. Landscape Ecology 34: 2353–2369, https://doi.org/10.1007/s10980-019-00893-w.

Webster, J. R., & E. F. Benfield, 1986. Vascular plant breakdown in freshwater ecosystems. Annual Review of Ecology and Systematics 17: 567–594, https://doi.org/10.1002/ar.a.20165.

Wijewardene, L., N. Wu, P. Giménez-Grau, C. Holmboe, N. Fohrer, A. Baattrup-Pedersen, & T. Riis, 2021. Epiphyton in agricultural streams: Structural control and comparison to epilithon. Water (Switzerland) 13: 1–17, https://doi.org/10.3390/w13233443.

Winter, J. G., & H. C. Duthie, 2000. Stream biomonitoring at an agricultural test site using benthic algae. Canadian Journal of Botany 78: 1319–1325, https://doi.org/10.1139/cjb-78-10-1319.

Winter, T. C., J. W. Harvey, O. L. Franke, & W. M. Alley, 1998. Ground Water and Surface Water - A single Resource - U.S. Geological Survey Circular 1139. USGS Publications Circular 1: 79.

Winter, T. C., J. W. LaBaugh, & D. O. Rosenberry, 1988. The design and use of a hydraulic potentiomanometer for direct measurement of differences in hydraulic head between groundwater and surface water. Limnology and Oceanography 33: 1209–1214, https://doi.org/10.4319/lo.1988.33.5.1209.

Woodward, G., M. O. Gessner, P. S. Giller, V. Gulis, S. Hladyz, A. Lecerf, B. Malmqvist, B. G. McKie, et al., 2012. Continental-scale effects of nutrient pollution on stream ecosystem functioning. Science 336: 1438–1440, https://doi.org/10.1126/science.1219534.

Wyatt, K. H., F. R. Hauer, & G. F. Pessoney, 2008. Benthic algal response to hyporheic-surface water exchange in an alluvial river. Hydrobiologia 607: 151–161, https://doi.org/10.1007/s10750-008-9385-1.

Appendices

Appendix A

Appendix A1. Site location (E indicates East branch, W indicated West branch), distance to source of branch, radon-222 (^{222}Rn) concentration for each season, canopy cover (%) and discharge ($m^3\ s^{-1}$) in summer

Site	X	Y	Distance to Source (m)	^{222}Rn - Autumn ($Bq\ m^{-3}$)	^{222}Rn - Winter ($Bq\ m^{-3}$)	^{222}Rn - Spring ($Bq\ m^{-3}$)	^{222}Rn - Summer ($Bq\ m^{-3}$)	Canopy Cover - Summer	Discharge ($m^3\ s^{-1}$) - Summer
1E	-81.0230	43.16314	2547	527	1176	515	311	82.75	0.044
2E	-81.0277	43.16081	3099	704	962	492	232	82.75	0.081
3E	-81.0272	43.15215	4464	203	1026	670	360	72.25	0.110
4E	-81.0257	43.14457	6023	209	692	284	55	85.25	0.154
5E	-81.0265	43.14300	6223	846	702	255	48	79	0.158
6E	-81.0258	43.14069	6482	273	497	181	130	93.25	0.162
7E	-81.0196	43.1297	7952	433	829	276	62	82.5	0.190
1W	-81.0558	43.16141	2597	337	553	445	30	89.5	0.008
2W	-81.0564	43.164	2900	530	682	460	124	86.75	0.013
3W	-81.0517	43.15618	3596	337	877	830	566	84.5	0.018
4W	-81.0508	43.1544	3810	261	768	808	412	85.25	0.024
5W	-81.0511	43.15083	4070	482	820	760	361	87	0.044
6W	-81.0508	43.15212	4217	424	614	602	358	81.5	0.020
7W	-81.0443	43.14645	4581	92	598	512	285	91.5	0.025
8W	-81.0485	43.14841	5012	91	776	668	198	89.5	0.032
9W	-81.0404	43.14371	5477	70	880	767	340	91.75	0.036

10W	-81.032	43.13785	6464	349	868	664	228	89	0.050
11W	-81.0306	43.13587	6710	392	1082	954	724	79	0.048
12W	-81.0199	43.12903	8002	202	831	757	354	84.75	0.065

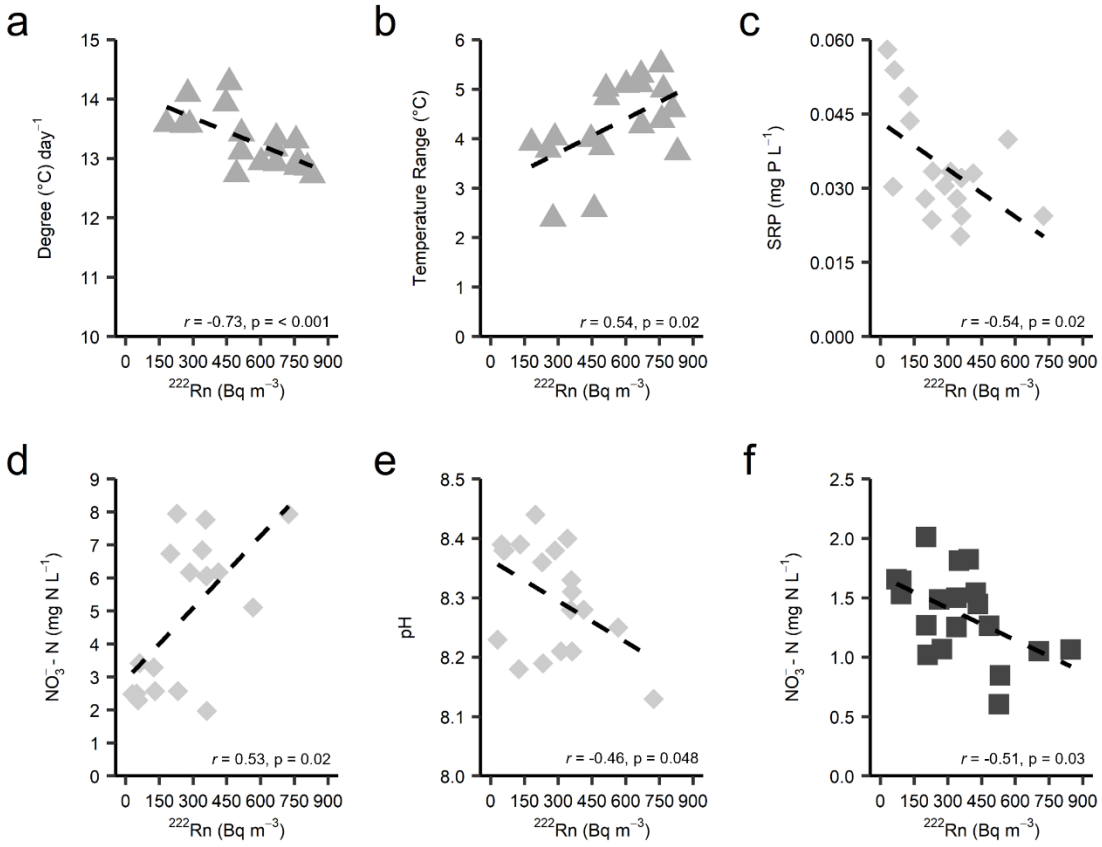

Appendix A2. Significant ($p < 0.05$) Pearson product-moment correlations with Pearson correlation coefficients (r) and p-values for: (a) Average degree day^{-1} and ^{222}Rn in spring; (b) Mean daily temperature (°C) range and ^{222}Rn in spring; (c) SRP (mg P L^{-1}) and ^{222}Rn in summer; (d) NO_3^-N (mg N L^{-1}) and ^{222}Rn in summer; (e) pH and ^{222}Rn in summer, and; (f) NO_3^- N (mg N L^{-1}) and ^{222}Rn in autumn.

Appendix B

Appendix B1. Radon-222 mass balance model

Groundwater discharge along each stream reach was estimated by applying a steady state ^{222}Rn mass balance model in which gas exchange and radioactive decay of ^{222}Rn in the stream was taken into account. Using this model, groundwater inflows (q_{gw}, m^3/m/d) along the stream reaches were estimated via (Atkinson et al., 2015; Cook, 2013; Mullinger et al., 2007):

$$q_{gw} = \frac{Q_s \frac{(C_{out} - C_{in})}{L} - kdwC_s + \lambda \mathrm{d}\mathrm{w}C_s}{(C_{gw} - C_s)}$$

where C_{in} and C_{out} are the ^{222}Rn activities measured at the downstream and upstream sampling for the reach (Bq/m^3), C_s is the average ^{222}Rn activity in the stream reach considering the upstream and downstream activities (Bq/m^3), C_{gw} is a representative ^{222}Rn activity in the groundwater, d and w are the average stream depth and width, respectively (m), Q_s is the average stream discharge (m^3/day), λ is the radioactive decay rate (0.181 day^{-1}) and k is the reaeration coefficient (day^{-1}). ^{222}Rn loss due to evaporation was not included as it is not expected to considerably affect the ^{222}Rn concentrations in the stream (Atkinson et al., 2015). C_{gw} was based on sampling of six shallow groundwater wells located within 20 m of Kintore Creek (6700 ± 1400 Bq/m^3).

The reaeration coefficient (k) defines the rate of degassing of ^{222}Rn across the air-water interface and is related to stream turbulence. Following Atkinson et al. (2015), the following empirical relationship which is a modification of the gas transfer model of O'connor and Dobbins (1958) was used to calculate k:

$$k = 9.301\ x\ 10^{-3}\left(\frac{v^{0.5}}{d^{1.5}}\right)$$

where v is the average river velocity in the stream reach. Other empirical relationships were explored to estimate k including that based on the gas transfer model of Negulescu and Rojanski (1969), but the calculated groundwater inflow patterns were consistent regardless of which relationship was adopted.

Appendix B2. Additional input information for ^{222}Rn steady state mass balance model for three reaches in Kintore Creek, Ontario, Canada receiving high (HG), moderate (MG) and low (LG) inputs of groundwater.

	HG	MG	LG
^{222}Rn Above Reach (Bq m^{-3})	1183	294	679
^{222}Rn Below Reach (Bq m^{-3})	1121	679	762
Average stream flow (m^3/s)	0.041	0.010	0.015
Distance between sampling points (m)	174	191	210
Average stream depth (m)	0.15	0.11	0.12
Average stream width (m)	2.00	0.89	0.87
Average stream velocity (m/s)	0.14	0.10	0.15

Appendix C

Appendix C1. Descriptive statistics (mean, standard deviation, coefficient of variation, median, minimum, and maximum) for each of the environmental and biotic parameters.

Parameter	Mean	Standard Deviation	Coefficient of Variation	Median	Minimum	Maximum
Environmental						
Subsurface Temperature (°C)	17.7	1.6	0.09	17.9	14.0	20.1
SRP (µg/L)	42.2	1.1	0.03	42.2	40.0	44.5
NO_3^--N (mg/L)	7.2	2.0	0.3	8.1	2.1	10.4
Mean Daily Temperature (°C)	18.6	0.2	0.01	18.67	17.81	19.04
Mean Daily Temperature Range (°C)	3.0	0.5	0.2	2.93	1.90	5.09
Stream Velocity (m/s)	0.082	0.050	0.617	0.078	0.002	0.205
Stream Depth (cm)	11.7	2.8	0.2	11.7	5.0	17.5
pH	8.17	0.07	0.008	8.17	7.91	8.28
Specific Conductivity (µS/cm)	615	6	0.009	615	593	629
PAR (µmol/s/m^2)	1667	75	0.04	1469	1469	1783
Biotic						
Streambed Tensile Loss	5.0	0.7	0.1	5.2	3.3	6.1
Subsurface Tensile Loss	2.6	0.7	0.3	2.9	0.9	3.3
Chl-*a* Accumulation	0.07	0.06	0.93	0.05	0.001	0.27
Biofilm Growth Rate	0.0076	0.0067	0.8864	0.0063	0.0002	0.0315

	Subsurface Temperature (°C)	SRP (µg/L)	NO_3^--N (mg/L)	Mean Daily Temperature (°C)	Mean Daily Temperature Range (°C)	Stream Velocity (m/s)	Stream Depth (cm)	pH	Specific Conductivity (µS/cm)	PAR (µmol/s/m^2)
Subsurface Temperature (°C)		-	-	-	-	-	-	-	-	-
SRP (µg/L)	**0.67**		-	-	-	-	-	-	-	-
NO_3^--N (mg/L)	-0.21	-0.24		-	-	-	-	-	-	-
Mean Daily Temperature (°C)	**0.69**	**0.56**	-0.11		-	-	-	-	-	-

Mean Daily Temperature Range (°C)	0.16	**0.31**	-0.05	**0.58**		-	-	-	-	-
Stream Velocity (m/s)	0.05	-0.09	-0.01	0.19	0.07		-	-	-	-
Stream Depth (cm)	**0.37**	**0.37**	-0.05	**0.36**	0.14	**-0.41**		-	-	-
pH	**-0.34**	**-0.46**	**0.28**	-0.20	-0.01	-0.18	-0.02		-	-
Specific Conductivity (µS/cm)	0.15	0.15	-0.13	0.03	0.00	-0.12	0.26	**-0.54**		-
PAR (µmol/s/m^2)	0.24	0.09	0.01	0.26	0.12	**0.38**	**-0.29**	-0.11	-0.18	-

Appendix C2. Pearson correlation coefficient (r) between environmental variables where significant ($\alpha = 0.05$) correlations are bolded. "-" denotes duplicate data on upper diagonal and " " denotes correlation of a variable with itself.

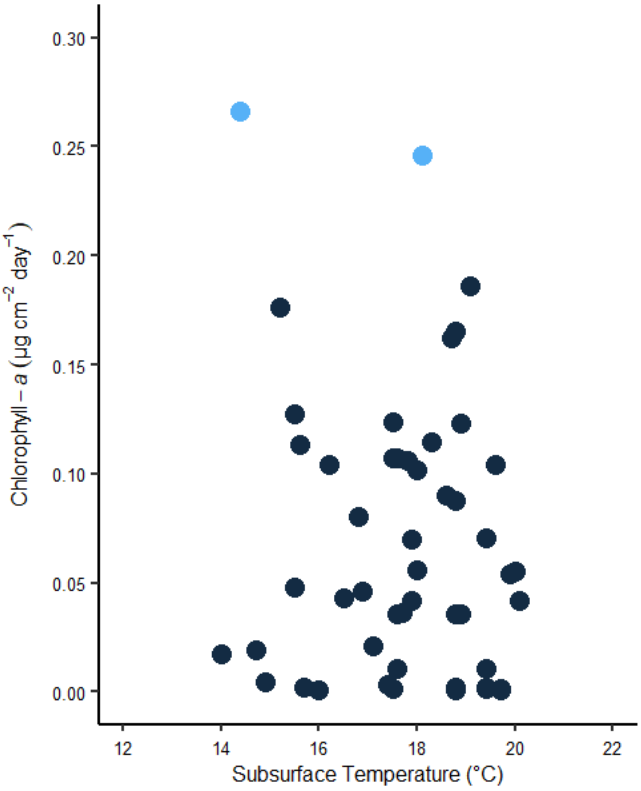

Appendix C3. Scatterplot of subsurface temperature (°C) and chl-a accumulation (µg cm^{-2} day^{-1}) with outlier locations identified using Tukey's IQR method in light blue, and all other locations in dark blue.